The Dissertation Committee for Larissa Anne Durfee Certifies that this is the approved version of the following dissertation:

The Enzymology and Substrate Selectivity of the ISG15 Conjugation System

Committee:

Jon Huibregtse, Supervisor

Robert Krug

Rick Russell

Sara Sawyer

Chris Sullivan

The Enzymology and Substrate Selectivity of the ISG15 Conjugation System

by

Larissa Anne Durfee, B.S.

Dissertation

Presented to the Faculty of the Graduate School of

The University of Texas at Austin

in Partial Fulfillment

of the Requirements

for the Degree of

Doctor of Philosophy

The University of Texas at Austin

May, 2010

Dedication

To my family, Gloria, and Courtney for their belief in me and their unending support.

Acknowledgements

I am extremely grateful to my advisor, Dr. Jon Huibregtse, for his encouragement, guidance, patience, and enthusiasm for science. I could not have asked for a better mentor. I am also grateful to the members of my committee, Drs. Robert Krug, Rick Russell, Sara Sawyer, and Chris Sullivan, for their constructive criticism, helpful suggestions, and advice. To all of the Huibregtse lab members, past and present, thank you for your friendship and help throughout the years. You have made each day in lab more enjoyable. Finally, I would like to thank my family, Courtney, and my friends, for their love and support during all of the ups and downs of graduate school.

The Enzymology and Substrate Selectivity of the ISG15 Conjugation System

Publication No._____

Larissa Anne Durfee, Ph.D.

The University of Texas at Austin, 2010

Supervisor: Jon M. Huibregtse

ISG15 is an interferon-induced and anti-viral ubiquitin-like protein (Ubl). Ube1L, UbcH8, and Herc5 have been identified as the E1-E2-E3 enzymes for ISG15 conjugation, and, like ISG15, their expression is induced by type I interferons. Although Herc5 is the major E3 for ISG15, over 300 proteins have been identified as ISG15 target proteins in interferon-stimulated cells. In this work, I address two aspects of the human ISG15 conjugation system: 1) the specificity of the Ube1L-UbcH8 interaction and 2), the basis of substrate recognition by Herc5. Regarding the selection of UbcH8 by Ube1L, my experiments show that although UbcH8 had been reported to function as an E2 for both Ub and ISG15, UbcH8 is preferentially activated by Ube1L compared to Ube1 ($E1^{Ub}$). The basis of this preference is a result of specific interactions between the ubiquitin-fold domain (UFD) of Ube1L and the amino-terminal α1-helix and β1–β2 region within UbcH8. Examination of the interferon-induced and transfected expression levels of UbcH8, combined with the kinetic constants, suggest that UbcH8 is unlikely to function

as a Ub E2 in most cell lines. In examining the selection of target proteins by Herc5, I show that the range of substrates extends far beyond the proteins identified in proteomics studies and includes many exogenously expressed foreign proteins. Furthermore, I show that ISG15 conjugation is restricted to newly synthesized pools of proteins and Herc5 is associated with polyribosomes. I propose a model for ISGylation in which Herc5 broadly modifies newly synthesized proteins in a co-translational manner and suggest that, in the context of an interferon-stimulated cell, newly translated viral proteins may be primary targets of ISG15. Consistent with this, I show that ISGylation of human papillomavirus (HPV) L1 capsid protein has a dominant-inhibitory effect on the infectivity of HPV16 pseudoviruses. These discoveries have greatly increased our understanding of the mechanism of ISG15 pathway and provide a framework for establishing an *in vitro* ISG15 conjugation system and further examination of the anti-viral function of ISG15.

Table of Contents

List of Tables

List of Figures

Chapter 1: Introduction

1.1 A BRIEF OVERVIEW OF THE UBIQUITIN SYSTEM

In 2004, the Nobel Prize in Chemistry was awarded to Aaron Ciechanover, Avram Hershko and Irwin Rose for their discovery of the ubiquitin system and its role in regulated protein degradation. The lysosome, discovered in the 1950s, was assumed to mediate all protein degradation, however several lines of evidence suggested an additional ATP-dependent mechanism existed as well (Ciechanover, 2009). Hershko, Ciechanover, and colleagues published the first of many papers in 1978 on the selective post-translational modification of cellular proteins with a 8.5 kDa protein now known as ubiquitin (Ciehanover et al., 1978). They discovered an ATP-dependent system in which a protein tagged with ubiquitin is selectively degraded by the proteasome. Today, ubiquitination is known to function in a wide range of cellular processes, including DNA repair, transcription, endocytosis, membrane transport, protein localization, and antigen processing.

1.1.1 Conjugation of Ubiquitin

Ubiquitin (Ub) is covalently conjugated to proteins through amide bonds formed between their terminal carboxyl groups and, in most cases, ε-amino groups of lysine residues of target proteins. The Ub conjugation pathway consists of E1, E2, E3 and de-ubiquitinating enzymes (DUBs) (Figure 1.1) (Passmore and Barford, 2004). Ub is expressed as an inactive precursor and before it can be conjugated to a target protein a DUB must cleave Ub to reveal a Gly-Gly motif at the C-terminus. Once processed, E1 forms an ATP-dependent Ub-adenylate followed by an enzyme-bound Ub-thioester at the

active site cysteine of the E1. The activated E1 then binds a specific E2 enzyme and transfers Ub to the E2 active-site cysteine in a transthiolation reaction, preserving the Ub-thioester linkage. The Ub charged E2 enzyme dissociates from the E1 and binds an E3 ligase that facilitates transfer of Ub to a target protein. Ubiquitination can be reversed when DUBs hydrolyze the isopeptide bond between Ub and the substrate or between two Ub molecules. This reversal by DUBs functions to recycle Ub, edit the Ub chain topology of target proteins, and rescue proteins from proteasome-mediated degradation (Love et al., 2007). In humans, there are two E1s (Uba1 and Uba6), approximately 60 E2s, 100 DUBs, and between 600-1000 E3s for the Ub pathway (Rape, 2009).

Once the target protein has been selected, ubiquitin is added either as one molecule (monoubiquitination and multi-monoubiquitination) or as a chain of molecules (polyubiquitination). Ubiquitin has seven lysines (K6, K11, K27, K29, K33, K48, K63) available to link with other ubiquitin molecules resulting in homotypic chains or mixed-linkage chains (Kim et al., 2007). All seven lysines of ubiquitin have been shown to form chains *in vivo,* however the function of some chain types is still unknown (Peng et al., 2003). K48-linked chains have been well established as the main chain type involved in proteasomal degradation, but all other chain types (with the exception of K63-linked chains) are capable of targeting proteins to the proteasome *in vivo* (Xu et al., 2009). For example, Xu *et al.* demonstrated that K11-linked chains were shown to be required for targeting misfolded proteins in the ER for proteasomal degradation. Although K63-linked chains do not signal protein degradation, they function in processes ranging from cell surface receptor internalization to signaling events leading to NF-κβ activation (Bennett and Harper, 2008; Hayden and Ghosh, 2008; Mukhopadhyay and Riezman, 2007). Recently, unanchored K63-polyubiquitin chains have been shown to be required

for the activation of RIG-I, a viral RNA detector involved in the innate immune response (Zeng et al., 2010). Physiological roles for monoubiquitination include DNA repair and endocytosis (Haglund and Dikic, 2005; Hicke, 2001).

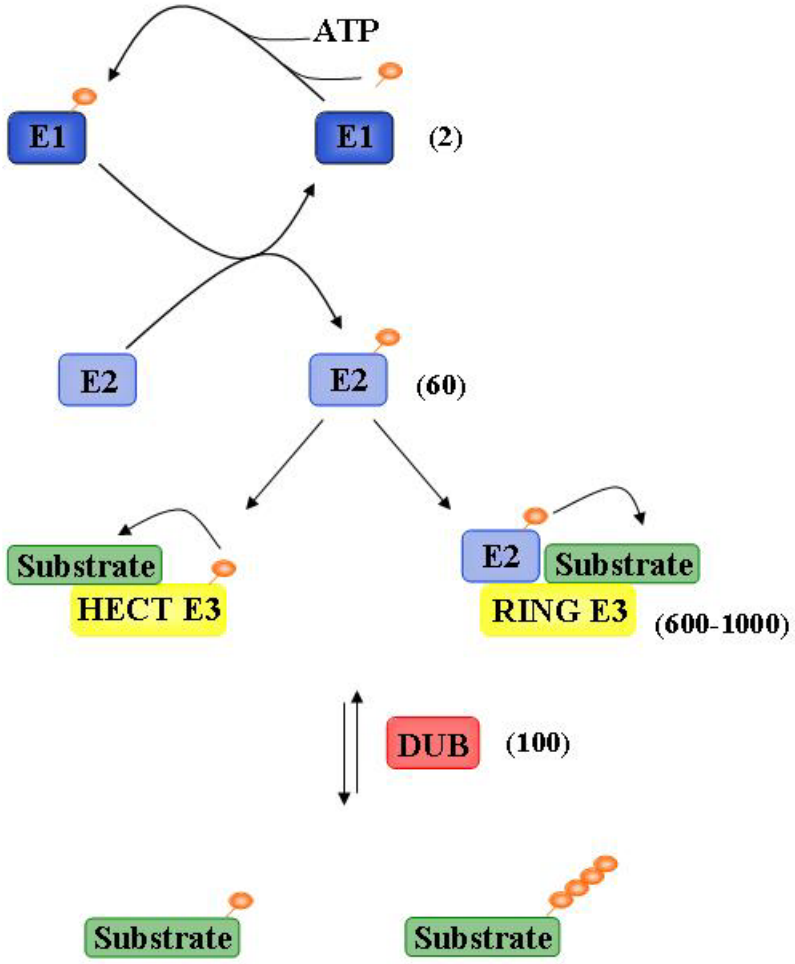

Figure 1.1: The Ubiquitin Pathway.

1.1.2 E1 activating enzymes

Structural studies of E1 enzymes have identified three functional domains: 1) an adenylation domain which binds Ub and ATP and catalyzes adenylation of the C-

terminus of Ub forming Ub~AMP, 2) a cysteine domain which contains the catalytic cysteine, and 3) a ubiquitin-fold domain (UFD) which recruits E2 enzymes (Schulman and Harper, 2009). The catalytic reaction cycle begins with the formation of Ub~AMP which is then attacked by the catalytic cysteine to form an enzyme-bound Ub-thioester. Adenylation of a second Ub molecule occurs resulting in a doubly loaded E1 enzyme that presents the UFD for interaction with the E2 enzyme. Transthiolation occurs, E2~Ub is released, and remaining Ub~AMP serves as the precursor the next reaction cycle. The E1 enzyme must undergo major conformational changes during this process. For example, the site of Ub~AMP formation is widely separated from the catalytic cysteine. Recent structures of SUMO and its E1 reveal that once SUMO~AMP is formed, the cysteine domain rotates 130 degrees and secondary structure must refold for E1~SUMO thioester formation (Olsen et al., 2010). E1 active site remodeling may also be required to facilitate transfer of Ub/Ubl from the E1 cysteine to the E2 cysteine. A complete understanding of E1 conformational changes is important for the development of small molecule inhibitors. For example, the Nedd8 pathway is involved in cell cycle control, and a recently developed Nedd8 E1 inhibitor is currently in phase I clinical trials for solid tumor malignancies (Soucy et al., 2009). The work by Olsen *et al.* will aid in developing additional E1 small molecule inhibitors in the future.

1.1.3 E2 conjugating enzymes

All E2 conjugating enzymes consist minimally of a core ubiquitin-conjugating domain (UBC) of approximately 150 residues, one of which is the catalytic cysteine (Pickart, 2001). E2 enzymes must bind E1 and E3 enzymes however, these events are mutually exclusive (Eletr et al., 2005; Eletr and Kuhlman, 2007). Structures of E2 enzymes in complex with either an E1 or E3 enzyme reveal the E2 N-terminal α1-helix

interacts with both the E1 and E3 enzymes (Bencsath et al., 2002; Eletr and Kuhlman, 2007; Huang et al., 2005; Huang et al., 1999; Reverter and Lima, 2005). In addition, some studies have shown E1 enzymes prefer uncharged E2s, while E3 enzymes prefer Ub-charged E2 enzymes (Hershko et al., 1983; Kawakami et al., 2001; Pickart and Rose, 1985; Siepmann et al., 2003). While the α1-helix is important for both interactions, the E1-E2 interaction also requires the β1-β2 region whereas the E2-E3 interaction requires additional residues from Loops 4 and 7 of the E2 enzyme. For example, a phenylalanine residue in Loop 4 is important for the E2 interaction with both HECT and RING E3 ligases, while a tryptophan residue in Loop 7 is important for RING E3 interactions (Huang et al., 1999; Martinez-Noel et al., 1999; Zheng et al., 2000). Until recently, E2 enzymes were considered to function only as "carriers" of Ub between the E1 and E3. Many new studies have shown that some E2 enzymes play a role in the type and length of Ub chain formed on substrates (Ye and Rape, 2009). This function is limited to E2s that interact with RING E3s most likely because RING E3s are docking proteins with no catalytic activity.

1.1.4 E3 ligase enzymes

E3s function minimally as docking or scaffolding proteins, binding both the activated E2 and a substrate protein. There are two major types of E3 ligases: RING E3s and HECT (Homologous to E6AP C-terminus) E3s. In the case of the HECT E3 ligases, the E2 transfers Ub to the active-site cysteine of the E3, with the E3 directly catalyzing the final transfer to the target protein. Alternatively, RING E3 ligases have no catalytic activity and instead facilitate the transfer of Ub from the E2 directly to the target protein. In humans, there are 28 HECT E3 ligases compared to over 600 RING E3 ligases (Deshaies and Joazeiro, 2009; Rotin and Kumar, 2009).

RING E3 ligases

The RING domain is composed of two zinc atoms bound to cysteines and histidines to form a cross-brace which stabilizes the RING E3 and mediates the interaction with the E2 enzyme (Deshaies and Joazeiro, 2009). Cbl, a monomeric RING E3 ligase, contains a phosphotyrosine-binding domain (PTB) upstream of its RING finger domain that allows Cbl to recognize tyrosine-phosphorylated target proteins (Joazeiro et al., 1999). Recently STUbls (SUMO-targeted ubiquitin ligases) were identified as a new type of monomeric RING E3 ligase (Perry et al., 2008). STUbls contain two N-terminal SUMO-interactions motifs (SIMs) which are required for recognition and ubiquitination of its SUMOylated target proteins. Many RING E3 ligases are part of larger complexes where target protein recognition is mediated by a different subunit of the complex. Cullin-RING E3 ligases (CRLs) form complexes with different substrate binding proteins such as the F box, SOCS box, and BTB domain-containing proteins (Petroski and Deshaies, 2005). These substrate binding proteins often contain WD40 repeats, leucine rich repeats, or ankyrin repeats to mediate the interaction with target proteins.

HECT E3 ligases

The HECT domain is C-terminal domain of ~350 residues. This domain was first described in E6AP, a E3 ligase hijacked by the human papillomavirus (HPV) E6 protein to mediate degradation of p53 (Scheffner et al., 1993). E6AP was the first E3 to be purified and when used in an *in vitro* assay, it was shown to form a thioester with Ub before transferring it to p53. Sequence analysis revealed several protein sequences with C-terminal residues similar to E6AP that were also capable of thioester formation (Huibregtse et al., 1995). E6AP and these related proteins were classified as a new group of Ub E3 ligases, the HECT E3s.

The first crystal structure of a HECT E3 was of the HECT domain of E6AP bound to the E2 enzyme, UbcH7 (Huang et al., 1999). This U-shaped structure revealed a bilobal HECT domain with the N-terminal lobe mediating E2 binding and a C-terminal lobe containing the catalytic cysteine for thioester formation. Interestingly, the catalytic cysteines on UbcH7 and the C-lobe of E6AP were found to be separated by 41 Å (Figure 1.2). This distance was much greater than the 2.5Å required for transthiolation and it was proposed that transfer of Ub from E2 to E3 would require a large conformational change of the HECT domain. Subsequent crystal structures of HECT domains (WWP1, SMURF2, HUWE1, NEDD4L) revealed different orientations of the N- and C-lobes (Kamadurai et al., 2009; Ogunjimi et al., 2005; Pandya et al., 2010; Verdecia et al., 2003). An L-shape, similar to that of $HECT^{E6AP}$, was observed for the $HECT^{SMURF2}$, while an inverted T shape was observed for $HECT^{HUWE1}$, $HECT^{NEDD4L}$, and $HECT^{WWP1}$. The shift of the C-lobe to the middle of the N-lobe placed the E2 and E3 cysteines much closer; in the case of $HECT^{NEDD4L}$ and UbcH5B, only 8Å apart.

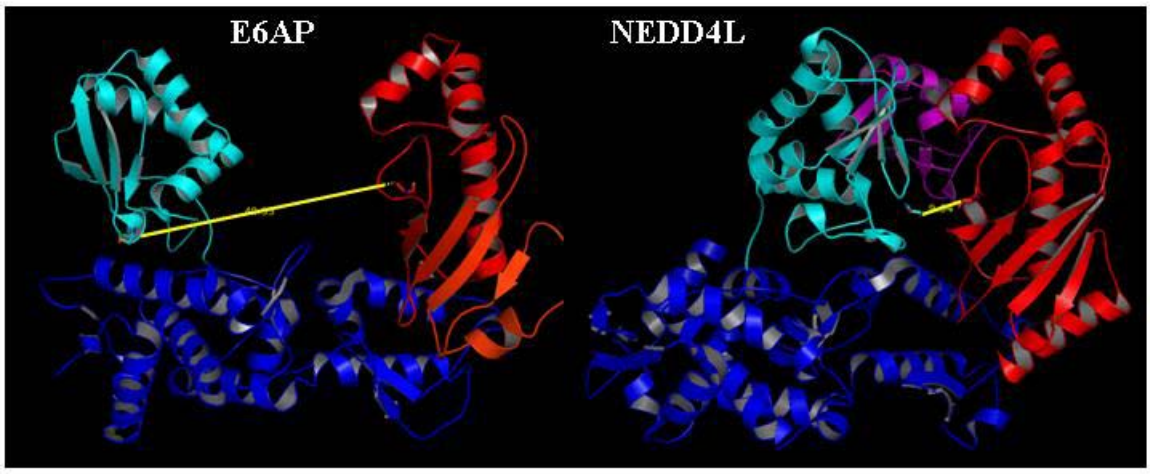

Figure 1.2: E2-HECT domain structures

The crystal structures for UbcH7-HECT^{E6AP} (left) and UbcH5B-HECT^{NEDD4L} (right) indicate the C lobe of the HECT domain is very flexible. The E2 is displayed in red, N-lobe in dark blue, C-lobe in light blue, and ubiquitin in purple (NEDD4L structure only). The distance between the catalytic cysteines is indicated by the yellow line. Structures were created using PyMol and the PDB files 1DF5 and 3JW0.

While the C-terminal HECT domain is the catalytic domain of the E3, the N-terminal regions of HECT E3s mediate target protein recognition. For example, the Nedd4 family of HECT E3 ligases has WW domains which interact with PPXY (Pro-Pro-X-Tyr) motifs found in their target proteins. The HPV E6 protein binds E6AP at a 17 amino acid peptide approximately 100 residues upstream of the HECT domain. N-terminal RCC1-like domains (RLDs), known to mediate protein-protein interactions, distinguish the Herc family of HECT E3 ligases (discussed in more detail below).

HECT E3 ligases are a major focus of our lab and currently we are interested in the mechanism by which HECT E3 ligases control the type of linkage formed between molecules of Ub. E6AP preferentially catalyzes K48-linked chains, while Rsp5, a *S. cerevisiae* HECT E3, preferentially synthesizes K63-linked chains. Our lab recently

determined that chain type specificity among HECT E3 ligases is a function of the C lobe of the HECT domain (Kim and Huibregtse, 2009). Kim *et al.* showed that exchanging the C lobe of the K63-specific HECT E3 Rsp5 for the C lobe of the K48-specific HECT E3 E6AP resulted in Rsp5 preferentially catalyzing K48-linked chains. In addition to chain type specificity, our lab is also interested Ub chain elongation. The sequential-addition model of polyubiquitination proposes a single Ub molecule is added to the substrate and then the chain is elongated by conjugation of additional Ub monomers. One problem with this model is accounting for the formation of long chains composed of up to 30 Ub molecules. Recently, a non-covalent ubiquitin binding domain (UBD) was discovered on the N-lobe of the HECT domains for RSP5 and SMURF1 (French et al., 2009; Ogunjimi et al.). Mutational analysis of the SMURF1 UBD found a decrease in polyubiquitination of SMURF1 itself as well as the substrate Rho. Ogunjimi *et al* proposed a role for the N-lobe UBD in stabilizing and positioning Ub at the growing end of the chain for addition of another molecule of Ub. We are in the process of characterizing the role of the N-lobe UBD in polyubiquitination with other HECT E3s such as RSP5 and E6AP.

1.2 ISG15: UBIQUITIN-LIKE PROTEIN

Ubiquitin-like proteins (Ubls) are proteins that structurally resemble the β-grasp fold of Ub and contain a C-terminal glycine required for isopeptide bond formation with target proteins (Figure 1.3). To date, seventeen human Ubls have been identified, including Nedd8, FAT10, SUMO1-4, and ISG15 (Schulman and Harper, 2009). Ubls are conjugated to cellular proteins via an enzymatic cascade similar to that of Ub. Ubls also have specific Ubl-specific proteases (ULPs) which cleave the C-terminus to process the Ubl before conjugation as well as hydrolyze Ubls from target proteins. With the

exception of SUMO2/3 and Nedd8, Ubls have not been found to form poly-Ubl chains (Jones et al., 2008; Vertegaal, 2010).

While the Ub system has 60 E2s and over 600 E3s, no more than two E2s and at most a few E3s have been identified for any Ubl (Kerscher et al., 2006). Until recently, it was thought that each Ubl had dedicated E1, E2, and E3 enzymes and therefore Ubl pathways were considered to be parallel, but distinct from the Ub pathway. This paradigm has been challenged with the discovery of new pathway enzymes. For example, a newly discovered E1 for Ub, Uba6, has been reported to be the E1 for FAT10 as well (Chiu et al., 2007). In addition, two structurally-distinct Ubls involved in autophagy, Atg8 and Atg12, are activated by a single E1 (Ichimura et al., 2000; Mizushima et al., 1998).

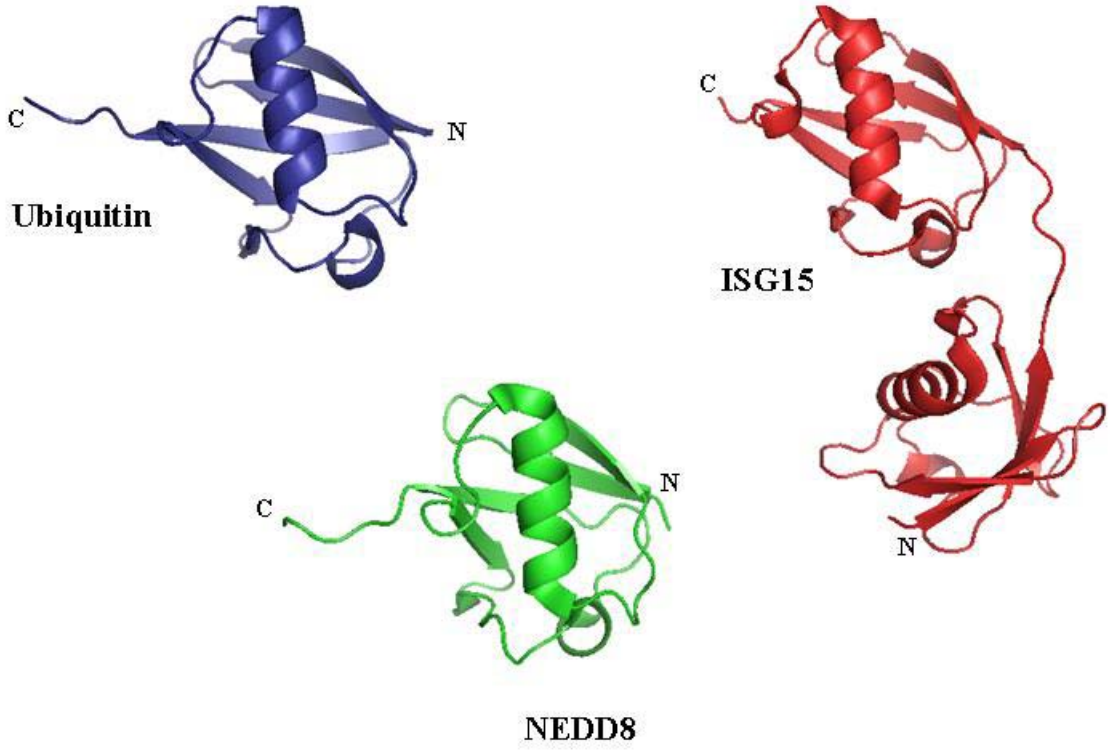

Figure 1.3: Ubiquitin-like proteins structurally resemble ubiquitin.

Nedd8 (green) and ISG15 (red) structurally resemble ubiquitin (blue). Structures created with Pymol using the PDB files 1Z2M, 2KO3, and 1UBQ.

1.2.1 Nedd8

Nedd8 (neural precursor cell expressed, developmentally down-regulated 8) is the most similar of all Ubls to Ub and is highly conserved in most eukaryotes. Model organisms such as *Schizosaccharomyces pombe*, *Caenorhabditis elegans*, *Drosophila*, *Arabidopsis*, and mouse require Neddylation for viability with the exception of *S. cervisiae* (Rabut and Peter, 2008). Analysis of mouse embryos deficient in Neddylation revealed an essential role for Nedd8 in cell cycle progression (Tateishi et al., 2001). The

primary targets of Nedd8 appear to be cullin-RING E3 Ub ligases (CRLs), although targets not related to CRLs exist as well (Jones et al., 2008). Nedd8 modification of the cullin subunit of CRLs induces a conformational change that activates the Ub E3 ligase (Duda et al., 2008). At the same time, this modification prevents the cullin inhibitor, CAND1, from binding CRLs. The fact that many substrates of CRLs are involved in cell cycle control corresponds with the role of Nedd8 in cell cycle progression.

Despite its similarity to Ub, there is no apparent cross-reactivity of Nedd8 with enzymes of the Ub system. The features of the Nedd8 E1 that confer specificity for Nedd8 have been identified. Nedd8 E1 specifically charges Nedd8 due to a unique Arg present in the Nedd8 E1 that repels Arg72 of Ub, but accepts Ala72 of Nedd8 (Souphron et al., 2008). The specificity of the Nedd8 E2 is dictated by its interaction with the E1 rather than Nedd8. The ubiquitin-fold domain of the Nedd8 E1 recruits the E2 through interactions with the E2 α1-helix and the β1-β2 loop (Huang et al., 2005). In addition, the Nedd8 E2 contains a unique N-terminal extension that interacts specifically with a unique groove in the adenylation domain of the Nedd8 E1 (Huang et al., 2004). The identity of a Nedd8 specific E3 enzyme is unclear. While Dcn1 has been reported to act as a scaffold-type E3 ligase for the modification of CRLs, the Nedd8 E2s have also been reported to interact directly with the RING domain of CRLs in order to mediate cullin Neddylation (Huang et al., 2009; Kurz et al., 2008).

1.2.2 SUMO

SUMO (small ubiquitin-related modifier) proteins share little amino-acid identity with Ub, but maintain a similar structure (Bayer et al., 1998). Organisms such as *S. cervisiae* and *C. elegans* have only one SUMO protein compared to the four found in humans. Like Nedd8, most organisms require SUMOylation for viability (Geiss-

Friedlander and Melchior, 2007). While SUMO is known to function in many cellular processes including DNA repair, RNA metabolism, and mitochondrial activity, SUMOylation is frequently associated with regulation of transcription. In addition, many of the SUMO target proteins identified to date are transcription factors (TFs). Interestingly, several studies found SUMOylated TFs were maximally repressed despite the fact that only a small fraction of the TF was modified (Hay, 2005). One model suggests this is a result of short-term modification: SUMOylation is required to recruit a repressor complex which, once bound, allows deSUMOylting enzymes to remove SUMO without altering the bound complex thus continuing repression.

A unique aspect of the SUMO pathway involves the recognition of target proteins. Ubc9, the E2 for SUMO, is capable of directly interacting with and modifying target proteins containing the consensus motif Φ-K-x-E/D (Φ is a hydrophobic, K is the lysine attached to SUMO, x is any amino acid, and E or D is an acidic residue) (Bernier-Villamor et al., 2002). While several E3 ligases exist for SUMO, reports suggest they function non-enzymatically to enhance SUMO conjugation or confer additional specificity in target recognition. For example, Siz/PIAS-RING (SP-RING) E3 ligases enhance and redirect SUMOylation via their PINIT domain. Structural and mutational analysis showed the PINIT domain of Siz1 is required to position a non-consensus lysine residue in PCNA for SUMOylation by Ubc9 (Yunus and Lima, 2009). SUMOylation of PCNA at this lysine residue has been proposed to inhibit recombination repair events (Papouli et al., 2005; Pfander et al., 2005).

1.2.3 Characteristics of ISG15

ISG15 was the first Ubl identified (Figure 1.4) (Farrell et al., 1979). ISG15 is a 17 kDa protein resembling two molecules of Ub connected by a linker of six amino acids

(Narasimhan et al., 2005). There are several unique features of ISG15 relative to other Ubls. First, and most importantly, ISG15 is transcriptionally induced by type I interferons (IFN-α/β) and is therefore conjugated to proteins only in the context of a viral or microbial infection. Second, ISG15 is found only in vertebrates. Third, ISG15 is not well conserved between species compared to Ub and other Ubls. Human ISG15 is only 65% identical to mouse ISG15, whereas Ub is 100% identical between human and mouse; mouse and rat ISG15 are 73% identical. Finally, ISG15 is the only Ubl where the last six residues of the protein (LRLRGG) are identical to that of Ub. These residues are important for $E1^{Ub}$ discrimination between Ub and other Ubls and the identity suggested potential overlap between the ISG15 and Ub pathways.

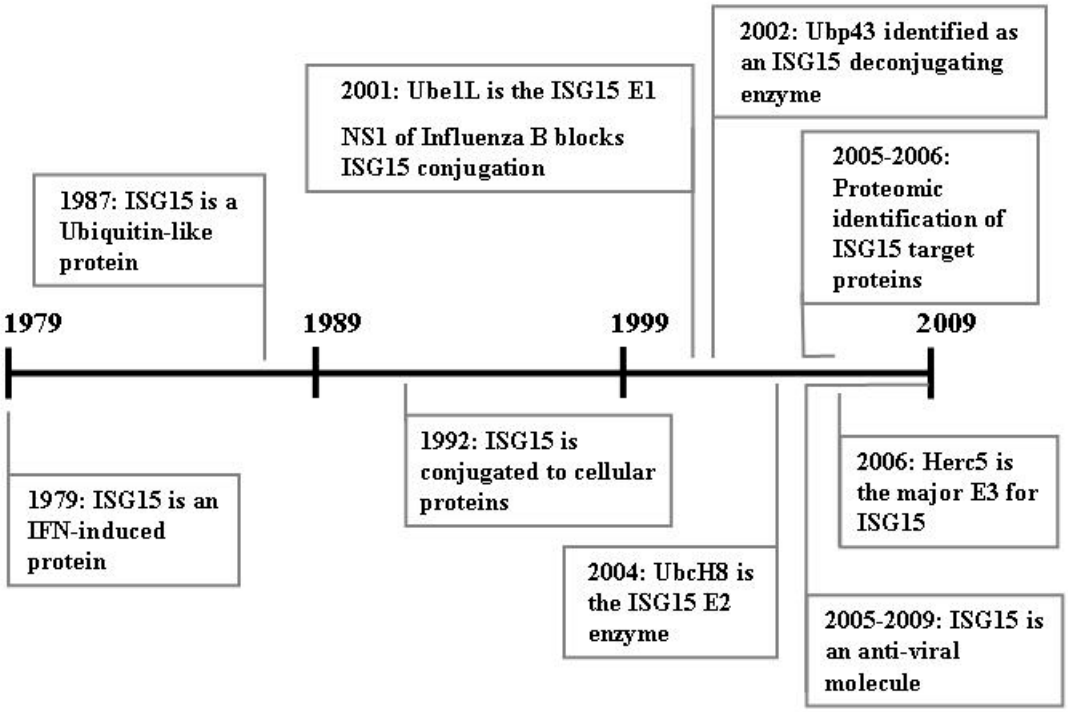

Figure 1.4: Timeline of important discoveries in the ISG15 field.

1.2.4 The ISG15 pathway enzymes

Although ISG15 was first identified as a Ubl in 1992, it was not until 2001 that the first enzyme involved in its conjugation was identified (Loeb and Haas, 1992; Yuan and Krug, 2001). Using ^{32}P-labeled ISG15 and IFN-treated A549 cell lysates, the Krug lab identified Ube1L as the ISG15 E1. Ube1L is the most similar human E1 enzyme compared to $E1^{Ub}$ (62% similar). Unlike other Ub/Ubl E1 enzymes, Ube1L is the only E1 transcriptionally induced by IFN-α/β (Kim et al., 2004; Yuan and Krug, 2001). Crystal structures of the E1s for Nedd8, SUMO, and Ub reveal three common domains: an adenylation domain, a catalytic-cysteine-containing domain, and a C-terminal Ub-fold domain (UFD). The UFD of E1s for Nedd8, SUMO, and Ub have been shown to be important in the recruitment of their respective E2s (Figure 1.5) (Huang et al., 2005; Lee and Schindelin, 2008; Lois and Lima, 2005). Based on structural propensities of residues conserved with Uba3, Ube1L is also predicted to contain a C-terminal UFD as well.

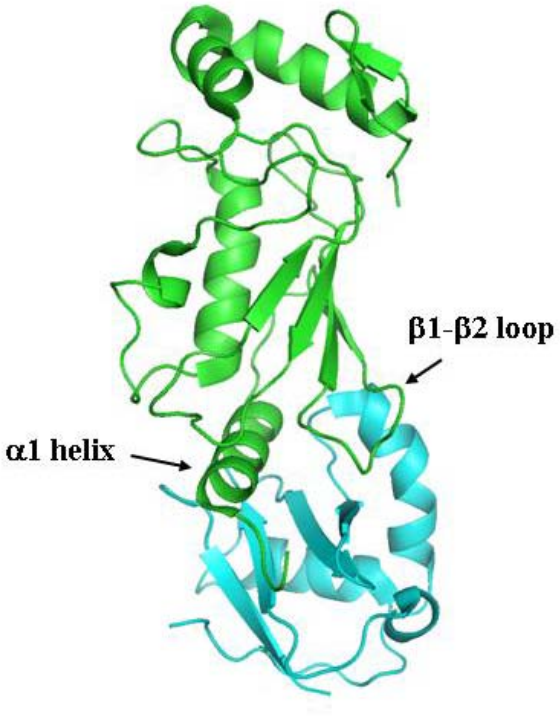

Figure 1.5: Crystal structure of the interaction of Nedd8's E2 ($Ubc12^{core}$) with the ubiquitin-fold domain of the Nedd8 E1 ($NE1^{UFD}$).

$NE1^{UFD}$ is in light blue while $Ubc12^{core}$ is in green. $NE1^{UFD}$ has two grooves: one holds the α1 helix and the other holds the β1-β2 loop of $Ubc12^{core}$. $Ubc12^{core}$ is missing a 26 residue N-terminal extension which interacts with a unique groove in the NE1 adenylation domain. Structure created with PyMol using the PDB file 1Y8X.

Following identification of Ube1L, the Krug and Huibregtse labs used recombinant purified ISG15 to isolate the ISG15 E2, UbcH8 from IFN-β-treated A549 cells (Zhao et al., 2004). A previous study had shown UbcH8 was transcriptionally induced by IFN-α (Nyman et al., 2000) and Zhao *et al*. confirmed UbcH8 mRNA induction following IFN-β treatment. UbcH8 had been reported in several cases to function in Ub conjugation pathways (Chin et al., 2002; Urano et al., 2002; Wheeler et al., 2002; Zhang et al., 2000). In addition, many studies reported UbcH8 to function in a

manner that was redundant with UbcH7 (Fortier and Kornbluth, 2006; Imai et al., 2000; Moynihan et al., 1999; Shimura et al., 2000), suggesting that UbcH8 might function in both the Ub and ISG15 conjugation systems. UbcH7 is the most closely related E2 (55% identity, 72% similarity to UbcH8) and recent phylogenetic analysis of E2 enzymes grouped UbcH7 and UbcH8 into their own family (Michelle et al., 2009). Despite the similarity, depletion of UbcH8 by siRNAs eliminated virtually all ISG15 conjugation in IFN-β-treated cells, whereas depletion of UbcH7 had no effect on ISG15 conjugation (Zhao et al., 2004). These results strongly suggested that UbcH8 is the only E2 enzyme for the ISG15 pathway, however given the functional redundancy of E2s in the Ub system it was difficult to unambiguously determine whether UbcH8 functions in Ub conjugation *in vivo*.

Herc5 was identified as the major E3 for ISG15 by the Huibregtse and Krug labs (Dastur et al., 2006). The enzymes for Ub/Ubl conjugation pathways often undergo auto-conjugation, a process in which the enzyme transfers Ub/Ubl to itself. As a result, these components are often identified in the process of identifying target proteins by mass spectrometry. Consistent with this, proteomic analysis to find ISG15 target proteins identified the ISG15 enzymes Ube1L and UbcH8 (Zhao et al., 2005). Interestingly, a single HECT E3 ligase, Herc5, was also identified. In addition, microarray analysis of IFN-β treated HeLa cells showed that like ISG15, Ube1L, and UbcH8, the expression of Herc5 is transcriptionally induced by IFN-β. These results suggested that Herc5 might be an E3 ligase for the ISG15 conjugation pathway. Dastur *et al.* showed that depletion of Herc5 by siRNA eliminated nearly all ISG15 conjugation to target proteins in IFN-β treated cells. Furthermore, ISGylation could be reconstituted by co-transfection of Ube1L, UbcH8, ISG15, and Herc5 in non-interferon treated cells.

The microarray analysis identified several other IFN-induced E3 ligases in addition to Herc5, including TRIM25 and Herc6 (Dastur et al., 2006). TRIM25 (Efp) is known to act as a Ub RING E3 ligase for 14-3-3σ, a negative regulator of the cell cycle. One report showed that TRIM25 could auto-conjugate with ISG15 (although not as well as with Ub), while another report stated TRIM25 could transfer ISG15 to 14-3-3σ.(Nakasato et al., 2006; Zou and Zhang, 2006) Our lab found that depletion of TRIM25 by siRNA had no effect on ISG15 conjugation, nor did the transfection of plasmids expressing E1, E2, ISG15, and TRIM25 reconstitute ISG15 conjugation (Dastur, 2007). Herc6, a HECT E3 ligase, is 50% identical to Herc5 and has a very similar domain organization. Similar to TRIM25, depletion of Herc6 by siRNA or addition of Herc6 by plasmid transfection had no effect on ISG15 conjugation (Dastur et al., 2006; Dastur, 2007). It is unclear what, if any, role exists for human Herc6 in ISG15 conjugation.

Interestingly, human Herc5 does not have a direct equivalent in mice or rats. However, the human Herc5 and Herc6 genes are adjacent to each other on chromosome 4 and are very likely related to each other through a gene duplication event (Hochrainer et al., 2005). As stated previously, both genes are transcriptionally regulated by interferon signaling and the human Herc5 and Herc6 proteins are 50% identical with very similar domain organizations. Mouse Herc6 is also interferon-induced and located at the corresponding genomic position as human Herc6. While it was proposed that Herc5 was the result of a gene duplication of Herc6 in the primate lineage, this is likely incorrect since other mammals (dogs, cows, sheep, monkeys) have both the Herc5 and Herc6 genes in a similar arrangement as in the human genome, suggesting that Herc5 was lost in the evolution of the rodent lineage. Although there is no evidence that human Herc6 plays a

significant role in ISG15 conjugation, it is conceivable that mouse Herc6 plays the equivalent role to human Herc5 in conjugation of mouse ISG15. In support of this hypothesis, Versteeg *et al.* found that ISGylation could be reconstituted by transfection of mUbe1L, mUbc8, mISG15, and mHerc6 (Versteeg et al., 2010). Conjugation was dependent on all four components as well as the active-site cysteine present in the HECT domain of mHerc6.

Deconjugating enzymes function in Ub precursor cleavage, recycling of Ub, editing of Ub chain topology, and rescuing of proteins from the proteasome. Like Ub, ISG15 is expressed as an inactive precursor and it must be cleaved to expose a Gly-Gly motif at the C-terminus. Unlike Ub, there is no evidence that ISGylated proteins are sent to the proteasome or that poly-ISG15 chains are formed. The first Ubl-specific protease (ULP) identified for ISG15 was Ubp43 (Usp18 in humans) (Malakhov et al., 2002). While Ubp43 is considered an ISG15 deconjugating enzyme, it is not required for precursor processing of ISG15, as ISG15 conjugates still accumulate in Ubp43 -/- mice. In addition, mice lacking Ubp43 have a severe phenotype characterized by hydrocephalus, premature death, and neurological symptoms that can not be rescued by the simultaneous knockout of ISG15 and Ubp43 (Knobeloch et al., 2005; Ritchie et al., 2002). These results suggest ISG15-independent or enzymatic-independent functions exist for Ubp43. To date, two enzymatic-independent functions have been found for Ubp43: 1) Ubp43 negatively regulates IFN-α/β signaling by competing with Janus activated kinase (JAK) for binding to IFNAR2 and 2) Ubp43 limits apoptosis in IFN-α-treated cells (Malakhova et al., 2006; Potu et al., 2010). Since Ubp43 is not required to process the inactive ISG15 precursor, other ULPs must exist for ISG15. Recently, a screen for ISG15 ULP's identified Usp2, Usp5, Usp13, and Usp14, in addition to Ubp43

(Catic et al., 2007). It is not known whether any of these newly identified ULPs can cleave the C-terminal region of the precursor ISG15 or remove ISG15 from target proteins.

1.2.5 The di-ubiquitin like structure of ISG15

Sequence alignment of Ub with the N-terminal and C-terminal domains shows 32% and 37% identity, respectively. The two ubiquitin-like domains are connected by a six residue linker and contact each other via van der Waals interactions between N-terminal histidine 39 and phenylalanine 41 and the C-terminal proline 136 and glycine 138 (Narasimhan et al., 2005). Mutation of either the N-terminal or C-terminal contact sites reduces conjugation *in vivo*, although the C-terminal mutations have a larger effect on conjugation (Appendix I). It is possible that the C-terminal contact sites have a function in addition to stabilization such as E1 activation. While the C-terminal domain of ISG15, including the terminal Gly-Gly motif, is clearly required for substrate conjugation, the role of the N-terminal domain is unclear. Chang *et al*. reported deletion of the N-terminal domain of ISG15 (ISG15-ΔN) did not inhibit activation by Ube1L or transfer to UbcH8 *in vitro*, but did impair overall conjugation when transfected with Ube1L and UbcH8 *in vivo* (Chang et al., 2008). In contrast, in our hands, overall conjugation did not appear to be decreased when ISG15-ΔN was co-transfected with Ube1L, UbcH8, and Herc5 (Appendix I). Conclusions regarding the contact site mutants or the N-terminal domain of ISG15 can not be made without careful kinetic analyses of these mutants at each step of conjugation. In this regard, it is important to note that while Ube1L and UbcH8 activation has been analyzed *in vitro*, conjugation of ISG15 target proteins has not been fully reconstituted.

1.2.6 Identification of ISG15 target proteins

More than 300 cellular proteins have been identified as target proteins by three proteomics studies (Giannakopoulos et al., 2005; Wong et al., 2006; Zhao et al., 2005). The first study, by the Krug and Huibregtse labs, identified 158 high-confidence target proteins. Zhao *et al.* expressed a double-tagged ISG15 protein (6XHis and FLAG N-terminal tags), along with Ube1L and UbcH8, in HeLa cells, and then treated the transfected cells with IFN-β. Extracts were prepared 24 hours before preparation for mass spectrometry. In a second study, Giannakopolous *et al*. identified ISG15 conjugates in interferon-treated human cells (U937 cells) and in mouse Ubp43-null MEFs using an antibody recognizing endogenously expressed ISG15. Mass spectrometry identified a total of 76 mouse and human proteins in the immunoprecipitates. Finally, Wong *et al*. identified 174 target proteins using stably expressed FLAG-ISG15 in A549 cells were treated with IFN-β for 48 hours. Together, these three studies identified 312 unique proteins as potential ISG15 target proteins.

The identification of ISG15 target proteins was highly anticipated, as it was hoped that this would provide valuable insight into the biologic function of ISG15. This, for example, was the case for identification of targets of Sumo, where target identification revealed a very high percentage of targets to be nuclear proteins involved in regulation of DNA- and RNA-related processes. Unfortunately, the identification of ISG15 target proteins was, at least initially, not particularly revealing. The targets were largely abundant constitutively expressed proteins, with the exception of approximately 15 targets that were themselves interferon-induced proteins. The interferon-induced targets included some of the better-characterized antiviral ISGs, including PKR, MxA, RIG-I, p56, and STAT1 (discussed further below). The constitutively expressed proteins

encompassed both cytoplasmic and nuclear proteins involved in a diverse array of cellular functions, including cytoskeletal organization, stress responses, translation, transcription, RNA splicing, and general metabolism. A prediction of the biological function for ISG15 could not be inferred from the diverse set of target proteins. Furthermore, the fraction of an ISGylated protein is often no more than 10-20% of the total pool of the target protein examined (Zhao et al., 2005). This low level of modification is an additional complication in predicting a function for ISG15.

1.2.7 Recognition of ISG15 target proteins

Ub E3 ligases function to transfer Ub to specific substrates, so it is no surprise that more than 600 human genes encoding putative Ub E3 ligases have been identified. Generally, the recognition of target proteins by E3 ligases is mediated through protein-protein interaction motifs found in both sets of proteins, but no common primary sequence motif has been identified in ISG15 target proteins. Herc HECT E3 ligases possess N-terminal regulator of chromosome condensation 1 (RCC1)-like domains (RLDs) known to mediate protein-protein interactions (Hadjebi et al., 2008). RCC repeats were first identified in the RCC1 protein, a guanine nucleotide exchange factor. RCC1 contains seven RCC repeats which form a seven-bladed β-propeller structure which binds Ran on one face and chromatin on the other. The RLD of Herc5 consists of three less conserved RCC repeats (residues 1-150) followed by four canonical RCC repeats between residues 151-350 (Hadjebi et al., 2008). Herc5 mutants lacking either the entire RLD or the first two RCC repeats cannot support target protein ISGylation however, both mutants are able to conjugate ISG15 to themselves (auto-conjugation). The role of the Herc5 RLD in target protein recognition will be discussed in more detail in Chapter 4.

1.2.8 The effects of ISGylation on target protein function

Only modest progress has been made on determining the functional implications of ISG15 conjugation. Currently, there are a number of cell-based approaches that can be used to generate ISGylated proteins and validate modification of individual proteins. However, it is important to note that an *in vitro* ISGylation system has not yet been established. Without such a system, it is not possible to easily generate purified ISGylated target proteins for biochemical analyses. There are two broad possibilities for the biochemical function of ISGylated target proteins: 1) ISG15 is a specific signaling molecule (in the manner that Ub signals to the proteasome), or 2) ISG15 non-specifically disrupts the function of its target proteins by physical occlusion or obstruction. There is little or no evidence in support of the first idea, however there are a few studies discussed below which provide support for the second idea. One major issue with these studies is only a very small fraction of the total pool of any target protein is modified with ISG15 and therefore, it is hard to imagine that overall protein function would be disrupted (discussed further in Chapter 6). The targets described below are Ubc13, PP2Cβ, and filamin B.

Ubc13 is a ubiquitin E2 enzyme that functions in the generation of K63-linked polyubiquitin chains. Two reports showed that Ubc13 is ISGylated at lysine residue K92, which lies near the active-site cysteine residue of the protein (C87) (Takeuchi and Yokosawa, 2005; Zou et al., 2005). Both studies showed that the ISGylated form of Ubc13 was defective for ubiquitin thioester formation. Given the proximity of the C87 to K92 in the structure, the inhibition of thioester formation is likely to be simply a result of steric occlusion of C87 by the conjugated ISG15 molecule. The downstream effects of this inhibition have been suggested to result in prevention of NF-κB activation, as K63-

linked polyubiquitination catalyzed by the Ubc13/Mms2 complex is a critical component of the signaling pathway that leads to NF-κB activation. NF-κB activation, in turn, is critical for transcriptional activation of genes involved in the innate immune response, including IFN-β. An unresolved problem with this proposed mechanism is that only a small fraction of Ubc13 is ISGylated, and it is not clear how this would lead to a significant inhibition of overall Ubc13 activity.

PP2Cβ is a protein phosphatase that dephosphorylates the TAK1 and IKK kinases, leading to inhibition of NF-κB signaling. Using a NFκB luciferase reporter assay, it was shown that ISGylation of PP2Cβ inhibited its activity and lead to a slight increase in luciferase activity (Takeuchi et al., 2006). Similar to Ubc13, only a small fraction of PP2Cβ is ISGylated and it is unknown what effect the resulting changes in NF-κB activation would have in the context of a viral infection.

Filamin B is one of three related actin binding proteins that are critical for crosslinking of cortical actin filaments. At early time points after interferon stimulation, filamin B tethers RAC1 and a MAP kinase module, which promotes activation of JNK and JNK-mediated apopotosis. The ISGylation of filamin B was shown to lead to release of RAC1, MEKK1, and MKK4 from the scaffold, preventing JNK activation (Jeon et al., 2008). A model was proposed whereby ISGylation of filamin B, at relatively late time points after interferon stimulation, leads to the eventual inactivation of JNK.

1.3 ISG15: ANTI-VIRAL PROTEIN.

1.3.1 The innate immune system

When cells are infected by bacteria or viruses, the innate immune system is first to detect pathogens using pattern recognition receptor proteins (PRRs) (Mogensen, 2009). PRRs can quickly detect pathogen-associated molecular patterns (PAMPs) present on

bacteria or viruses. Recognition of pathogens via PRRs triggers the recruitment of adaptor molecules and the activation of multiple signaling cascades involving NF-κβ, mitogen-activated protein kinases (MAPKs), and interferon-regulatory factors (IRFs). Ultimately, pro-inflammatory cytokines and type I interferons, also known as IFN-α and IFN-β (IFN–α/β), are produced (Figure 1.6). IFN-α/β is then secreted where it can bind IFN-α/β receptors on uninfected cells nearby, as well as the initially infected cell, resulting in transcription over a hundred of interferon stimulated genes (ISGs) and the formation of an anti-viral state in the uninfected cells (Figure 1.7). ISG15 (interferon-stimulated gene of 15 kDa) is one of the most strongly induced ISGs (Birmachu et al., 2007; Blomstrom et al., 1986; Der et al., 1998).

Virus recognition by PRRs

Toll-like receptors (TLRs) are the most extensively studied PRRs. TLRs are a family of membrane proteins which, upon recognition of PAMPs, dimerize and undergo conformational changes that allow them to recruit adaptor proteins such as MyD88 and/or TRIF to mediate signal transduction (Mogensen, 2009; Trinchieri and Sher, 2007). Viral glycoproteins are recognized by TLR2 and TLR4 on the cell surface, while viral RNA or DNA is recognized by TLRs localized at the endosome. Each of the endosomal TLRs is specific for a type of viral nucleic acid: TLR3 for dsRNA, TLR7/8 for ssRNA, and TLR9 for CpG DNA. Some cell types express only a subset of the TLRs described. For example, plasmacytoid dendritic cells (pDCs) express TLR7 and TLR9. With the exception of TLR2, the TLRs recognizing viruses trigger both pro-inflammatory cytokines and type I interferons. The MyD88-dependent pathway, utilized by all TLRs except TLR3, is responsible for the activation of NF-κβ and AP-1. Additionally, TLR7/8 and TLR9 trigger a MyD88-dependent pathway that leads to IRF7 activation. TRIF-

dependent signaling, used by TLR3 and TLR4, can mediate the activation of all four transcription factors: NF-κβ, AP-1, IRF3, and IRF7.

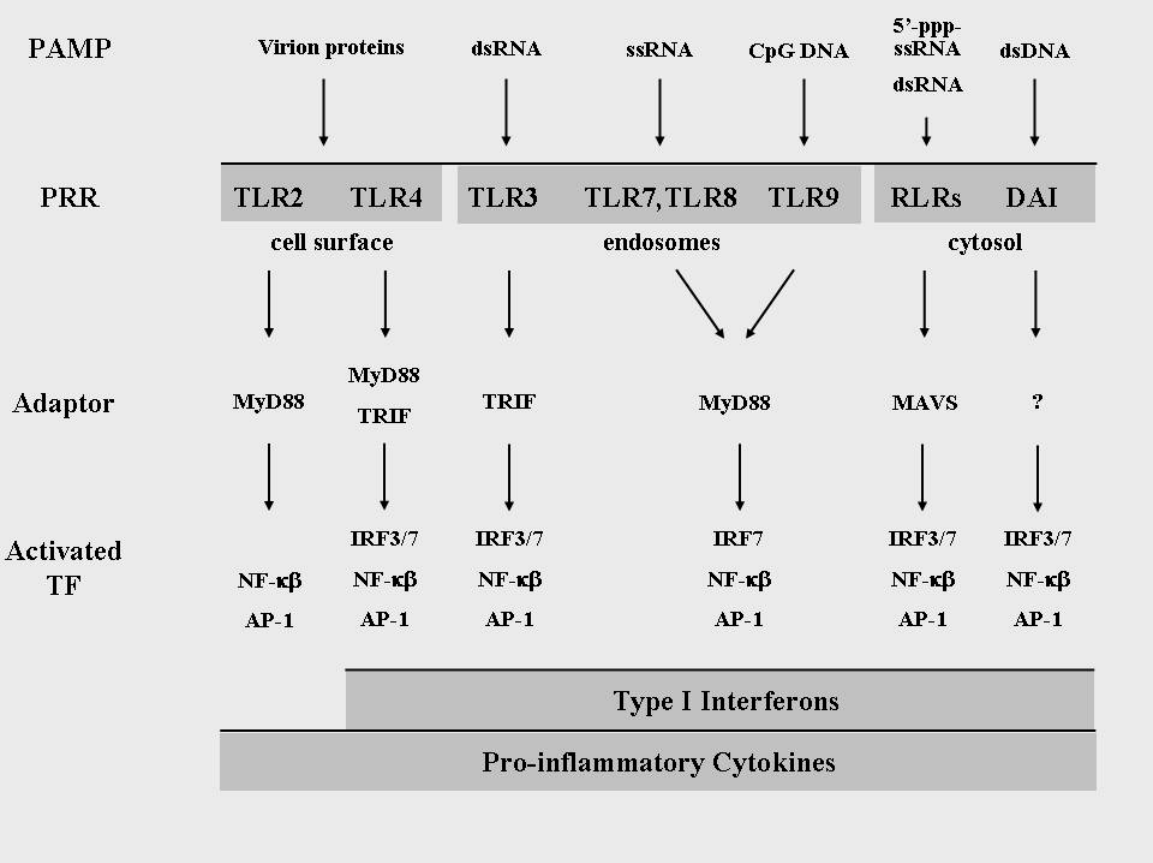

Figure 1.6: Activation of the innate immune response by viruses.

Pattern recognition receptor proteins (PRRs) are activated by viral pathogen-associated molecular patterns (PAMPs) leading to the induction of type I interferons and pro-inflammatory cytokines. Adapted from Gillet *et al.* 2008, Trinchieri and Sher 2007, and Fensterl and Sen 2009.

RIG-I like receptors (RLRs), including RIG-I (retinoic acid-inducible gene I), Mda5 (melanoma differentiation-associated gene 5), and LGP2 (laboratory of genetics and physiology 2), are characterized by a DExD/H-box RNA helicase domain and contain a C-terminal regulatory domain for RNA binding. While RLRs such as RIG-I and Mda5 possess CARD (caspase recruitment) domains to initiate downstream

signaling, LGP2 does not and a recent study suggests it assists RIG-I and Mda5 with viral RNA recognition rather than mediating a response on its own (Satoh et al.). RLRs sense specific viruses and appear to have preferential ligands: RIG-I recognizes short dsRNAs and 5' triphosphate RNA, while Mda5 recognizes long dsRNAs (Kato et al., 2008; Kato et al., 2006). Viral dsRNA is also recognized by protein kinase R (PKR) however, RLRs appear to be the major contributors to dsRNA-activated responses. Like the TLRs, activation of the RLRs and PKR by viral RNA ultimately leads to the production of cytokines and type I interferons. While it is clear that RLRs with CARD domains interact with the adaptor protein MAVS (also known as IPS-1, CARDIF, or VISA) to mediate these responses, it is unclear if PKR assists RIG-I and Mda5 like LGP2 or if it independently leads to induction of cytokines and type I interferons.

Cytosolic DNA can trigger type I interferons independently of TLR9 and studies have identified the cytoplasmic DNA sensors, DAI (DNA dependent activator of IRFs) and AIM2 (absent in melanoma 2) (Schroder et al., 2009; Takaoka et al., 2007). While AIM2 does not induce IFNs, results suggest DAI interacts with IRF3 to mediate IFN induction. Alternative sensors for pathogenic DNA recognition have been proposed as knockdown of DAI had little effect on IFN induction. Recently, a new mechanism for cytosolic DNA recognition has been identified. RNA polymerase III has been shown to transcribe dsDNA into dsRNA which is then capable of activating RIG-I (Ablasser et al., 2009; Chiu et al., 2009).

PRRs and type I interferons

As discussed above, recognition of pathogens via PRRs triggers multiple signaling cascades which result in the activation of the transcription factors NF-κβ, AP-1 (via MAPKs), interferon-regulator factor-3, and -7 (IRF3 and IRF7). NF-κβ regulates

the induction of pro-inflammatory cytokines with the help of AP-1, while IRF3 and IRF7 are the key regulators of the type I interferon response. IFN-α is only induced by homodimers of IRF7, but homodimers of IRF3 or heterodimers of IRF3 and IRF7 can induce IFN-β. IFN-β is most stably induced by a complex known as the enhanceosome. This complex is formed when IRF3 and/or IRF7 form a complex with AP-1, NF-κβ, and the co-activator CBP or p300 (Honda and Taniguchi, 2006).

The induction of type I interferons is biphasic and results in a positive feedback loop that strengthens the interferon response (Haller et al., 2006). During the early phase, IFN-β is induced and secreted in an autocrine and paracrine manner. This leads to the upregulation of IRF7 and results in the late phase induction of IFN-α and the continued production of IFN-β. Originally it was thought that the early phase induction of IFN-β was entirely dependent on homodimers of IRF3 because IRF3 is constitutively expressed, while IRF7 is expressed at very low levels (in all cells except for pDCs). However, both mice lacking IRF3 and mice lacking IRF7 showed very reduced levels of IFN-β indicating IRF7 plays a role in the early phase induction of IFN-β (Honda et al., 2005).

The anti-viral response of interferons

Interferons (IFNs) are secreted cytokines with anti-viral activity (Samuel, 2001). Type I IFNs include IFN α, β, ε, κ, and ω, however IFN α and β are the major members. Type I IFNs can be produced by all cell types and function to directly inhibit viral activity. IFN-γ is the sole member of Type II IFNs. It is primarily produced by T cells and NK cells and acts on macrophages to upregulate MHC molecules. The most recently discovered group of IFNs, Type III IFNs, are composed of three IFN-λ molecules (Ank and Paludan, 2009). Type III IFNs are induced by IRF3 and IRF7 and function similarly

to Type I IFNs, however they are limited to primarily to epithelial cells (Ank et al., 2008; Sommereyns et al., 2008).

Each type of interferon has its own heterodimeric receptor. IFNAR1/2 and IFNAG1/2 are the receptors for IFN-α/β and IFN-γ, respectively, and are ubiquitously expressed (Samuel, 2001). In contrast, The IFN-λ receptor is composed of IL-10Rβ and the cell-type specific IFNλR1 limiting this receptor to epithelial cells primarily (Ank and Paludan, 2009). Regardless of the type of interferon, the binding of the ligand to the receptor activates the JAK-STAT signaling pathway. Janus activated kinases (JAKS) are recruited to the receptor and activate themselves via autophosphorylation. In addition, JAKS phosphorylate the IFN receptor and members of the signal and activator of transcription (STAT) family of proteins. Phosphorylated STAT proteins dimerize and can form complexes with other proteins before translocation into the nucleus and binding of specific DNA sequences within the promoters of interferon stimulated genes (ISGs). Type II IFN induces a STAT1 homodimer which binds GAS (gamma activated sequences) elements of IFN-γ target genes. Type I IFN induces the formation of a complex known as the interferon stimulated gene factor 3 complex (ISGF3). This complex is composed of a STAT1/STAT2 heterodimer bound to IRF9. IFN-α/β inducible genes are transcribed following the binding of ISGF3 to promoters containing interferon stimulated response elements (ISREs).

Mice lacking the IFN-α/β receptor are susceptible to numerous viruses indicating the requirement of IFN-α/β and the transcription of ISGs for an effective response against viral infection (Muller et al., 1994; Ryman et al., 2000). These hundreds of ISGs are able to mount an anti-viral response via many different mechanisms. For example, MxA is known to accumulate at the ER membrane where it can detect and trap viral

nucleocapsid-like structures (Haller et al., 2007). Cellular and viral translation is inhibited through the action of several different proteins: activated PKR phosphorylates EIF2α (Dar et al., 2005), while human p56 and p54 inhibit translation through the binding of eIF3 (Terenzi et al., 2006). The 2'-5' OAS-RNaseL pathway functions to degrade viral RNA (Hovanessian and Justesen, 2007). Viral dsRNA activates 2'-5' OAS which in turn activates RNaseL. The RNA degraded by RNaseL can also activate the RLRs RIG-I and Mda5 (Malathi et al., 2007). ISG15 is a highly induced ISG, however the mechanism behind its role in the anti-viral response is unclear and will be discussed in more detail in Chapter 5.

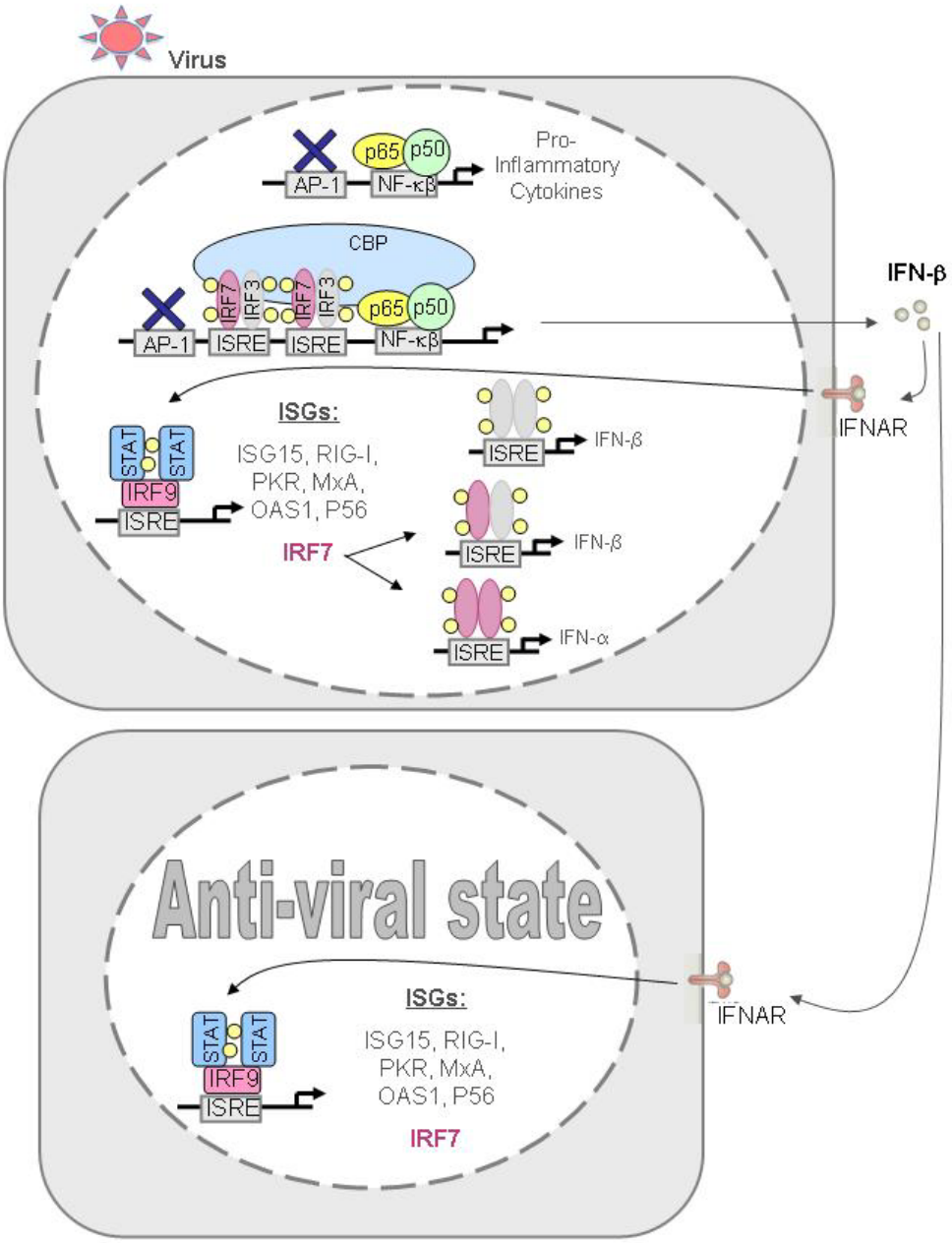

Figure 1.7: Innate immune response to viruses

Viral recognition by the innate immune system results in the production of pro-inflammatory cytokines and a biphasic induction of type I interferons. During the early phase, IFN-β is induced and secreted where it can then bind to the initially infected cell as well as neighboring cells. This leads to the upregulation of IRF7 and results in the late phase induction of IFN-α, continued production of IFN-β, and induction of interferon stimulated genes (ISGs).

1.3.2 Anti-viral function of ISG15

Support for an antiviral function for ISG15 was first reported in 2001 when it was found that the influenza B virus NS1 protein bound ISG15 thereby blocking the conjugation of ISG15 to cellular proteins (Yuan and Krug, 2001). Since then, many studies have examined ISG15 and influenza virus. In 2007, mice lacking ISG15 were found to be more susceptible to both influenza A and B (Lenschow et al., 2007). Recent studies using Ube1L-null mice showed that the anti-viral effect of ISG15 against influenza B was a result of conjugated ISG15 rather than free ISG15 (Lai et al., 2009). Using human cell lines, Hsiang *et al* showed that ISG15 conjugation in human cells inhibited influenza A gene expression which resulted in virus replication inhibition (Hsiang et al., 2009). Furthermore, inhibition of influenza A viral replication has been shown to be mediated by ISGylation of the viral protein, NS1 (Zhao et al., 2009). The mechanism by which ISG15 conjugation inhibits influenza B replication is still unclear. A new study on NS1 of influenza B demonstrated that NS1B binds and sequesters human ISG15, but not mouse ISG15, in nuclear speckles (Sridharan et al., 2010). This result may explain why mice infected with either mouse-adapted or non-mouse adapted versions of influenza B virus are sensitive to mouse ISG15 conjugation.

ISG15 has also been reported to have antiviral effects against Sindbis, Vaccinia (VACV), Herpes Simplex I (HSV-1), murine γ-Herpesvirus 68 (γHV68), human immunodeficiency virus 1 (HIV-1), avian sarcoma leukosis virus (ASLV), and Ebola virus (Harty et al., 2009). The first study using ISG15-null mice determined no difference in survival rate when infected with VSV (vesicular stomatitis virus) or LCMV (lymphocytic choriomeningitis virus) (Osiak et al., 2005). A subsequent study found mice lacking ISG15 have increased susceptibility to influenza A and B, HSV-1, γHV68,

and Sindbis virus infection (Lenschow et al., 2007). In addition, the anti-viral effect of ISG15 against Sindbis virus was also shown to be dependent on the conjugation of ISG15 (Giannakopoulos et al., 2009; Lenschow et al., 2005).

In the case of HIV-1, Ebola, and ASLV, expression of ISG15 has been shown to inhibit virus-like particle (VLP) release. Two separate studies demonstrated ISG15 inhibition of Nedd4, a Ubiquitin E3 ligase, decreased VP40 ubiquitination and Ebola VLP release (Malakhova and Zhang, 2008; Okumura et al., 2008). Similarly, ISG15 was proposed to inhibit the release of HIV-1 VLPs by inhibiting the ubiquitination of HIV-1 Gag and Tsg101, an ESCRT I protein required for efficient HIV-1 budding (Okumura et al., 2006). A recent study on HIV-1 and ASLV VLP release suggested an additional mechanism exists at the last step of budding (Pincetic et al., 2010). Pincetic *et al* found that Vps4, an ATPase which releases ESCRT complexes at the last step of budding, was unable to associate with HIV-1 or ASLV budding complexes in the presence of ISG15. ISGylation of CHMP5, an ESCRT III protein, was proposed to be ultimately responsible for the loss of Vps4 during the last stage of virus release. Together these studies indicate possible conjugation-independent and –dependent functions for ISG15 inhibition of VLP budding.

In addition to Influenza B, other viruses have also evolved mechanisms for interfering with ISG15 conjugation. SARS coronavirus and human coronavirus NL63 both encode proteases (PLpro and PLP2, respectively) that can deconjugate ISG15 from target proteins (Clementz et al., 2010; Lindner et al., 2007). Vaccinia virus encodes a viral early protein, E3, which binds ISG15 and prevents its anti-viral activity (Guerra et al., 2008). ISG15 can also be deconjugated by ovarian tumor (OTU) domain-containing proteases encoded by both nairoviruses and arteriviruses (Frias-Staheli et al., 2007).

1.4 GOALS OF MY DOCTORAL WORK

The goals of my doctoral work have been two-fold: 1), to understand the specificity of the Ube1L-UbcH8 interaction and 2), to understand the basis of substrate recognition by Herc5. In 2005, Ube1L, the most closely related E1 to Uba1, and UbcH8, a previously reported Ub E2, had been identified as the E1 and E2 for ISG15. Other Ubl pathways had dedicated E1 and E2 enzymes, so the discovery of UbcH8 represented a potential point of convergence between the ISG15 and Ub pathways. In addition, it was unclear how Ube1L discriminated between UbcH8 and other closely related Ub E2 enzymes. At the same time, hundreds of cellular proteins were reported to be targets for ISG15 conjugation, while only one major E3 ligase, Herc5, had been identified.

The first part of my dissertation work focused on the specific interactions between Ube1L and UbcH8 that allow Ube1L to discriminate between UbcH8 and closely related Ub E2s such as UbcH7. Using kinetic analyses, I determined a strong preference of Ube1L for UbcH8 compared to UbcH7 and of Ube1 ($E1^{Ub}$) for UbcH7 compared to UbcH8. I then demonstrated the basis of this preference was a result of specific interactions between the ubiquitin-fold domain (UFD) of Ube1L and the amino-terminal α1-helix and β1–β2 region within UbcH8. I also examined the interferon-induced and transfected expression levels of UbcH8, and combined with the kinetic constants, determined that UbcH8 is unlikely to function as a Ub E2 in most cell lines. The second part of my dissertation work focused on the recognition of substrates by Herc5. I discovered the list of target proteins that Herc5 ISGylates extends beyond the proteins identified by the proteomics and includes many exogenously expressed foreign proteins. In addition, I found that ISG15 conjugation is restricted to newly synthesized pools of proteins and that Herc5 is physically associated with polyribosomes. These results led to

a model for ISGylation in which Herc5 broadly modifies newly synthesized proteins in a co-translational manner. In a third part of my work I focused on how ISG15 modification of newly synthesized proteins might mediate an anti-viral effect. In the context of a viral infection, newly translated viral proteins may be the targets of ISGylation. I demonstrated that ISGylation of human papillomavirus (HPV) L1 capsid protein has a dominant-negative effect on the infectivity of HPV16 pseudoviruses. This effect may not be restricted to capsid proteins; low-level ISGylation of any viral protein that multimerizes might have a dominant-negative effect on production of infectious virus. These discoveries have greatly increased our understanding of the mechanism of ISG15 pathway and provide a framework for establishing an *in vitro* ISG15 conjugation system and further examination of the anti-viral function of ISG15.

.

Chapter 2: Methods and Materials

2.1 Materials and Methods for Chapter 3

Plasmids and Mutagenesis. Plasmids containing Ube1L, UbcH8, Herc5, and ISG15 were described previously. Additional pcDNA3 (Invitrogen)-based ISG15 plasmids were made encoding either the HA (YPYDVPDYA) epitope at the N terminus of ISG15 or cloning ISG15 into the pcMV10 vector, which introduces a N-terminal 3X-FLAG epitope (Sigma). The HA epitope was also added to the N terminus of the pcDNA3-Ube1L and pcDNA3-Ube1LΔUFD plasmids. UbcH8 was introduced into the pcMV14 vector which contains a C-terminal 3X-FLAG epitope (Sigma). All E2s (chimeric and wild type), Ube1L^{UFD}, Ube1LΔUFD, and Ube1L-UFD^{Ub} expression plasmids were constructed by standard PCR ligation methods using pcDNA3 and pFastBac (Invitrogen) as vectors. Sequences of all constructs were verified by DNA sequencing.

Protein expression and purification. Recombinant baculoviruses were generated using the Bac-to-Bac Baculovirus Expression System (Invitrogen) for the following: wild-type Ube1L and all Ube1L derivatives, UbcH7, UbcH8, and all chimeric E2 proteins. All proteins were expressed as GST fusion proteins in High Five insect cells. Insect cells were collected 48-72 hours post-infection, and lysed in buffer containing 1% NP-40, 100 mM Tris, pH 7.9, 100 mM NaCl, 1 mM DTT, 100 μM phenylmethylsulfonyl fluoride, 4 μM leupeptin, 0.3 μM aprotinin. Proteins were affinity purified using GST-Bind Resin (Novagen). Ub and ISG15 were expressed as GST fusion proteins using the pGEX6p-1 vector (GE Healthcare) in *Escherichia coli* strain BL21 with an added cAMP-dependent kinase recognition motif (RRASV). Cells were

collected and resuspended in 1X PBS containing 1% Triton and lysed by sonication. Ub and ISG15 were purified on GST-Bind Resin and resuspended in 50 μl of kinase buffer (40 mM TRIS pH 7.5 and 20 mM MgOAc). The proteins were labeled by adding 2 μl of adenosine 5' triphosphate [γ–^{32}P] (Perkin Elmer) and 2 μl of cAMP-dependent protein kinase (Promega), and the reaction mixtures were rotated at room temperature for one hour. Unincorporated label was removed by washing the beads in kinase buffer. GST fusion proteins on beads were subjected to site-specific cleavage with PreScission protease (GE Healthcare) to remove GST. All proteins, with the exception of DEAE-purified E1^{Ub}, were subjected to SDS-PAGE followed by staining with Coomassie blue G250 and quantified relative to BSA standards using a near-infrared fluorescence scanner (Odyssey, Li-Cor Biosciences). Ube1L and E1^{Ub} enzymes used in K_m assays were purchased from Boston Biochem. E1^{Ub} used in all other assays was expressed using a recombinant baculovirus in High Five insect cells (Invitrogen) and partially purified on DEAE-Sepharose as described previously.

Biochemical Assays. All thioester assays were carried out in reactions containing 25 mM Tris (pH 7.5), 50 mM NaCl, 10 mM $MgCl_2$, 5 mM ATP, 0.1 mM DTT, and 2.25 μM ^{32}P-labeled ISG15 (~9 X 10^9 cpm/μmol) or 2.7 μM ^{32}P-labeled ubiquitin (~4 X 10^9 cpm/μmol). All reactions were initiated with the addition of [^{32}P]Ub/[^{32}P]ISG15, incubated at room temperature, terminated with SDS-PAGE loading buffer lacking DTT, and analyzed by SDS-PAGE and autoradiography or by Bio-Rad Phosphorimager with Quantity One Software. E1^{Ub}/Ube1L activity was determined in a similar manner using excess E1^{Ub}/Ube1L and minimal UbcH7/UbcH8. All concentrations listed are of active enzyme. Except where indicated, all thioester assays used 0.5 μM wild type and chimeric E2s. Assays in Fig. 3.2 were incubated for 5 or 75 min and contained 0.5 μl DEAE-

purified $E1^{Ub}$/13.2 nM Ube1L. Assays in Figure 3.4 contained 0.5 μl DEAE-purified $E1^{Ub}$ or 4.8 nM Ube1L and ISG15 samples were incubated 4 minutes, while Ub samples were incubated for both 1 and 10 minutes. The reactions in Figure 3.5*A* contained 4.4 nM Ube1L or Ube1LΔUFD and were incubated for 10 minutes, while the reactions in Figure 3.5D contained 4.4 nM Ube1L/Ube1L-UFD^{Ub} and were incubated for 5 minutes and 30 minutes, respectively. For the $Ube1L^{UFD}$ competition assay (Figure 3.5C), 0.5 μM UbcH8 was incubated with 0, 1, 2, or 4 μM $Ube1L^{UFD}$ for 3 minutes. A reaction mix containing 4.4 nM Ube1L, 25 mM Tris (pH 7.5), 50 mM NaCl, 10 mM $MgCl_2$, 5 mM ATP, 0.1 mM DTT, and 2.25 μM [^{32}P]ISG15 was added to each of the UbcH8 reactions for 4 minutes before the reaction was terminated. For the K_m and k_{cat} values in Table 3.1, initial velocity conditions were determined for each E2 so that the E1 concentration and incubation time resulted in linear product formation, where less than 10% of the E2 was converted to E2~Ubl. Preliminary K_m assays using 0.23 nM $E1^{Ub}$/3.4 nM Ube1L, and the proper incubation time were performed to determine the appropriate range of E2 concentrations for each wild-type or chimeric E2 protein. A minimum of three K_m assays were performed and known amounts of [^{32}P]Ub or [^{32}P]ISG15 were included to convert counts to a concentration value. After quantitation using the Bio-Rad Phosphorimager and Quantity One software, kinetic constants were determined using nonlinear regression of Michaelis-Menten plots with Graphpad Prism software. All kinetic constants reported include the standard error.

Transfection Assays. Human HeLa and HEK293 cells were grown in Dulbecco's modified Eagle's medium supplemented with 10% fetal bovine serum. Plasmid DNA transfections were performed with cells at 80% confluence using Lipofectamine transfection reagent (Invitrogen). For the experiment shown in Figure

3.5B, plasmids expressing Herc5 (0.5 μg), 3X-FLAG ISG15 (0.5 μg), and UbcH8 (0.25 μg) were transfected with HA-Ube1L, HA-Ube1LΔUFD (0.25 μg), or no E1. Cells were harvested and lysed 48 hours post-transfection or post-IFN-β treatment in lysis buffer containing 1% Nonidet P-40, 100 mM Tris, pH 7.9, 100 mM NaCl, 1 mM DTT, 100 μM phenylmethylsulfonyl fluoride, 4 μM leupeptin, 0.3 μM aprotinin. 30 μg of total cell proteins were separated by SDS-PAGE, transferred to nitrocellulose membrane, and probed with anti-FLAG antibody (Sigma) to detect ISG15-conjugated proteins and anti-HA antibody (Covance) to detect E1 expression.

UbcH8 expression levels in HeLa cells. For Figure 3.6, UbcH8 levels were determined by immuoblotting of 30 mg whole cell extracts of untreated HeLa cells (lane 2), HeLa cells treated with 1000 units/ml of interferon-β (Berlex) for 48 hours (lane 1), or HeLa cells transfected with a 0.25 mg UbcH8 expression plasmid (pCMV-3X-FLAG-UbcH8). UbcH8 was detected with anti-UbcH8 followed by IRDye 800 goat anti-rabbit secondary (Licor Biosciences). The membrane was scanned using the Odyssey system (Licor Biosciences) and signal intensities were quantitated with Quantity One software (Biorad). Transfection efficiency (33%) was determined by analysis of cells transfected with a GFP reporter plasmid.

2.2 MATERIALS AND METHODS FOR CHAPTER 4

Antibodies, Plasmids, and siRNAs. All antibodies and target plasmids used in this study are listed in Tables 2.1 and 2.2, respectively. Table 2.3 lists the ISG15 pathway related plasmids used in this study. The IQGAP1 SMARTpool siRNA was supplied by Dharmacon. Additional siRNA sequences: p53, 5'-GACTCCAGTGGTAATCTACTT-3' and hTfr, 5'-AAGGTGTAGTGGAAGTATC-3'.

Cell Culture, IFN-β Treatment, Transfections, and Immunoblotting. Maintenance, transfection, harvest, and immunoblotting of HeLa and 293T cells were as described in section 2.1. ISG15 conjugation was induced by treating HeLa cells with 1000 units/mL IFN-β (Betaseron) for either 24 or 48 hours. For the experiment shown in Figure 4.9, Lipofectamine 2000 (Invitrogen) was used in the initial transfection, while XtremeGENE siRNA Transfection Reagent (Roche) was used for the co-transfection of DNA and siRNA.

^{35}S-Labeling and Puromycin Labeling Experiments. HEK293T cells in 35 mm dishes were transfected with the indicated plasmids, as described above, and labeled for two hours with 80μCi of ^{35}S-cysteine (1000 Ci/mmole). The FLAG-ISG15 construct used in this experiment contained the C78S mutation, eliminating the only cysteine residue in ISG15. The C78S mutant is fully functional for conjugation, and the use of this mutant ensured that the ^{35}S-cysteine-containing proteins detected in the immunoprecipitation represented labeled cellular proteins that had been conjugated to unlabeled ISG15, as opposed to unlabeled proteins being conjugated to ^{35}S-labeled ISG15. Similarly, the ΔN-ISG15 construct lacked C78. Cells were washed w/ PBS and either harvested immediately (late labeling period) or replenished with fresh media. Cell lysates were collected and immunoprecipiations were performed with anti-FLAG M2 agarose beads (Sigma). Immunoprecipitates were separated by SDS-PAGE and labeled proteins were detected by autoradiography. For puromycin experiments, cells were transfected with the indicated plasmids and treated, 24 hours post-transfection, with puromycin (1 mM final concentration) for 2 minutes. Total cell extracts were prepared and FLAG-ISG15 conjugates were precipitated with anti-FLAG M2 agarose beads

(Sigma). The immunoprecipitates were then analyzed by immunoblotting with an antibody recognizing puromycin.

Sucrose Gradient Fractionation. HEK293T or HeLa cells were harvested 24 hours after transfection or IFN-β stimulation, as described, with the exception that heparin (200 μg/ml) was added to the polysome lysis buffer and RNasin was omitted. Lysates were centrifuged for 10 min at 16,300 x *g* at 4°C, and supernatants were loaded onto linear 7-47% (w/v) sucrose gradients containing cycloheximide (200 μg/ml). For EDTA treatment, cells were lysed in polysome lysis buffer containing 50 mM EDTA ($MgCl_2$ and heparin omitted) before applying to a linear 10-30% (w/v) sucrose gradient (supplemented with 10 mM EDTA instead of $MgCl_2$). For the RNase treatement, RNase (Sigma) was added to the lysate (heparin omitted) at a final concentration of 10 μg/ml and incubated at 30°C for 15 minutes before applying to a linear 7-47% (w/v) sucrose gradient. Gradients were centrifuged at 222,000 x *g* for 90 min (180 min for EDTA samples) at 4°C in a Beckmann SW41Ti rotor. Polysome profiles were monitored by absorbance at 254 nm and gradient fractions were collected on an ISCO density gradient fractionator. Trichloroacetic acid (TCA) was added to each sucrose-gradient fraction to a final concentration of 10 % (v/v) for protein precipitation. Precipitated proteins were then prepared for SDS-PAGE and immunoblotting analyses.

2.3 Materials and Methods for Chapter 5

Transfections. 293TT cells and the plasmid p16shell expressing HPV16 L1 and L2 were provided by John Schiller (NCI, Bethesda, MD). 293TT cells are a 293T cell line stably transfected with an expression plasmid encoding a cDNA for large T antigen. These cells were maintained as previously described. 293TT cells were ~80% confluent at the time of transfection with Lipofectamine 2000 at a DNA (μg) to reagent ratio of 1:2.

For Figure 5.1, 293TT cells were transfected with plasmids expressing p16shell (0.5 μg) alone or with plasmids expressing Ube1L (0.25 μg), UbcH8 (0.25 μg), HA-Herc5 (0.5 μg), and 3X-FLAG ISG15 (0.5 μg), or this set of plasmids without ISG15 (see also Table 2.4). Cells were harvested and lysed 48 hours post-transfection as previously mentioned in section 2.1. Total extracts were probed with anti-HPV16 L1 antibody (Santa Cruz Biotechnology) followed by IRDye 800 goat anti-rabbit secondary (Licor Biosciences). The membrane was scanned using the Odyssey system (Licor Biosciences) to detect L1-conjugated proteins.

Mass Spectrometry. 293TT cells were co-transfected with p16shell and the ISGylation components as described above. HPV16 L1-ISG15 conjugates were immunoprecipitated with anti-HPV16 L1 antibody, followed by electrophoresis on a 8% SDS polyacrylamide gel. The purified protein band was analyzed by mass spectrometry at the Taplin Biological Mass Spectrometry Facility.

HPV Pseudovirus Production and Infectivity Assays. 293TT cells (in 100mm dishes) were co-transfected with p16shell (5 μg), pcVM10-GFP (3 μg), HA-ISG15 (3 μg), and either Ube1L (1.5 μg), UbcH8 (1.5 μg), and Herc5 (3 μg) or the inactive mutant enzyme forms: Ube1L-ΔUFD (1.5 μg), UbcH8 F62A (1.5 μg), and Herc5 C994A (3 μg). After 48 hours, 293TT cells were collected and pseudovirus was purified according to the previously described protocols. The lysate was applied to the Optiprep (Sigma) gradients and subjected to ultracentrifugation. Fractions were collected and peak L1 content was determined via SDS-PAGE and immunoblotting for HPV16 L1. Relative amounts of L1 (ISGylated and non-ISGylated) were determined using a fluorescent secondary antibody and the Odyssey system (LiCor). L1 protein concentration was determined by quantitation with BSA standards on colloidal Coomassie-stained SDS–PAGE gels using

the Odyssey system as well. For the infection assay, 293T cells were grown in 12 well plates and infected with equal amounts of PsV-containing-fractions. Sixty hours post-infection, cells were trypsinized and subjected to FACS analysis using a FACSCalibur machine (Becton Dickinson). CellQuest Pro v5.2.1 (Becton Dickinson) was used for data acquisition and analysis of 10,000 live cell events.

Transmission electron microscopy (TEM). TEM analysis of purified HPV16 PsV was performed on carbon-coated copper grids stained with 1% uranyl acetate using a FEI Tecnai Transmission Electron Microscope (TEM). Image acquired by Dwight Romanovicz.

ANTIBODIES	DESCRIPTION
Anti-Hsc70	Santa Cruz Technologies
Anti-IQGAP1	BD Biosciences
Anti-Ube1	Abcam
Anti-Moesin	Cell Signaling Technology
Anti-Flag M2	Sigma Aldrich
Anti-V5	AbD Serotec
Anti-HA	Covance
Anti-C-Myc	Covance
Anti-TAP (Peroxidase-anti-peroxidase)	Rockland Immunochemicals for Research
Anti-p56	Kindly provided by Ganes Sen (Cleveland Clinic, Cleveland, OH)
Anti-Herc4	Novus Biologicals
Anti-Herc5	Kindly provided by Enzo Life Sciences
Anti-Puromycin	Kindly provided by Peter Walter (UCSF, San Francisco, CA)
Anti-E6AP	Prepared as described (Talis et al., 1998)

Table 2.1: Antibodies used in Chapters 4 and 5.

PLASMID	DESCRIPTION
pc3XFLAG-ISG15 & pcHA-ISG15	Previously described (Zhao et al., 2005)
pcFLAG-ISG15 & pcFLAG-ΔN-ISG15	Plasmids were made by introducing a sequence encoding an N-terminal FLAG epitope (DYKDDDDK) into a pcDNA3.1 plasmid containing either full length human ISG15 or residues 80-158 of ISG15 (ΔN)
pcDNA Ube1L	Previously described (Zhao et al., 2005)
pcDNA Ube1LΔUFD	Previously described (Durfee et al., 2008)
pcDNA UbcH8	Previously described (Zhao et al., 2005)
pcDNA UbcH8 F62A	Previously described (Dastur et al., 2006)
pCS2+MT (Myc)-Herc5	M. Ohtsubo of Hiroshima University
pcTAP Herc5 pcTAP Herc5 C994A	Previously described (Dastur et al., 2006)
pcHA-Herc5, pcHA-Herc5ΔRCC, and pcHA-Δ100	Herc5, Herc5ΔRCC, and Herc5Δ100 were subcloned from the pcTAP vector into the pcHA vector (Dastur et al., 2006)
pcTAP IQGAP1, A, B, C	The cDNA of IQGAP1 was previously described (Ho et al., 1999).
pcMV10 IQGAP1	Same as above, but IQGAP1 was cloned into the pcMV10 vector.
pcTAP Ube1	Ube1 was previously described (Beaudenon and Huibregtse, 2005; Huibregtse et al., 1995), and was subcloned into the pcTAP vector.
pcV5 Ube1	Same as above, but Ube1 was cloned into the pcV5 vector.
pcHA Ube1	Same as above, but Ube1 was cloned into the pcHA vector.
pcV5 Moesin	Previously described (Zhao et al., 2005)
pcV5 TrxR1	Previously described (Zhao et al., 2005)
pcV5 Ran	Previously described (Zhao et al., 2005)
pcFLAG Cofilin	Cofilin cDNA was cloned into the pcFLAG vector.
pcTAP Hsc70	pcTAP Hsc70 was provided by R. Krug.
pcMyc Hsc70	pcMyc Hsc70 was provided by Dr. D. Manor.
pcTAP p56	His-3X FLAG-p56 was provided by Dr. Robert Krug (UT Austin, Austin, TX), and was subcloned into the pcTAP vector.
pcTAP MxA, A, B	pcTAP MxA was provided by Dr. Robert Krug (UT Austin,

	Austin, TX), and was used to generate the TAP fusion proteins A and B.
pcMV10 MxA	Same as above, but MxA was cloned into the pcMV10 vector.
pcTAP	Previously described (Dastur et al., 2006)
pcTAP E6AP (C-A mutant)	The cDNA of E6AP C-A mutant was previously described (Huibregtse et al., 1995), and was subcloned into the pcTAP vector.
pcHA p53	The cDNA of p53 was previously described (Huibregtse et al., 1991), and was subcloned into the pcHA vector.
pcTAP p53	Same as above, but p53 was subcloned into the pcTAP vector.
pcHA β-Gal	β-Gal was amplified from pSVβgal (Promega) and cloned into the pcHA vector.
pcTAP Herc6 (C-A mutant)	Herc6 was amplified from cDNA, cloned into the pcTAP vector, and the active site cysteine mutated (C985A).
pcTAP p56	His-3X FLAG-p56 was provided by Dr. Robert Krug (UT Austin, Austin, TX), and was subcloned into the pcTAP vector.
pcTAP HIV Integrase	HIV-1 Integrase cDNA was subcloned into the pcTAP vector.
pcTAP SopA	The cDNA of SopA was subcloned from a plasmid provided by J. Chen (Purdue University) into the pcTAP vector.
p16shell, p18shell	Provided by John Schiller (NCI, Bethesda, MD)
pcV5-HPV18L1	HPV18 L1 ORF was cloned into the pcV5 vector
pcTAP OSPG	OSPG was amplified from Shigella genomic DNA provided by S. Payne, and cloned into the pcTAP vector.
pcFLAG Dlg	Dlg cDNA (Lee et al., 1997), and was cloned into pcFLAG vector.
pcMV10 GFP	GFP was amplified from pEGFP-C1 (Clontech) and cloned into the pcMV10 vector (Sigma)

Table 2.2: Plasmids used in Chapters 4 and 5

Chapter 3: The basis for selective E1-E2 interactions in the ISG15 conjugation system

3.1 INTRODUCTION

Ub and Ubls are covalently conjugated to proteins through amide bonds formed between their terminal carboxyl groups and, in most cases, ε-amino groups of lysine residues of target proteins. Two groups of enzymes, the E1 and E2 enzymes, are essential for all known Ub/Ubl conjugation pathways. These enzymes function cooperatively in reactions that involve enzyme-bound thioester intermediates (Pickart, 2001). E1 enzymes catalyze Ub/Ubl activation by first forming an ATP-dependent Ub/Ubl-adenylate, followed by an enzyme-bound Ub/Ubl-thioester at the active-site cysteine of the E1. The activated E1 then transfers the Ub/Ubl to the active-site cysteine of specific E2 enzymes in a transthiolation reaction, preserving the Ub-thioester linkage. In some cases, the E2 may directly interact with target proteins (*e.g.*, Ubc9 in Sumo conjugation (Melchior, 2000)), however conjugation of Ub and most Ubls requires E3 activities. E3s function minimally as docking or scaffolding proteins, binding both the activated E2 and a substrate protein, orienting them for reaction of the ε-amino group of a lysine side chain of the target protein with the activated carboxyl group of the Ub/Ubl. In the case of the HECT domain E3s, the E2 transfers Ub to the active-site cysteine of the E3, with the E3 directly catalyzing the final transfer to the target protein (Scheffner et al., 1995).

The E1, E2, and E3 enzymes for conjugation of Ub and Ubls are generally highly specific for function with either Ub or a single Ubl (Kerscher et al., 2006), however potential overlap of the conjugation pathways for Ub and ISG15 was suggested based on identification of the ISG15 E2 enzyme (Kim et al., 2004; Zhao et al., 2004). ISG15 is a

17 kDa Ubl that is rapidly and strongly induced by type-1 interferons (IFN-α/β). Over 300 cellular proteins are modified by ISG15 in IFN-β-treated cells (Giannakopoulos et al., 2005; Wong et al., 2006; Zhao et al., 2005). The E1 and E2 enzymes for ISG15 are Ube1L and UbcH8, respectively, and like ISG15, expression of both proteins is induced at the transcriptional level by IFN-α/β (Kim et al., 2004; Nyman et al., 2000; Yuan and Krug, 2001; Zhao et al., 2004). Depletion of UbcH8 by siRNAs eliminates virtually all ISG15 conjugation in IFN-β-treated cells, while depletion of the most closely related E2, UbcH7 (55% identity, 72% similarity to UbcH8), had no effect on ISG15 conjugation (Zhao et al., 2004). These results strongly suggest that UbcH8 is the only E2 enzyme for the ISG15 pathway. UbcH8 has been reported in several cases to function in Ub conjugation pathways (Chin et al., 2002; Urano et al., 2002; Wheeler et al., 2002; Zhang et al., 2000), often in a manner that is redundant with UbcH7 (Fortier and Kornbluth, 2006; Imai et al., 2000; Moynihan et al., 1999; Shimura et al., 2000), suggesting that UbcH8 might function in both the Ub and ISG15 conjugation systems. Importantly, given the functional redundancy of E2s in the Ub system, it is difficult to unambiguously demonstrate that UbcH8 functions in conjugation *in vivo*. The fact that UbcH8 expression is transcriptionally regulated by IFN-α/β signaling suggests that there may be insufficient amounts of UbcH8 protein present in most cell types in the absence of interferon to significantly influence Ub conjugation.

Structural and biochemical studies on Sumo and Nedd8 E1s have revealed the basis for interaction of these enzymes with their cognate E2 enzymes (Huang et al., 2005; Lois and Lima, 2005). Both of these E1s are heterodimeric enzymes (Sae1/Sae2 for Sumo, AppBp1/Uba3 for Nedd8), with the Sae1 and AppBp1 proteins corresponding to the N-terminal domain of monomeric E1s, and the Sae2 and Uba3 proteins corresponding

to the C-terminal domain of monomeric E1s. Interestingly, a domain at the C-terminus of the Sae2 and Uba3 proteins adopts a structure that resembles ubiquitin (the Ub-fold domain; UFD). The UFD is the primary site for interaction of Sae2 and Uba3 with their cognate E2 enzymes (Ubc9 and Ubc12, respectively). Ube1L is also predicted to contain a C-terminal UFD (Huang et al., 2005). The core region of Ubc12 that interacts with the UFD is primarily the first alpha helix and the β1- β2 loop (Huang et al., 2005), and the analogous regions of Ubc9 were identified by mutagenesis as the $E1^{Sumo}$ interacting domain (Bencsath et al., 2002). These results were consistent with earlier work that suggested that the N-terminal regions of Ub E2s were critical for interacting with $E1^{Ub}$ (Pitluk et al., 1995; Sullivan and Vierstra, 1991).

We initiated the current study study to determine the basis for specific Ube1L-UbcH8 interactions in the ISG15 system, and in particular, to identify the features that distinguish UbcH8 from UbcH7 in its ability to be activated by Ube1L. Consistent with the studies described above, two primary determinants within the E2 N-terminal region (the α1 helix and β1–β2 region) were responsible for the differential interaction of UbcH8 and UbcH7 with Ube1L. The UFD of Ube1L bound specifically to UbcH8 and was essential for transfer of ISG15 to UbcH8. In addition, $E1^{Ub}$ was found to discriminate against activation of UbcH8 to a similar degree as Ube1L discriminated against UbcH7, suggesting that UbcH8 may be limited in its capacity to function in Ub conjugation *in vivo*.

3.2 RESULTS

3.2.1 E2~ISG15 thioester formation *in vitro*.

UbcH7 is 55% identical and 72% similar to UbcH8 and is the most closely related E2 to UbcH8 among all human E2 enzymes. Figure 3.1A shows an alignment of the

UbcH8 and UbcH7 protein sequences, along with their common secondary structure elements as determined from X-ray crystal structures (UbcH8: PDB 1WZW, K. Tanaka and colleagues, unpublished; UbcH7: PDB 1D5F (Huang et al., 1999)). Both proteins belong to the subgroup of E2s defined, in part, by a conserved sequence motif within the amino-terminal α-helix (α1): xRϕxx[D/E]x (where x is any residue and ϕ is a hydrophobic residue) (Winn et al., 2004). This motif constitutes residues 4-10 of UbcH8 and represents the most common motif found in the α1 helix among all ubiquitin E2s (Winn et al., 2004). With the exception of UbcH8, none of the E2s in this subgroup have been reported to function with Ubls other than Ub. UbcH7 and UbcH8 both contain a conserved phenylalanine residue (F63 in UbcH7, F62 in UbcH8) that is a key contact for interaction of these proteins with HECT and RING E3s (Huang et al., 1999; Zheng et al., 2000), and both proteins consist solely of the approximately 150 amino acid common core E2 structure with no amino- or carboxyl-terminal extensions. Comparing the sequences of the two proteins, the longest contiguous stretch of non-conserved residues is the six-residue random coil linker between the first alpha helix and the first beta strand (α1~β1 linker; residues 16 to 21 of UbcH8), where the UbcH8 sequence is KPPPYL and UbcH7 is CGMKNF. The α1 helix, the linker, and the β1-β2 region are highlighted in the UbcH8 ribbon structure shown in Figure 3.1B.

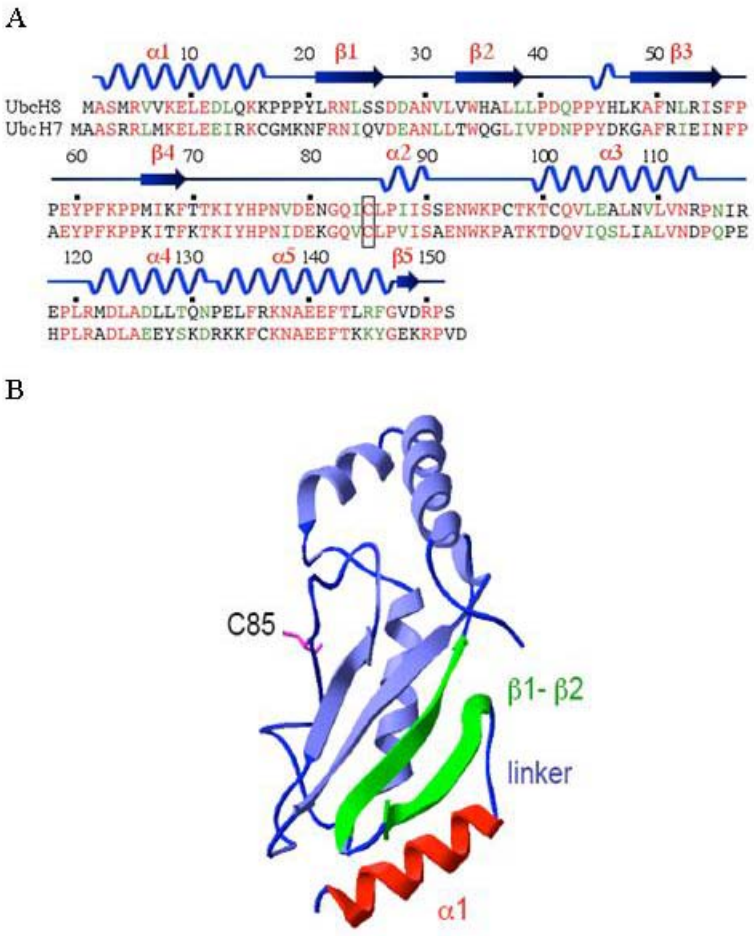

Figure 3.1: Sequence and structure of UbcH8.

A) Alignment of the UbcH8 and UbcH7 sequences, with secondary structure elements of UbcH8 indicated. Numbering is according to UbcH8 residues. Residues in red represent identical residues, green represent similar residues.

B) Structure of UbcH8 (PDB 1WZW, K. Tanaka and colleagues, unpublished). The α1 helix (red) and β1-β2 region (green) are indicated, along with the linker connecting these elements and the active site cysteine (C85, pink).

Both UbcH7 and UbcH8 have been reported previously to cooperate with $E1^{Ub}$ in catalyzing protein ubiquitination *in vitro* and *in vivo* (Kumar et al., 1997; Moynihan et al., 1999), while only UbcH8 functions in ISG15 conjugation *in vivo* (Zhao et al., 2004). To determine if these results are consistent with biochemical characteristics of $E1^{Ub}$ and Ube1L, we performed a preliminary examination of E1-E2 interactions using *in vitro* thioester assays and incubation times of either 5 or 75 minutes. As shown in Figure 3.2, at the 5 minute time point, $E1^{Ub}$ preferentially transferred Ub to UbcH7 compared to UbcH8. At the 75 minute time point the differences in UbcH7 and UbcH8 Ub thioester formation were minimized. Similar results were seen with ISG15 thioester assays, where UbcH8 activation was detected at the 5 minute time point, while UbcH7 activation was almost undetectable, but at the 75 minute time point the differences between UbcH8 and UbcH7 activation were minimized. These results indicate that both UbcH7 and UbcH8 can be charged with both Ub and ISG15 to varying degrees. They also demonstrate that *in vitro* experimental conditions may lead to inaccurate conclusions regarding E1 and E2 cooperativity, and suggested the need for more quantitative kinetic analyses.

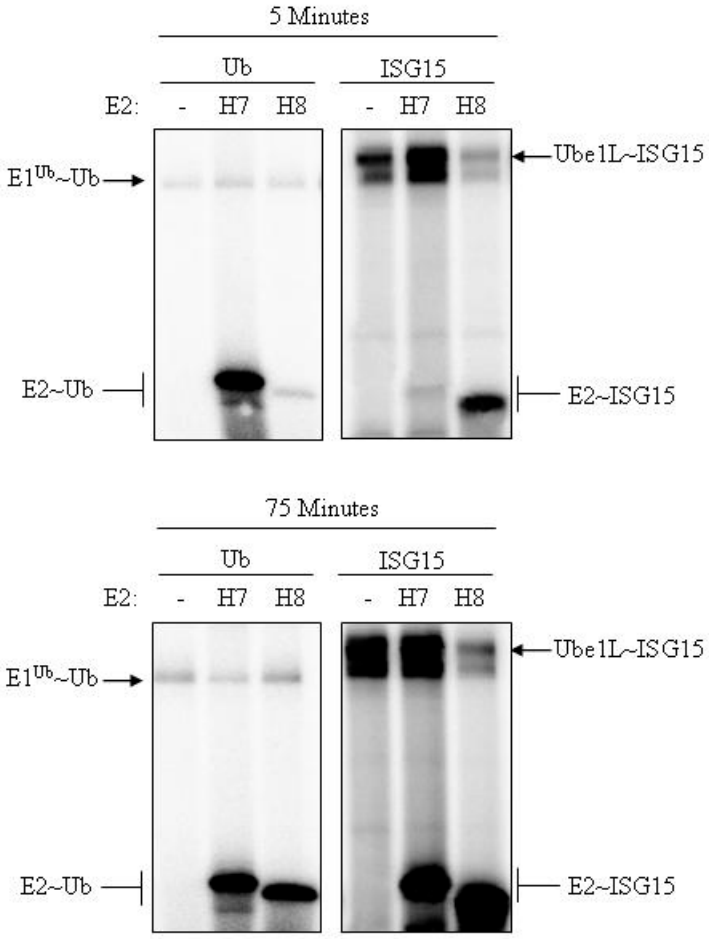

Figure 3.2: E1-E2 thioester assays with wild-type UbcH7 and UbcH8.

Thioester complex formation was analyzed after incubation with $E1^{Ub}$ or Ube1L for either 5 minutes (top panel) or 75 minutes (bottom panel) with wild-type UbcH7 or UbcH8. The Ub and ISG15 were labeled with ^{32}P and thioester adducts were detected by autoradiography.

The K_m values of $E1^{Ub}$ and Ube1L for both UbcH7 and UbcH8 (Table 3.1) were determined by quantifying E2~Ub/ISG15 thioester formation under initial rate conditions, using ^{32}P-labeled Ub and ISG15 (Table 3.1). The K_m of Ube1L for UbcH8 was determined to be 66 +/-8 nM and for UbcH7 it was approximately 29-fold higher (1891 +/- 368 nM). This difference was consistent with the fact that neither endogenous UbcH7 nor any other Ub E2 can substitute for UbcH8 in ISG15 conjugation in interferon-treated cells (Zhao et al., 2004). Similarly, the K_m of $E1^{Ub}$ for UbcH7 was determined to be 185 +/- 26 nM and for UbcH8 it was approximately 36-fold higher (6645 +/- 136 nM). The ratio of K_{cat}/K_m is an indicator of the specificity of an enzyme for a substrate, and this value for $E1^{Ub}$ was approximately 1,300-fold greater with UbcH7 than with UbcH8 (65,450 *versus* 51 $s^{-1}M^{-1}$; Table 1). For Ube1L, K_{cat}/K_m was approximately 114-fold greater with UbcH8 than with UbcH7 (42,580 *versus* 372 $s^{-1}M^{-1}$). Together, these kinetic parameters are consistent with previous demonstrations (Zhao et al., 2004) that no other endogenous E2 proteins can substitute for UbcH8 in the ISG15 system *in vivo*.

E1	E2	k_{cat} (s^{-1})	K_m (nM)	k_{cat}/K_m ($s^{-1}M^{-1}$)
$E1^{Ub}$ (Ub)	UbcH7	0.0115 +/- 0.001	185 +/- 26	65500 +/- 13000
$E1^{Ub}$	UbcH8	0.000340 +/- 0.0001	6650 +/- 140	50.7 +/- 19
Ube1L (ISG15)	UbcH7	0.000620 +/- 0.00001	1890 +/- 370	372 +/- 180
Ube1L	UbcH8	0.00265 +/- 0.0003	66.4 +/- 8.3	42600 +/- 790
Ube1L	A	0.000778 +/- 0.0004	86.1 +/- 33	8560 +/- 670
Ube1L	D	0.00218 +/- 0.0001	1770 +/- 150	1240 +/- 53
Ube1L	H	0.00282 +/- 0.0009	86.9 +/- 19	33900 +/- 10000
Ube1L	J	0.00106 +/- 0.0001	1940 +/- 220	573 +/- 130
Ube1L	K	0.00181 +/- 0.0002	1750 +/- 290	1210 +/- 370

Table 3.1: Kinetic constants of $E1^{Ub}$ and Ube1L for formation of E2~ubiquitin and E2~ISG15 thioesters.

3.2.2 Residues 1-39 are critical for UbcH8 interaction with Ube1L *in vitro*.

To identify the determinants of UbcH8 that confer specificity for Ube1L, we expressed and purified a set of chimeric UbcH8-UbcH7 proteins (Figure 3.3). These proteins were assayed for ISG15 thioester formation with purified Ube1L and ^{32}P-labeled ISG15, as well as for Ub thioester formation with $E1^{Ub}$ and ^{32}P-labeled Ub (Figure 3.4). To ensure incubation times were within the initial velocity period, reaction progress curves were examined for UbcH8 with Ube1L and UbcH7 with $E1^{Ub}$. Two time points were used for Ub thioester assays, as UbcH8~Ub thioester formation was nearly undetectable after one minute. Chimeras A and B, containing either the N-terminal 39 or 70 residues of UbcH8, functioned similar to UbcH8 in ISG15 thioester formation (87%

and 89%, respectively, relative to UbcH8), while thioester formation with chimera C (containing residues 1-122 of UbcH7) was undetectable. These results suggested that the N-terminal 39 residues of UbcH8 contain the major determinants for productive interaction with Ube1L. Interestingly, chimera C formed a Ub thioester with similar efficiency as wild-type UbcH7 in reactions programmed with $E1^{Ub}$, suggesting that the determinants of $E1^{Ub}$-UbcH7 specificity correspond, at least broadly, to the determinants of Ube1L-UbcH8 interaction. Chimeras A and B also formed Ub thioesters at a relatively low efficiency, similar to wild-type UbcH8, further suggesting that the N-terminal regions of UbcH8 and UbcH7 direct specificity for Ube1L and $E1^{Ub}$, respectively.

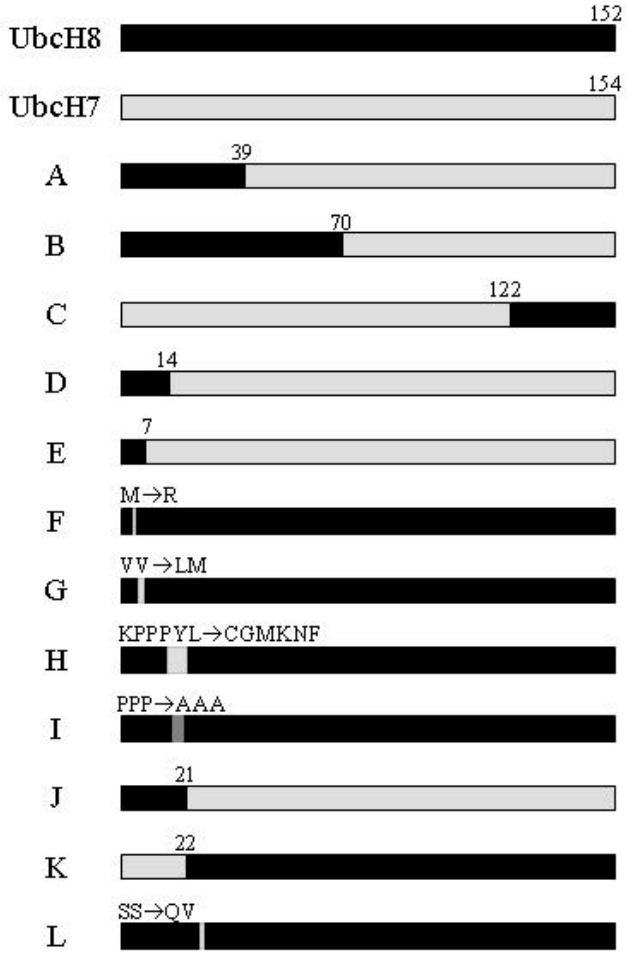

Figure 3.3: Schematic of chimeric and mutant E2 proteins.

UbcH8 sequences are shown in black and UbcH7 sequences are shown in gray. Numbering at chimera junctions represents the first residue (if the chimera contains UbcH8 in its C-terminus) of the last residue (if the chimera contains UbcH8 in its N-terminus) of the UbcH8 sequence present in the chimera. Specific amino acid changes are shown for some chimeras and mutants.

Additional chimeras (Figure 3.3) were made to further localize the determinants of UbcH8 required for functional interaction with Ube1L. Surprisingly, chimeras D and E, containing only the first 14 or first 7 residues of UbcH8, were positive for ISG15 thioester formation (at 23% and 24%, respectively, of level of UbcH8; Figure 3.4A, B). Chimera D contains the complete α1 helix, while E contains the amino terminal half of the α1 helix, which includes the conserved E2 sequence motif described above (xRϕxx[D/E]x, where ϕ is a hydrophobic residue and R is residue 5 of UbcH8). One significant difference between UbcH8 and UbcH7 within this region is that UbcH8 contains a methionine at residue 4, while UbcH7 contains an arginine at the analogous position. The M4R mutant of UbcH8 (chimera F) was diminished in thioester formation by 31% relative to UbcH8. In addition to residue 4, UbcH8 contains VV at residues 6-7, whereas UbcH7 contains LM at the analogous positions. ISG15 thioester formation was decreased by 69% when the LM sequence replaced the VV sequence of UbcH8 (chimera G). Furthermore, chimeras F and G functioned much better with Ub than wild-type UbcH8 when incubated for 10 minutes. These results indicate that the α1 helix of UbcH8 is an important determinant, but not the sole determinant, of specificity for Ube1L.

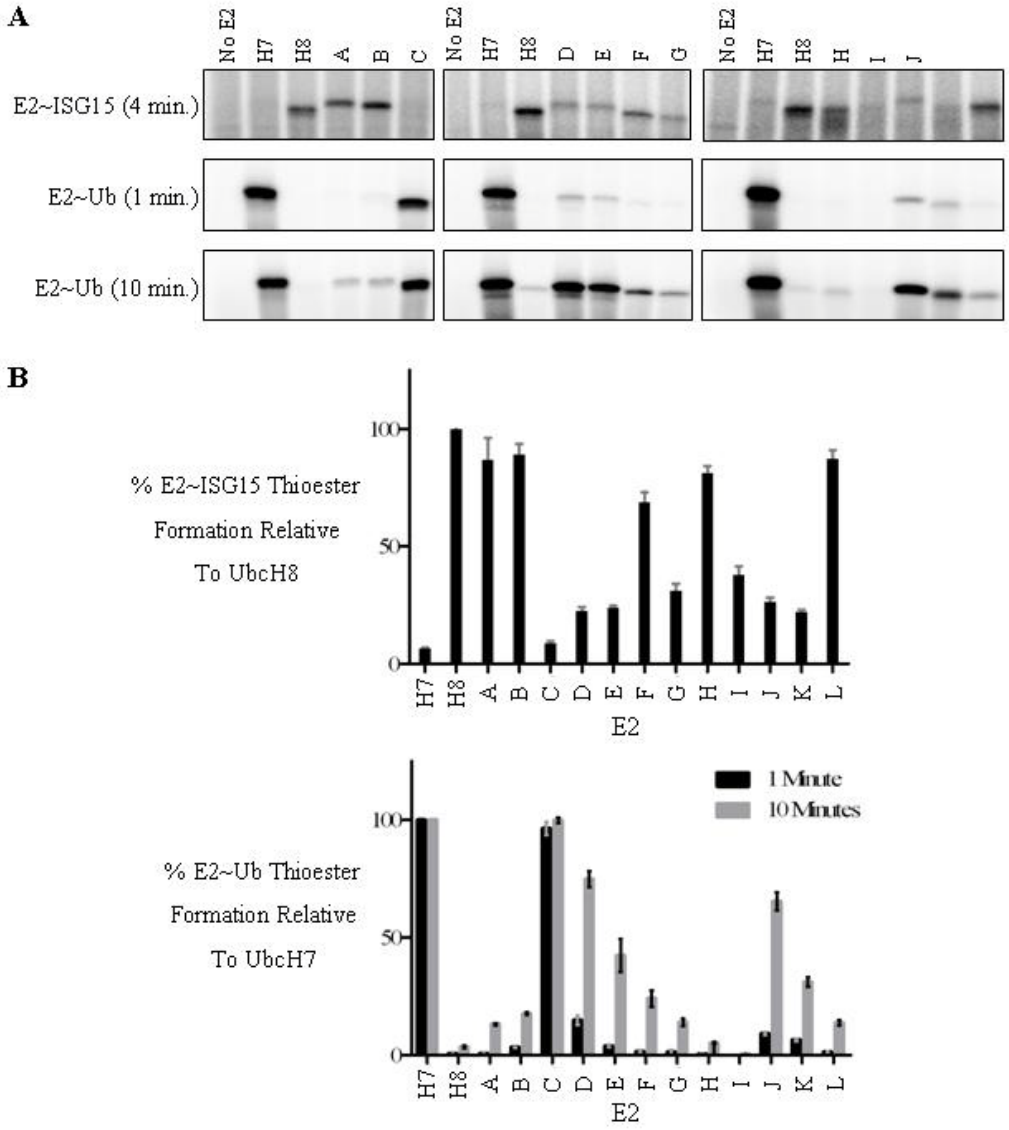

Figure 3.4: In vitro Ub and ISG15 thioester assays with chimeric E2s.

A) Equivalent amounts of the indicated E2 proteins were incubated with ^{32}P-ISG15 and Ube1L for four minutes (top panel), ^{32}P-Ub and E1^{Ub} (DEAE purified) for one minute (middle panel), or ^{32}P-Ub and E1^{Ub} (DEAE purified) for ten minutes (bottom panel). Reaction products were analyzed by SDS-PAGE without reducing agent.
B) E2 thioester adducts were quantitated and are represented as a percentage relative to UbcH8 (for ISG15 thioesters; upper panel); or relative to UbcH7 (for Ub thioesters; lower panel).

As noted above, linker residues between the α1 helix and the β1 sheet (UbcH8 resides 16-21) are very divergent between UbcH8 and UbcH7, and we therefore addressed whether these residues contributed to the specificity of UbcH8 for Ube1L *in vitro*. A chimera was constructed with the linker residues from UbcH7 replacing those of UbcH8 (chimera H). This resulted in a 19% decrease in thioester formation relative to UbcH8. A more dramatic decrease of 62% was observed when UbcH8 residues 17-19 (PPP) were mutated to AAA (chimera I). Ub thioester formation with chimera H was comparable to UbcH8 while no Ub thioester formation was observed with chimera I. This suggests that the linker sequence might not be a direct determinant of specificity for Ube1L, but rather that alterations of this sequence might have deleterious structural effects on the orientation of the α1 helix or the β1−β2 region (discussed further below). Consistent with this possibility, the crystal structure of $Ubc12^{core}$ with a fragment of Uba3 revealed no interaction of the UFD with the corresponding $Ubc12^{core}$ α1-β1 linker.

The third region the N-terminal 39 residues with the potential to influence Ube1L interactions was the β1-β2 region (residues 21-39). ISG15 thioester formation of Chimera K (containing residues 22-152 of UbcH8) was 22% of that of UbcH8, while thioester formation of chimera J (containing residues 21-154 of UbcH7) was 27% of UbcH8. This indicates that the UbcH8 β1-β2 region contributes to ISG15 thioester formation, but that it is not sufficient for full activation. There are few amino acid differences between UbcH7 and UbcH8 within the β1-β2 region, however UbcH8 contains SS at resides 25-26 while UbcH7 contains QV at the analogous positions. When these residues were exchanged in UbcH8 (chimera L), ISG15 thioester formation was reduced by 13%, and this chimera functioned four-fold better than UbcH8 with $E1^{Ub}$. These results are

consistent with the β1-β2 region of UbcH7 and UbcH8 being an additional determinant of E1 recognition.

Kinetic analyses of select chimeras were used to further analyze the role of structural elements within the first 39 residues of UbcH8. Replacement of the α1-helix or β1-β2 region of UbcH8 with UbcH7 residues (chimeras D, K, or J) resulted in a 27-29-fold increase in the K_m of Ube1L compared to wild-type UbcH8 (Table 3.1). These chimeras also showed a large decrease in k_{cat}/K_m compared to UbcH8. In contrast, residues in the linker region (chimera H) had a K_m and k_{cat} similar to that of wild-type UbcH8. This was reflected in a k_{cat}/K_m ratio that was 80% that of UbcH8 compared to ratios approximately 1-3% of UbcH8 for chimeras D, K, and J. Finally, the K_m of Ube1L for chimera A, containing the first 39 residues of UbcH8, was very similar to that of wild-type UbcH8, although k_{cat}/K_m for chimera A was approximately 5-fold lower than UbcH8. This suggests that chimera A contains the determinants necessary for efficient Ube1L interaction, but that it may be partially defective for accepting ISG15 from Ube1L. Overall, these results are consistent with the UbcH8 α1-helix and β1-β2 regions being the primary elements recognized by Ube1L.

2.2.3 Interaction of UbcH8 with the UFD of Ube1L.

The Sae2 and Uba3 proteins, components of the Sumo and Nedd8 E1 enzymes, respectively, contain a C-terminal Ub fold domain (UFD). This is the primary site for interaction with the core domains of their appropriate E2 enzymes (Huang et al., 2005; Lois and Lima, 2005). It was proposed that the C-terminus of Ube1L is also likely to contain a UFD based on structural propensities of residues conserved with Uba3. To determine whether the UFD of Ube1L has a similar role as in Sae2 and Uba3, a C-terminal deletion mutant of Ube1L (Ube1LΔUFD) was constructed, lacking the last 102

amino acids of the protein (residues 911-1012). If the UFD is the site of interaction with UbcH8 then the Ube1LΔUFD would be predicted to be able to form an ISG15 thioester, but be unable to transfer ISG15 to UbcH8. As shown in Figure 3.5A, this was the case. In addition, the Ube1LΔUFD mutant did not support ISG15 conjugation when co-transfected with ISG15, UbcH8, and Herc5 into non-interferon-treated HEK293 cells (Figure 3.5B).

The purified UFD fragment of Ube1L (consisting of residues 902-1013) was predicted to compete with full-length Ube1L for binding to UbcH8, and as shown in Figure 3.5C, the UFD inhibited UbcH8~ISG15 thioester formation in a concentration-dependent manner. Finally, a chimeric Ube1L protein was created in which the UFD of Ube1L was replaced with the UFD from $E1^{Ub}$ (Ube1L-UFD^{Ub}; replaces residues 910-1013 of Ube1L with residues 951-1059 of $E1^{Ub}$). *In vitro*, Ube1L-UFD^{Ub} would be expected to transfer ISG15 preferentially to UbcH7, rather than UbcH8, and this was indeed the case (Figure 3.5D). The chimeric Ube1L-UFD^{Ub} protein was much less stable and less active than wild-type Ube1L, and therefore the absolute efficiencies of UbcH7~ISG15 thioester formation in the presence of the chimeric and wild-type Ube1L enzymes were not directly comparable. Nevertheless, the fact that the chimeric Ube1L preferentially transferred ISG15 to UbcH7 over UbcH8 is consistent with a model where the primary determinants of E1-E2 interactions in the ISG15 system are specified by the UFD of Ube1L with the α1 helix and β1-β2 region of UbcH8.

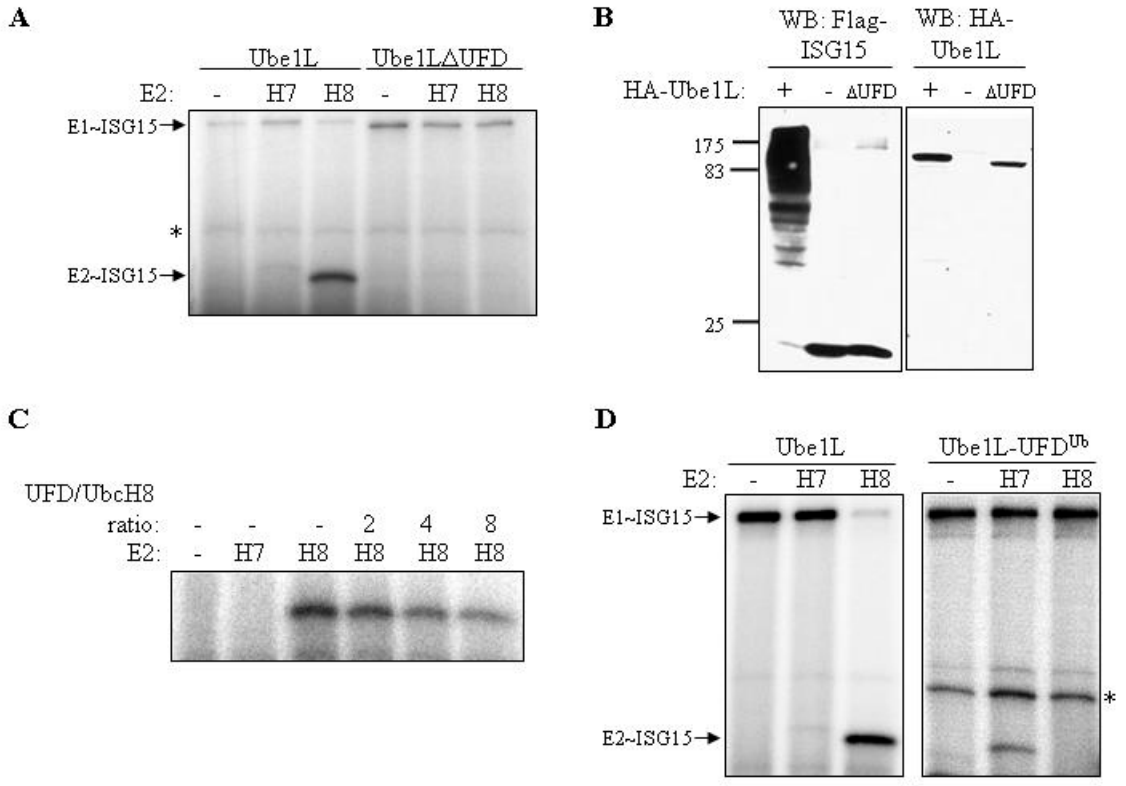

Figure 3.5: The UFD of Ube1L is required for the interaction with UbcH8.

A) ^{32}P-ISG15 was incubated for 10 minutes with Ube1L or Ube1LΔUFD, with the indicated E2 proteins, and reactions were analyzed by SDS-PAGE without reducing agent. An E2-independent background band is indicated (*).
B) HEK293 cells were transfected with plasmids expressing 3X FLAG-ISG15, UbcH8, Herc5, and either HA-Ube1L, no Ube1L, or HA-Ube1LΔUFD. Cell extracts were prepared and analyzed by immunoblotting with anti-FLAG antibody to detect ISG15 conjugates (left panel). Expression of HA-Ube1L and HA-Ube1LΔUFD was confirmed using anti-HA antibody (right panel).
C) The purified UFD of Ube1L is a competitive inhibitor of UbcH8~ISG15 thioester formation. UbcH8 thioester formation was analyzed as in (A), with increasing amounts of purified UFD protein present in the reaction (expressed as the molar ratio of UFD to UbcH8 protein).
D) A chimeric Ube1L protein containing the UFD of E1^{Ub} (Ube1L-UFD^{Ub}) preferentially transfers ISG15 to UbcH7. ^{32}P-ISG15 was incubated with Ube1L or Ube1L-UFD^{Ub} and either no E2, UbcH7, or UbcH8. Reaction products were analyzed by SDS-PAGE without reducing agent. An E2-independent background band is indicated (*).

3.2.4 Endogenous versus exogenous UbcH8 expression levels.

UbcH8 was initially reported to function in the conjugation of ubiquitin both *in vitro* and *in vivo*. As reported above, long incubation times and/or high enzyme concentrations *in vitro* can lead to inaccurate results regarding pathway specificity for UbcH8. A large number of studies suggesting UbcH8 functions as a ubiquitin E2 draw conclusions based on experiments where UbcH8 was expressed by transfection (Chin et al., 2002; Niwa et al., 2001; Wheeler et al., 2002; Zhang et al., 2000). We compared the expression levels of UbcH8 in HeLa cells after induction with interferon versus transfection of a CMV promoter-based UbcH8 expression vector (Figure 3.6). On a per cell basis, the level of UbcH8 in the transfected cells was approximately 60-fold higher than the level of UbcH8 in the interferon-treated cells. These results, in addition to the kinetic constants determined above, strongly suggest that overexpression of UbcH8 by transfection in vivo can potentially lead to the inaccurate designation of UbcH8 as a ubiquitin E2.

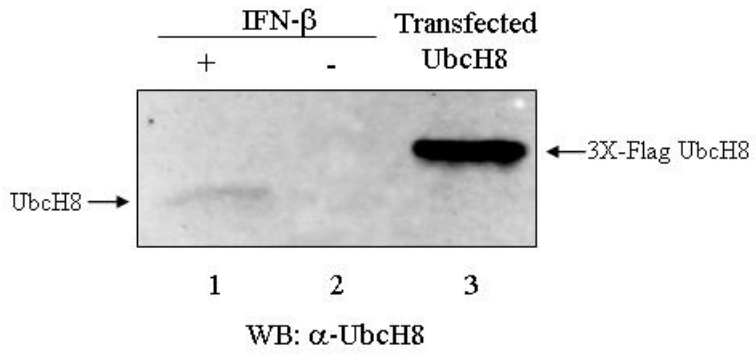

Figure 3.6: Protein expression levels of UbcH8 in HeLa cells.

UbcH8 levels were determined by immuoblotting of 30 mg whole cell extracts of untreated HeLa cells (lane 2), HeLa cells treated with 1000 units/ml of interferon-β for 48 hours (lane 1), or HeLa cells transfected with a 0.25 μg UbcH8 expression plasmid (pCMV-3X-FLAG-UbcH8).

3.3 DISCUSSION

The inherent similarities between Ub and Ubls and the enzymes of their conjugation systems leads to important questions about whether all Ub/Ubl pathways are separate and distinct, and if so, how specificity is determined. We have shown here that the basis for Ube1L-UbcH8 specificity is similar to that described previously in the Sumo and Nedd8 systems: interactions between the UFD of the Ube1L and the α1 helix and β1-β2 regions of UbcH8 are the major specificity determinants. Subtle differences in these regions between UbcH8 and UbcH7 are sufficient to allow effective discrimination against this very closely related Ub E2. Furthermore, the degree to which Ube1L

discriminates against UbcH7 (based on K_ms) is similar to the degree to which $E1^{Ub}$ discriminates against UbcH8, raising the question of whether UbcH8 functions in the Ub system. Similar results and conclusions concerning the role of UbcH8 in Ub conjugation have been discussed previously (Haas, 2006).

A UbcH8-UbcH7 chimeric E2 containing residues 1-39 of UbcH8 (chimera A) could interact efficiently with Ube1L. Within this N-terminal region, both the α1 helix and the β1-β2 region contributed to Ube1L specificity. Kinetic assays with chimeras containing either the α1 helix or the β1-β2 region of UbcH7 resulted in K_m and k_{cat}/K_m values similar to those of UbcH7. Within the α1 helix, there are only three non-conserved residues and alteration of these residues in UbcH8 to those found in UbcH7 decreased *in vitro* E2~ISG15 thioester formation significantly, while E2~Ub thioester formation was correspondingly increased. Two of the three residues, M_4 and V_7, correspond in position to residues of Ubc12 that make key interactions with the Uba3 component of the Nedd8 E1 (Huang et al., 2007; Huang et al., 2005).

The β1-β2 region also contributed to Ube1L-UbcH8 specificity (comparing, for example, chimeras A and J in ISG15 thioester formation), however it is likely that multiple subtle differences between UbcH8 and UbcH7 within this region contribute to this specificity. SS_{25-26} is the most divergent dipeptide in this region of UbcH8 (QV_{26-27} in UbcH7), and the residue corresponding to UbcH8 S_{26} in the Ubc9p and Ubc12 structures was previously shown to be important for SUMO and Nedd8 thioester formation, respectively. Exchange of SS_{25-26} in UbcH8 for QV_{26-27} led to a small but significant decrease in ISG15 thioester formation. Interestingly, this mutant formed a Ub thioester with an approximately 4-fold increased efficiency relative to wild-type UbcH8. It is therefore possible that SS_{25-26} may serve less as a specificity determinant for Ube1L-

UbcH8 interaction than as a barrier to $E1^{Ub}$-UbcH8 interaction. A role for such barriers in establishing E1-E2 specificities has recently been proposed in an analysis of the Nedd8 E2, Ubc12, where it was shown that certain surface residues of Ubc12 appear to function more in preventing mischarging by $E1^{Ub}$ than in specifying charging by the Nedd8 E1 (Huang et al., 2008).

The third structural element within residues 1-39 of UbcH8 is the linker between α1 and β1, and it is the most divergent region of sequence over the entire length of UbcH7 and UbcH8. A direct swap of UbcH7 linker into UbcH8 however, had little effect on the K_m of chimera H compared to wild type UbcH8. Furthermore, comparison of chimeras J (UbcH8 α1-helix and linker) and D (UbcH8 α1-helix only) revealed only a minor difference in thioester formation, suggesting that the linker sequence *per se* is not a determinant of Ube1L-UbcH8 specificity. This is consistent with the fact that the corresponding element in Ubc12 does not make contact with the Uba3 UFD in the co-crystal structure (Huang et al., 2005).

As in the Sumo and Nedd8 E1s, the C-terminal UFD of Ube1L is essential for transfer of ISG15 to UbcH8 and a chimeric Ube1L containing the UFD from $E1^{Ub}$ preferentially transferred ISG15 to UbcH7 over UbcH8. The fact that the chimeric Ube1L-UFD^{Ub} protein had very low activity compared to wild-type Ube1L precluded analyses to determine whether the UFD was the sole determinant of E2 specificity, and based on detailed structural studies of Ubc12 with the Nedd8 E1 complex it is likely that there is an additional surface(s) involved in the Ube1L-UbcH8 interaction (Huang et al., 2008). Nevertheless, the results presented here strongly support a model in which the primary basis for preferential transfer of ISG15 to UbcH8 is the ability to recruit the E2 via the UFD.

Interestingly, before UbcH8 was shown to be E2 for the ISG15 system (Kim et al., 2004; Zhao et al., 2004), it was reported to be an E2 for the Ub system (Chin et al., 2002; Fortier and Kornbluth, 2006; Shimura et al., 2000; Urano et al., 2002; Wheeler et al., 2002; Zhang et al., 2000). However, endogenous UbcH8 expression levels are very low in most non-interferon human cell lines, including HeLa, A549, and HEK293 cells, where it is virtually undetectable by immunoblotting (see Figure 3.6). While interferon-β treatment of HeLa cells leads to the induction of UbcH8, transient transfection of a CMV promoter-based UbcH8 expression vector led to an approximately 60-fold higher level of UbcH8 over the interferon-induced level of endogenous UbcH8. Combined with the relatively high K_m of $E1^{Ub}$ for UbcH8, these observations suggest that 1) UbcH8 is unlikely to function in Ub conjugation in many commonly utilized cell lines (at least in the absence of interferon stimulation), and 2) that experimental overexpression may lead to such high levels of UbcH8 that the relatively high K_m of $E1^{Ub}$ for UbcH8 might be overcome, allowing it to function in Ub conjugation and leading to potentially erroneous conclusions regarding the participation of UbcH8 in Ub-dependent processes. Alternatively, there may be cell or tissues types where UbcH8 expression is sufficient to allow its utilization in the Ub system. For example, global microarray gene expression profiling suggests that UbcH8 may be preferentially expressed in certain cells of the immune system (Su et al., 2002). Finally, a second E1 enzyme for Ub has been recently described, Uba6/E1-L2, raising the possibility that UbcH8 might normally be activated with Ub through Uba6 rather than $E1^{Ub}$ (Ube1) (Chiu et al., 2007; Jin et al., 2007). However, in end-point thioester assays, UbcH8 was not activated with Ub any more efficiently by Uba6 than $E1^{Ub}$ (Ube1) (Jin et al., 2007).

If UbcH8 does not function in Ub-dependent processes, why has the ISG15 system evolved to utilize an E2 that is so similar to UbcH7 (as well as other related E2s, such as the UbcH5 family of E2s)? Why has UbcH8 not diverged more extensively from E2s of the Ub system? One possibility may be related to the fact that the major E3 for the ISG15 system is a HECT E3, Herc5 (Dastur et al., 2006). Herc5 is the only HECT E3 known to function with a modifier other than Ub, and because of inherent HECT E3 structure and/or the unique mechanism of HECT E3s, Herc5 might place considerable constraints on the how far the primary sequence of UbcH8 can diverge from other human E2s that function with HECT E3s (e g., UbcH5a, b, c, UbcH6, UbcH7).

Interestingly, there are other features of the ISG15 system that more closely resemble features of the Ub system than other Ubl systems. For example, human Ube1L is the most closely related E1 enzyme to human Ube1/E1^{Ub}, and ISG15 is the only Ubl where the last six residues of the protein (LRLRGG) are identical to that of Ub. Are these similarities indicative of functional or regulatory overlap between these pathways? As with UbcH8, it is clear that no other E3 can substitute for the broad effect of Herc5 in ISG15 conjugation however, it is not known whether Herc5 might also function in Ub conjugation. There may be mechanistic or structural features of Herc5 that distinguish it from Ub HECT E3s, or Herc5 might simply preferentially recruit UbcH8 over other E2s. These unique problems make the ISG15 system of interest for addressing general mechanism and design of Ubl conjugation systems. In addition, understanding the biochemistry of ISG15 conjugation may ultimately aid in the elucidation of the biochemical function of ISG15 conjugation and the basis of its antiviral activity.

Chapter 4: The ISG15 Conjugation System Targets Newly Synthesized Proteins

4.1 INTRODUCTION

ISG15 is a 17 kD ubiquitin-like protein (Ubl) that is rapidly induced by type 1 interferons (IFN-α and β). Induction by interferon implied, over 20 years ago, that ISG15 was a component of the innate immune system (Farrell et al., 1979), however it has only been recently confirmed that ISG15 has anti-viral activity against several types of viruses, including Influenza, Sindbis, Herpes, HIV, and Ebolavirus (Hsiang et al., 2009; Lenschow et al., 2007; Okumura et al., 2006; Okumura et al., 2008). In addition, several viruses have evolved mechanisms for interfering with ISG15 function: the NS1 protein of Influenza B blocks ISG15 conjugation (Yuan and Krug, 2001), SARS coronavirus encodes an ISG15 deconjugating enzyme (Lindner et al., 2007), and the Vaccinia E3 protein binds to ISG15 and blocks its anti-viral activity (Guerra et al., 2008; Yuan and Krug, 2001). The ability of ISG15 to be conjugated to other proteins has been shown in some cases to be essential for its anti-viral activity (Giannakopoulos et al., 2009; Lai et al., 2009). The biochemical function of ISG15 conjugation and the basis of the anti-viral activities of ISG15 conjugation remain unknown.

While ISG15 is a very rapidly induced IFN-stimulated gene, conjugation does not become apparent until 18-24 hours after IFN stimulation, corresponding with the delayed induction of the ISG15 E1, E2, and E3 enzymes (Dastur et al., 2006). The human ISG15 E1 enzyme is Ube1L (Yuan and Krug, 2001) and the E2 enzyme is UbcH8/Ube2L6 (Kim et al., 2004; Zhao et al., 2004). The major E3 for human ISG15 is Herc5, a HECT domain ligase that contains N-terminal RCC1 repeats (Dastur et al., 2006; Wong et al.,

2006). Herc5 depletion results in a dramatic decrease in ISG15 conjugation, affecting conjugation to the vast majority of cellular target proteins, and co-expression of ISG15, Ube1L, UbcH8, and Herc5 in non-IFN-stimulated cells reconstitutes broad and robust ISG15 conjugation (Dastur et al., 2006). Herc5 has also been shown to have anti-viral activity against influenza A virus (Zhao et al., 2009). EFP, a RING E3, has been reported to be an additional E3 for ISG15, however only a single target has been reported (Zou and Zhang, 2006). Therefore, while additional proteins may play a role in ISG15 conjugation, Ube1L, UbcH8, and Herc5 represent the core IFN-induced components of this conjugation system in human cells.

Proteomics studies have identified over 300 cellular proteins that are targeted for ISGylation (Giannakopoulos et al., 2005; Wong et al., 2006; Zhao et al., 2005). These targets were present in many cellular compartments and no functional classes of proteins were particularly overrepresented, although twelve IFN-induced human proteins were identified (Zhao et al., 2005). A common structural or primary sequence element that confers ISG15 conjugation has not been identified, nor have poly-ISG15 chains been observed. Importantly, only a small fraction of the pool of a given target protein is generally modified (Zhao et al., 2005). These observations raise the following questions: 1) how can a single ISG15 ligase be responsible for targeting such a large and diverse set of proteins, 2) what is the biochemical effect of ISG15 conjugation on target proteins, and 3) how can modification of a small fraction of any individual target protein have a significant effect on the overall activity of that protein? The findings presented here lead to a model that accounts for broad substrate targeting in the ISG15 system and provide a basis for understanding the anti-viral activity of ISG15 conjugation.

4.2 RESULTS

4.2.1 The ISG15 system targets a broad range of proteins.

ISG15 conjugation can be observed experimentally by treating HeLa cells with IFN-β, preparing total cell lysate 24-48 hours post-treatment, and immunoblotting with anti-ISG15 antibody (Figure 4.1A). Surprisingly, when such lysates were immunoblotted with antibodies against previously identified target proteins it was difficult to observe their modification.

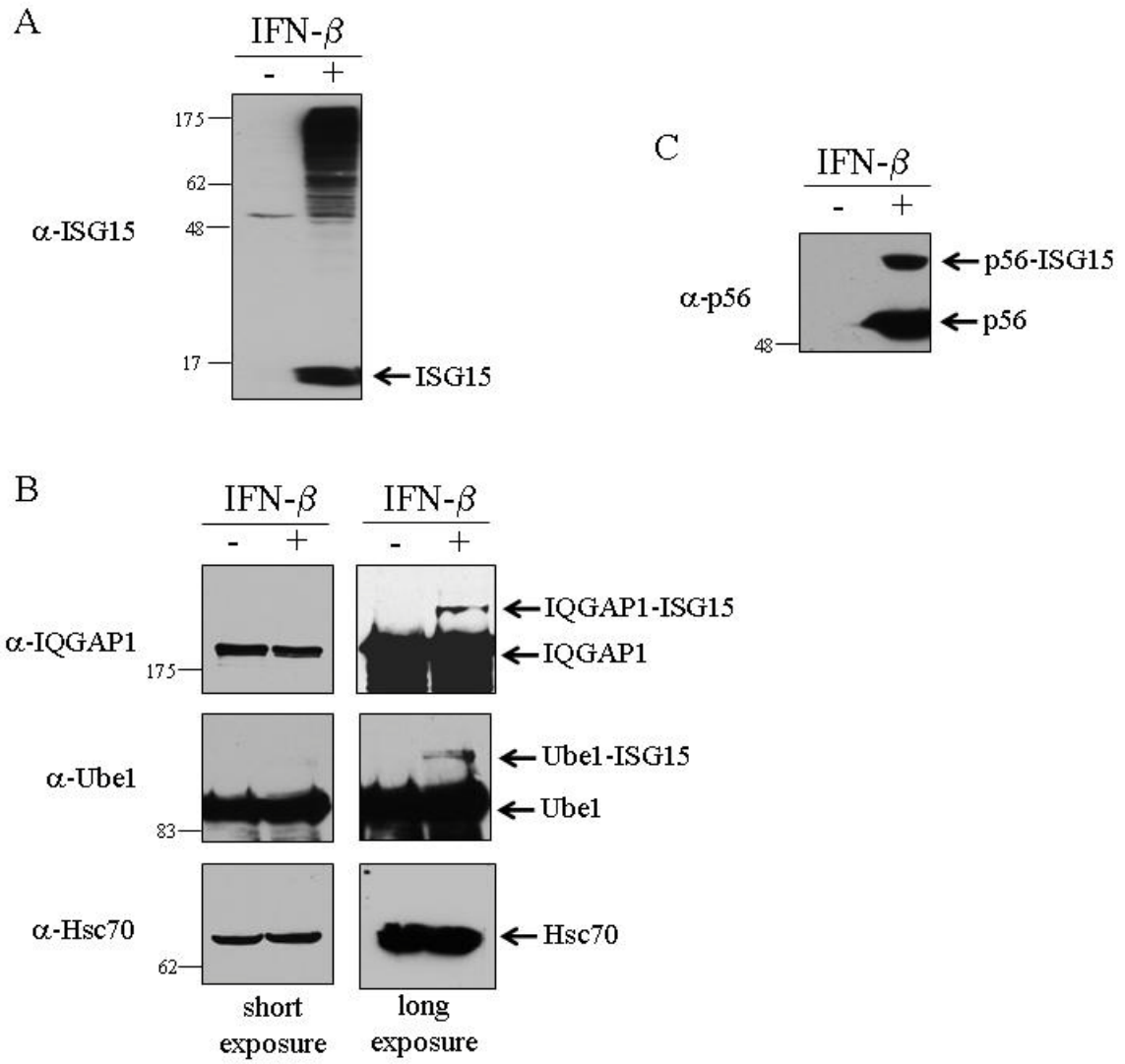

Figure 4.1: Detection of ISG15 conjugates in IFN-β treated HeLa cells.

A) Total ISG15 conjugates in HeLa cells. Cells were either untreated or treated with IFN-β for forty-eight hours. Cell extracts were analyzed by SDS-PAGE and immunoblotting with anti-ISG15 antibody
B) Modification of constitutively expressed target proteins. Cells were treated and extracts analyzed as in (A), using the indicated antibodies. Short (left) and long exposures (right) are shown for each immunoblot.
C) ISG15 modification of p56, an interferon-induced protein. Same as described in (A), with immunoblot analyzed with anti-p56 antibody.

This is seen in Figure 4.1B for two such proteins, IQGAP1 and Ube1. While modification of both proteins could be detected on very long exposures, modification of Hsc70 (Figure 4.1B) and four other constitutively expressed target proteins could not be detected (Table 4.1). The success rate for validation of IFN-induced target proteins was higher, with three out of five targets confirmed, as shown for p56 (Figure 4.1C) and summarized in Table 4.1. As negative controls, five proteins not previously identified as targets of ISG15 modification were examined, and none of these were detectably modified in IFN-β-stimulated cells (Table 4.1).

Target protein	Previously Identified Target?	Interferon-induced?	Detectable ISGylation in IFN-treated HeLa cells?	Detectable ISGylation in 4-Plasmid Transfection?
Ube1	yes	no	yes	yes
IQGAP1	yes	no	yes	yes
Hsc70	yes	no	no	no
Moesin	yes	no	no	no
Tubulin	yes	no	no	no
Matrin 3	yes	no	no	no
Enolase	yes	no	no	no
MxA	yes	yes	yes	na
RIG-I	yes	yes	yes	na
p56	yes	yes	yes	na
PKR	yes	yes	no	na
RIG-G	yes	yes	no	na
OAS1	no	yes	no	na
PLSCR1	no	yes	no	na
E6AP	no	no	no	no
hnRNPk	no	no	no	no
Nucleophosmin	no	no	no	no

Table 4.1: Summary of endogenously expressed target proteins.

ISG15 conjugates can also be generating by expressing the core components of the conjugation system (ISG15 or FLAG-ISG15, Ube1L, UbcH8, and Herc5) by a four-plasmid transfection of non-IFN-stimulated cells. As seen in Figure 4.2 (top), robust ISG15 conjugation was observed in HEK293T cells subjected to this four-plasmid transfection. However, it was again difficult to detect ISGylation of individual endogenously expressed target proteins, as shown for IQGAP1, Moesin, and Ube1

(Figure 4.2A), although, as in IFN-stimulated HeLa cells, a low level of modification of IQGAP1 and Ube1 could be detected on very long exposures (not shown). Modification of only two of seven previously identified targets could be validated by this method (Table 4.2).

To further investigate the problem of target protein validation, non-IFN-stimulated cells (HEK293T) were transfected with plasmids expressing individual epitope-tagged target proteins, along with plasmids encoding the four core ISG15 conjugation components (a five-plasmid transfection). Surprisingly, in this scenario, ISG15 modification was detected for IQGAP1, Ube1, and Moesin (Figure 4.2B), as well as all other previously identified target proteins tested (Figure 4.3 and summarized in Table 4.2).

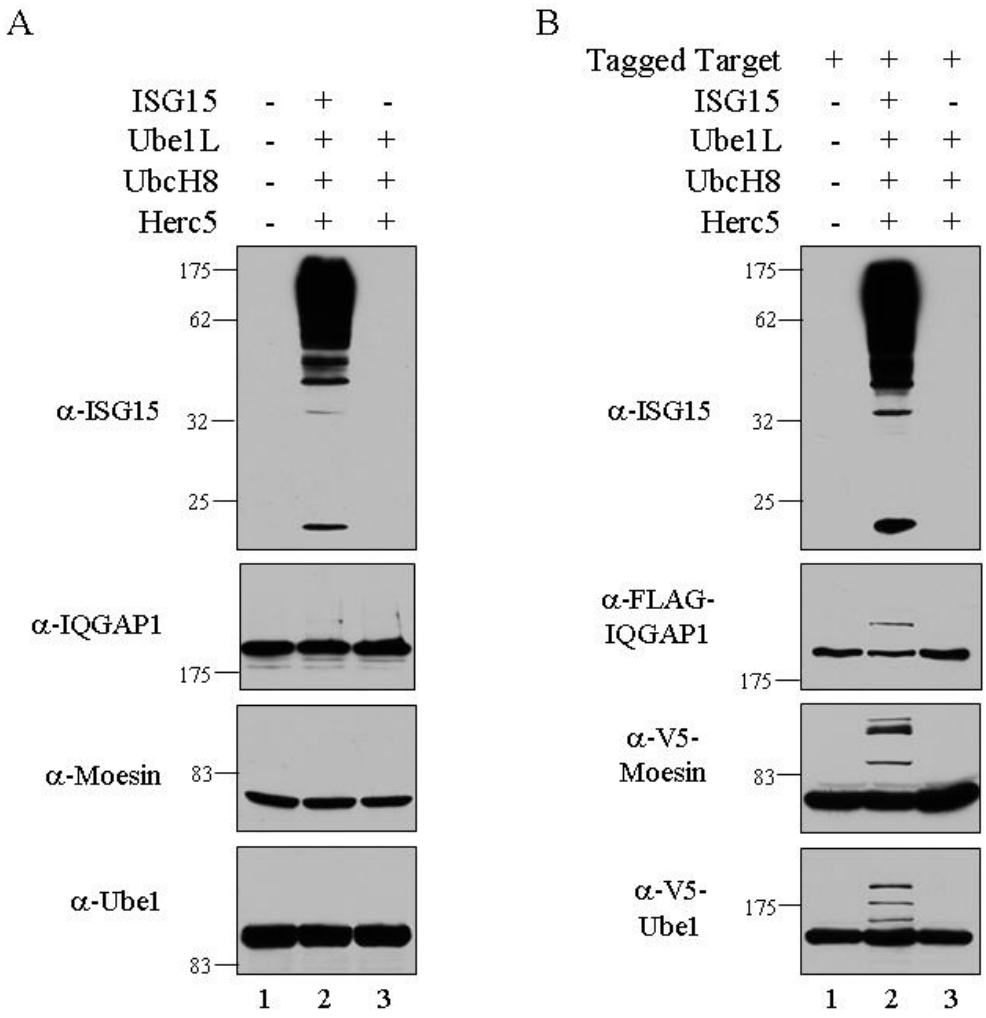

Figure 4.2: ISG15 conjugation to endogenously versus exogenously expressed target proteins.

A) ISGylation of endogenously expressed target proteins. HEK293T cells were either mock-transfected (lane 1), transfected with Ube1L, UbcH8, Herc5, and ISG15 (lane 2), or Ube1L, UbcH8, and Herc5 (lane 3). Cell extracts were prepared 48 hours post-transfection and analyzed for ISG15 conjugation by immunoblotting using the indicated antibodies.

B) ISGylation of exogenously expressed target proteins. HEK293T cells were transfected with a plasmid expressing an epitope-tagged target protein (FLAG-IQGAP1 in top two panels, V5-moesin, or V5-Ube1) either alone (lane 1), or combined with Ube1L, UbcH8, Herc5, and ISG15 (lane 2), or combined with Ube1l, UbcH8, and Herc5 (lane 3). Cell extracts were prepared 48 hours post-transfection and analyzed by immunoblotting using the indicated antibodies.

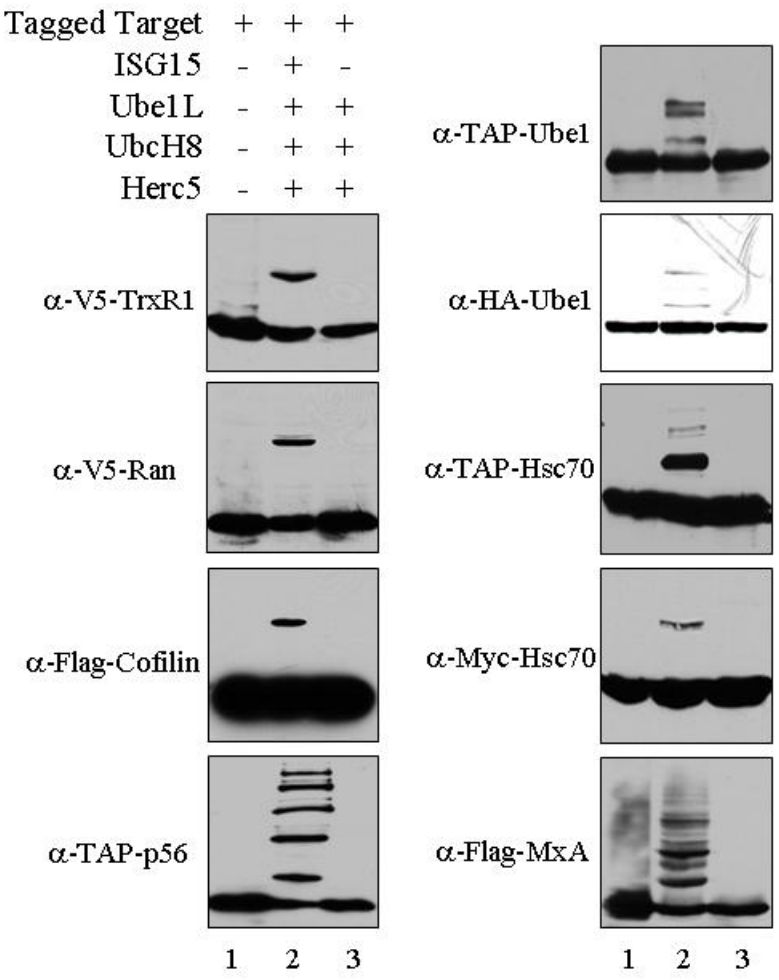

Figure 4.3: ISGylation of additional exogenously expessed target proteins.

HEK293T cells were transfected with a plasmid expressing an epitope-tagged target protein either alone (lane 1), or combined with Ube1L, UbcH8, Herc5, and ISG15 (lane 2), or combined with Ube1l, UbcH8, and Herc5 (lane 3). Cell extracts were prepared 48 hours post-transfection and analyzed by immunoblotting using the indicated antibodies.

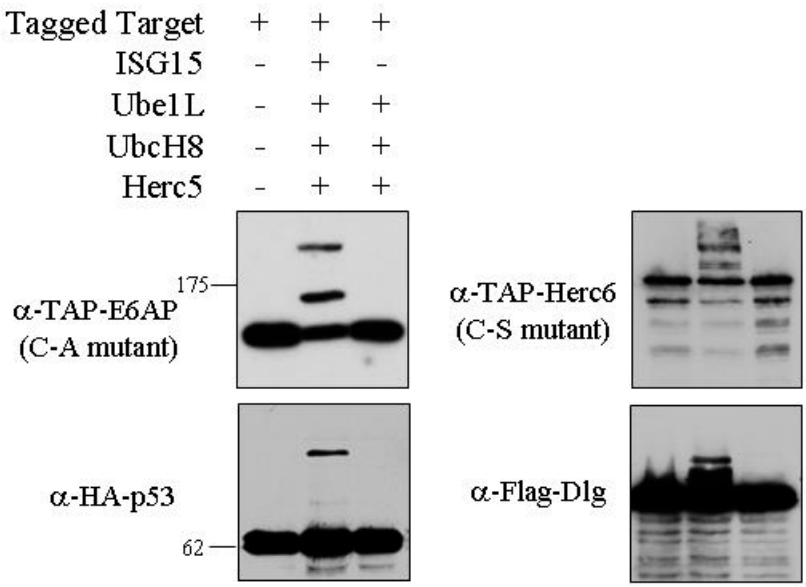

Figure 4.4: ISGylation of human proteins not previously identified as ISG15 targets. HEK293T cells were transfected with the indicated plasmids. Cell extracts were prepared 48 hours post-transfection and analyzed by immunoblotting using the indicated antibodies.

These results prompted us to assay, as presumptive negative controls, several epitope-tagged human proteins that had not been previously identified as ISG15 targets. Five out of seven of these were also found to be ISGylated, including E6AP, p53, Dlg, Herc4, and Herc6 (Figure 4.4 and Table 4.2). Several non-human proteins were also assayed, including the *E. coli* β-galactosidase, *Shigella flexneri* OspG, *Salmonella typhimurium* SopA, the TAP epitope tag (two copies of the protein A sequence and the calmodulin binding protein), and two viral proteins (HPV18 L1 and HIV integrase). All of these were modified when expressed along with the conjugation components (Figure 4.5 and Table 4.2). Three proteins were identified that were consistently not ISGylated in this assay system: GFP, human Wbp2, and a 35 kD carboxy-terminal fragment of

paxillin. We also confirmed that the nature of the epitope tag did not influence modification (see Figures 4.2 and 4.3 for modification of TAP-, HA-, and V5-Ube1, and Table 4.2 for others).

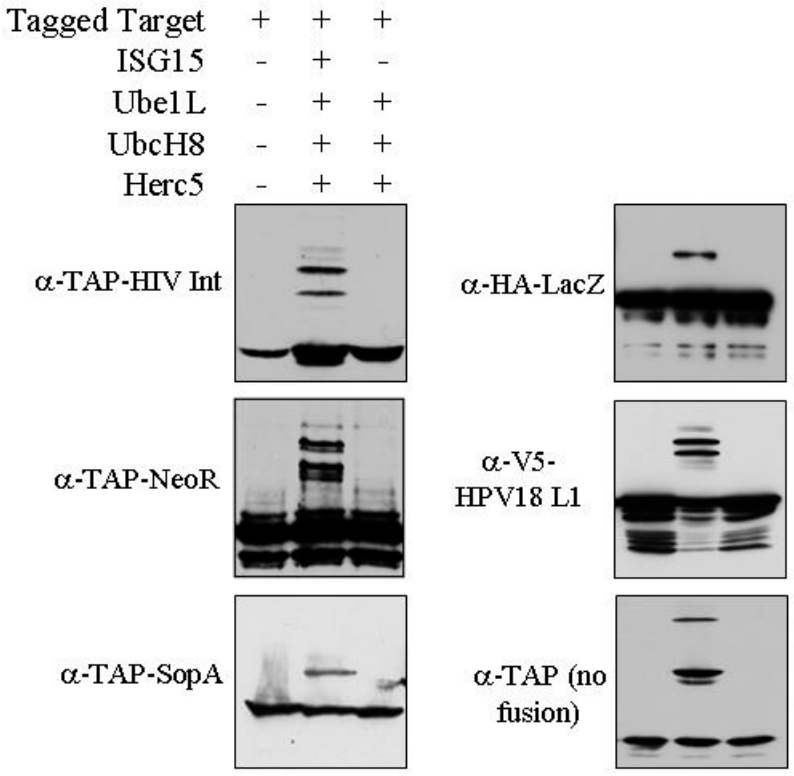

Figure 4.5: ISGylation of foreign proteins.

HEK293T cells were transfected with the indicated plasmids. Cell extracts were prepared 48 hours post-transfection and analyzed by immunoblotting using the indicated antibodies.

Target Protein	Previously Identified Target?	Detectable ISGylation in 5-Plasmid Transfection?
IQGAP1 (TAP, FLAG)	yes	yes
Moesin (V5)	yes	yes
Ube1 (V5, TAP, HA)	yes	yes
TrxR1 (V5)	yes	yes
Ran (V5)	yes	yes
Cofilin (FLAG)	yes	yes
p56 (TAP)	yes	yes
Hsc70 (TAP, Myc)	yes	yes
MxA (FLAG)	yes	yes
p53 (HA, TAP, FLAG)	no	yes
E6AP (C-A mutant; TAP)	no	yes
Herc6 (C-S mutant; HA, TAP)	no	yes
Herc4 (TAP)	no	yes
Dlg (FLAG)	no	yes
Paxillin (C-term.; FLAG)	no	no
Wbp2 (HA)	no	yes
Shigella OSPG (TAP)	na	yes
Salmonella SopA (TAP)	na	yes
TAP epitope, no fusion	na	yes
S. cerevisia Rsp5 (untagged)	na	yes
E. coli Neo^R protein (TAP)	na	yes
E. coli β-gal. (TAP, HA)	na	yes
HPV16 L1 protein (untagged)	na	yes
HPV18 L1 protein (V5)	na	yes
HIV Integrase (TAP)	na	yes
GFP	na	no

Table 4.2: Summary of proteins expressed by plasmid transfection.

In an attempt to map a domain on a target protein that was recognized by the ISGylation enzymes, three non-overlapping fragments of IQGAP1 were assayed for modification (Figure 4.6A). Surprisingly, all three fragments of the protein were ISGylated. Similar results were seen with two non-overlapping fragments of MxA (Figure 4.6B), indicating that the ISGylation machinery does not recognize a single epitope even within an individual protein. Together, these results suggested that, at least in the 5-plasmid transfection assay, the ISGylation machinery recognizes target proteins in a broad and relatively nonspecific manner.

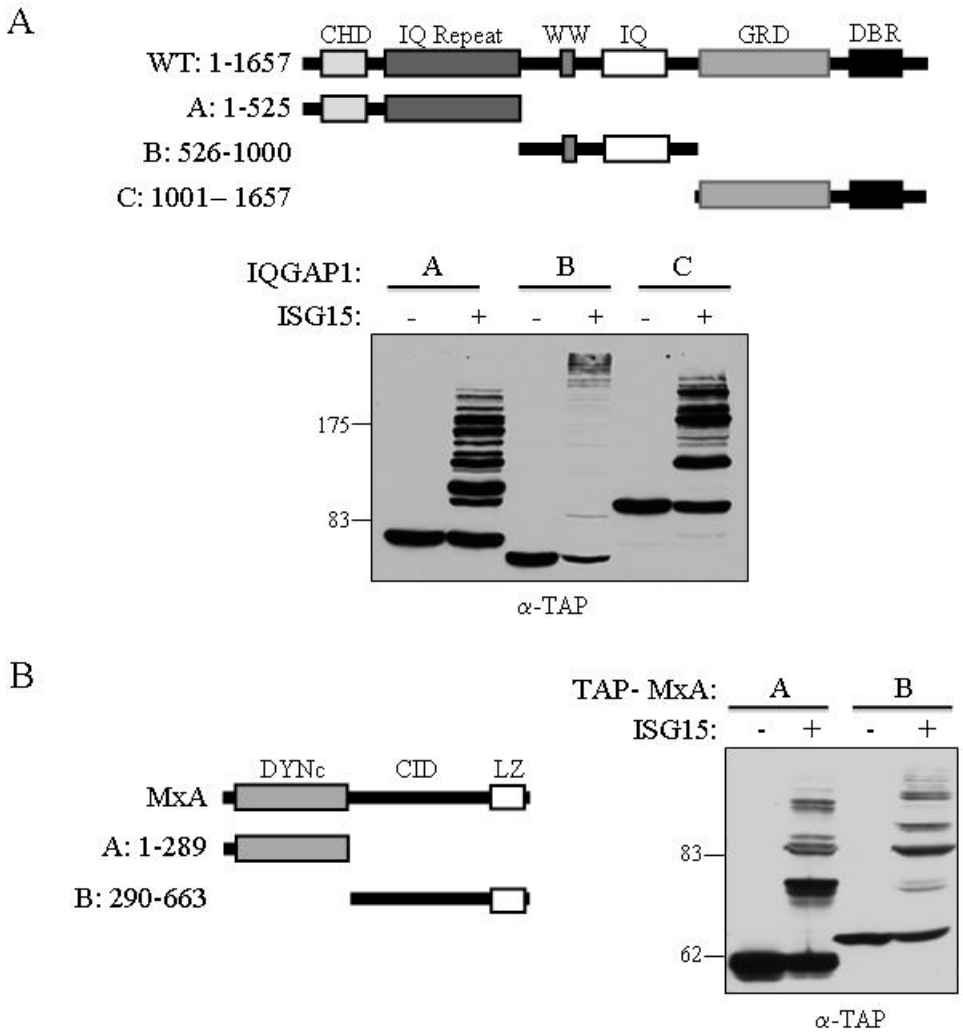

Figure 4.6: ISGylation of non-overlapping target protein fragments.

A) Schematic of IQGAP1, along with three non-overlapping fragments, A-C, with amino acid numbering shown (top). Plasmids expressing TAP-tagged fragments A-C were transfected into HEK293T cells with Ube1L, UbcH8, Herc5, and with or without ISG15. Extracts were prepared and analyzed with anti-TAP antibody.
B) Schematic of MxA, along with two non-overlapping fragments, A and B, with amino acid numbering shown (left). Plasmids expressing TAP-tagged fragments A and B were transfected into HEK293T cells and analyzed as in (A) using anti-TAP antibody.

To address whether the broad target recognition in the five-plasmid transfection assay was related to overexpression of the transfected target proteins, we monitored, at several time points after transfection, the protein levels and modification of two exogenously expressed target proteins (TAP-Ube1 and TAP-IQGAP1) relative to the corresponding endogenously expressed proteins. Figure 4.7 (left panels) shows the relative levels of exogenously and endogenously expressed proteins in the absence of ISG15 (expression of target protein with Ube1L, UbcH8, and Herc5, without ISG15), using an antibody that detects both proteins. The exogenously expressed proteins could be detected by 6 hours post-transfection for both TAP-Ube1 and TAP-IQGAP1. For Ube1, the levels of the exogenous protein did not exceed that of endogenous Ube1, even at 30 hours post-transfection, while for IQGAP1 the levels of exogenous protein were similar and perhaps slightly higher than endogenous IQGAP1 at 24 and 30 hours post-transfection (correcting for the ~50% transfection efficiency). However, at the 18-hour time point, when the exogenously expressed proteins were clearly less abundant than the endogenously expressed proteins, ISGylation of the exogenously expressed proteins was detected when the target protein was expressed with all four conjugation components (Figure 4A, middle panels). In contrast, modification of the endogenous proteins was not detectable at any time point (Figure 4.7, right panels). Therefore, the preferential modification of exogenously expressed proteins was not due to a higher steady state level of the exogenously expressed target proteins.

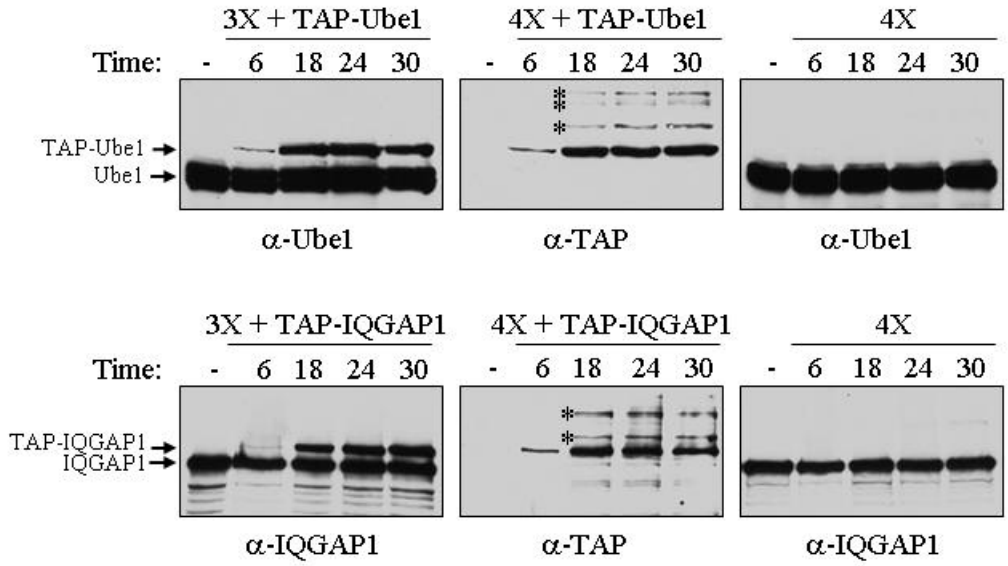

Figure 4.7: Time course of expression and ISGylation of exogenously versus endogenously expressed target proteins.

Left panels: HEK293T cells were transfected with plasmids expressing either TAP-Ube1 or TAP-IQGAP1 along with Ube1L, UbcH8, and Herc5 (3X). Cell extracts were prepared at the indicated time points after transfection and analyzed by immunoblotting with antibodies against Ube1 or IQGAP1 to compare exogenous and endogenous protein levels (left panels).
Middle panels: HEK293T cells were transfected with TAP-Ube1 or TAP-IQGAP1 plus Ube1L, UbcH8, Herc5, and FLAG-ISG15 (4X). Cell extracts were collected at the indicated time points and analyzed with an antibody against TAP to detect ISGylation of the exogenous targets. Asterisks mark the earliest detectable conjugates to TAP-Ube1 and TAP-IQGAP1.
Right panels: HEK293T cells were transfected with Ube1L, UbcH8, Herc5, and FLAG-ISG15 (4X, with no exogenous target protein), and extracts were analyzed for modification of endogenously expressed Ube1 or IQGAP1.

4.2.2 Newly synthesized proteins are targeted for ISGylation.

To account for the preferential modification of exogenously expressed target proteins, we considered that in the five-plasmid transfection assay the entire pool of the target protein was synthesized in the same window of time that the ISG15 conjugation machinery was active. In contrast, in all assays where endogenously expressed proteins were examined, only a fraction of the target protein was synthesized while the conjugation machinery was active (a function of the rate of synthesis of that protein). Also, in the five-plasmid transfections the mRNA levels encoding the exogenously expressed proteins were approximately 10-fold higher than the corresponding endogenously expressed mRNAs (based on three examples, Figure 4.8), suggesting that the exogenously expressed proteins, while not present at a higher steady-state level, were translated at a higher rate. These distinctions suggested that ISG15 conjugation might be limited to the newly synthesized pool of any given target protein. An additional observation consistent with this was the relatively high success rate for validation of IFN-induced ISG15 targets (*e.g.*, p56, MxA) in IFN-stimulated cells (see Table 4.1), where the entire pool of these proteins is, by definition, newly synthesized.

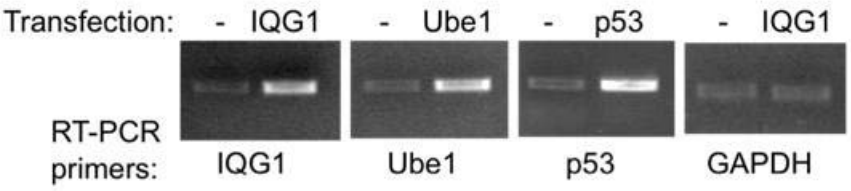

Figure 4.8: Exogenously expressed mRNAs are more abundant than the corresponding endogenously expressed mRNAs

Total mRNA was isolated from untransfected HEK293T cells (-) or cells transfected with TAP-IQGAP1 (IQG1), TAP-Ube1 (Ube1), or TAP-53 (p53) expression plasmids for 24 hours. After DNase treatment, cDNA was prepared with and without reverse transcriptase. RT-PCR reactions were performed using primer sets that detect both the endogenously and exogenously expressed mRNAs. A GAPDH primer set was used as a control for equal RNA in the each set of samples and is shown for the IQGAP1-transfected samples.

We tested the hypothesis that ISGylation is limited to newly synthesized proteins in three ways. In one approach (Figure 4.9A), an intracellular pool of a target protein was first established by plasmid transfection. Twenty-four hours later, the ISG15 conjugation machinery was expressed by a four-plasmid transfection, with or without co-transfection of an siRNA targeting the mRNA encoding the plasmid-expressed target protein. Extracts were prepared 22 hours after the second transfection, and the target protein was analyzed for ISGylation. Our hypothesis predicted that if ISG15 modification was dependent on protein synthesis, then siRNA-mediated destruction of the mRNA would result in a loss of ISGylation of the target protein. That is, the pre-existing pool of the target protein, synthesized in the first 24 hours, would not be modified. In contrast, in the absence of a specific siRNA or in the presence of an off-target siRNA, the target protein would continue to be synthesized and ISGylation would be observed.

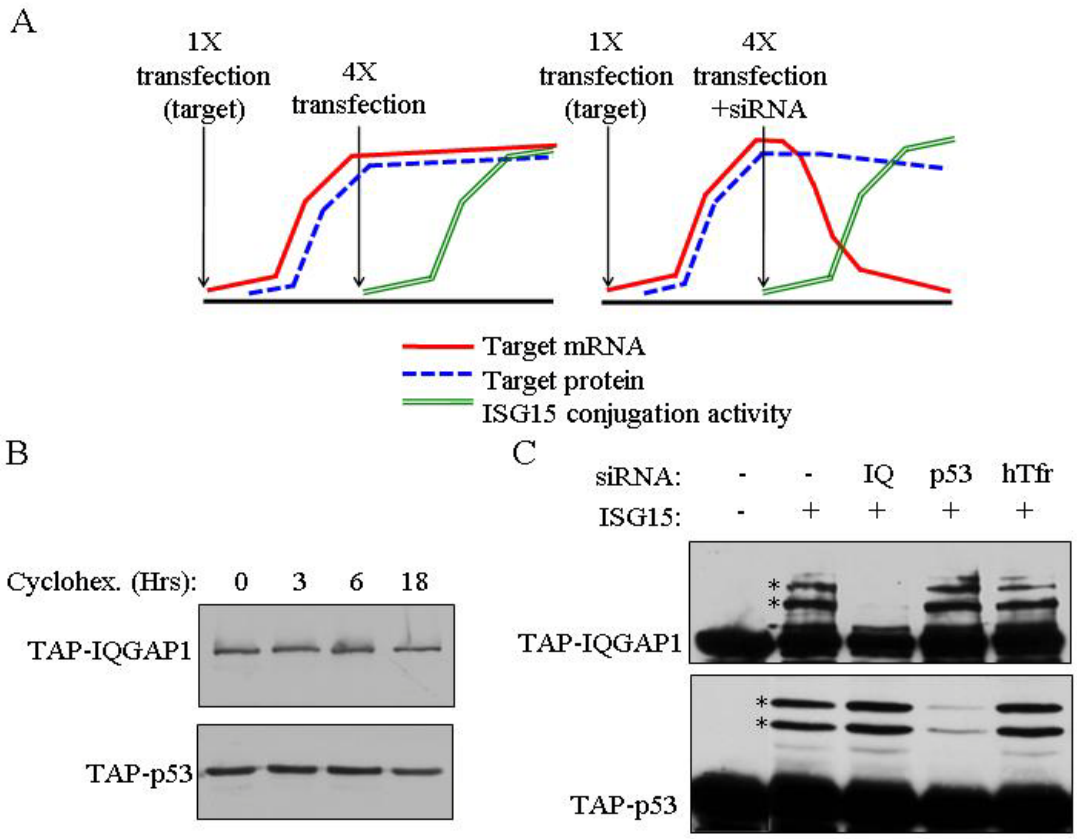

Figure 4.9: Blocking synthesis of an exogenous target protein blocks its ISGylation.

A) Schematic of experimental design. A plasmid expressing an epitope-tagged target protein was transfected at time zero; target mRNA (red line) and target protein (dashed blue line) accumulated over the next 24 hours. Plasmids expressing Ube1L, UbcH8, Herc5, and FLAG-ISG15 were then transfected, either without or with an siRNA that recognized the target protein mRNA. In the absence of the target siRNA (left), modification of the target protein was expected to occur as the ISG15 conjugation components (double green line) accumulated and the target protein continued to be synthesized. In the presence of the target siRNA (right), target protein mRNA would be destroyed as the conjugation components are expressed, but previously synthesized protein persist as a function of their rate of destruction.

B) TAP-IQGAP1 and TAP-p53 are long-lived proteins. Plasmids expressing TAP-IQGAP1 or TAP-p53 were transfected into HEK293T cells and treated with cycloheximide (40 μg/ml) 24 hrs after transfection. Extracts were prepared immediately, or 3, 6, or 18 hrs. later. Immunoblots with anti-TAP indicated that the protein levels did not decline more than 2-fold over 18 hrs.

C) Knockdown of target protein mRNA blocks target protein modification. HEK293T cells were transfected with either TAP-IQGAP1 or TAP-p53, and transfected again 24 hours later with Ube1L, UbcH8, Herc5, and ISG15, without or with siRNAs against IQGAP1, p53, or an off-target siRNA against hTfr (human transferrin receptor). Cell extracts were prepared 22 hrs after the second transfection and analyzed by immunoblotting with anti-TAP.

This experiment was dependent on the rate of degradation of the target protein, and for the targets analyzed, protein levels did not decline more than two-fold after siRNA transfection (Figure 4.9B). Figure 4.9C shows the results for analysis of TAP-IQGAP1 and TAP-p53. ISGylation of both proteins was observed in the absence of any siRNA or in the presence of off-target siRNAs, but was greatly diminished in the presence of a specific siRNA. These results were consistent with the hypothesis that a protein must be actively synthesized in order for it to be modified by ISG15.

A pulse-labeling scheme was used to globally determine whether ISGylation was limited to proteins synthesized in the same window of time that the conjugation machinery is active. In preliminary experiments, we determined that ISG15 conjugates became evident approximately 12 hours after a 4-plasmid transfection (FLAG-ISG15, Ube1L, UbcH8, and Herc5). Therefore, HEK293T cells were transfected with the four plasmids, then pulse-labeled with ^{35}S-labeled cysteine either before conjugation was occurring (6 hours post-transfection) or while conjugation was occurring (22 hours post-transfection). Total cell lysates were collected 24 hours post-transfection, and an anti-FLAG immunoprecipitation was analyzed by SDS-PAGE and autoradiography. Our hypothesis predicted that ^{35}S-containing proteins labeled at the early time point would not be ISGylated, while proteins labeled at the late time point, while conjugation was occurring, would be susceptible to ISGylation. A broad range of labeled proteins were conjugated to ISG15 in cells labeled at the 22 hour time point, while the pattern of labeled immunoprecipitated proteins from the early labeling period was only slightly above that seen in control untransfected cells (Figure 4.10B, compare lane 2 to lanes 1, 5, and 6). The slight signal over background in the lanes corresponding to the early labeling period may be due to either a secondary mode of ISG15 conjugation (*e.g.*, a minor Herc5-

independent conjugation pathway), or due to turnover of the ^{35}S-cysteine and re-incorporation into newly translated proteins at later time points. This experiment was also performed using a FLAG-ISG15 expression plasmid encoding an ISG15 mutant lacking the N-terminal ubiquitin-like domain (FLAG-ISG15-ΔN), which is conjugated similarly to wild-type ISG15. As above, ^{35}S-labeled proteins were co-immunoprecipitated with FLAG-ISG15-ΔN when cells were labeled at the 22-hour time point, but not when cells were labeled at the 6-hour time point (Figure 4.10B, lanes 3 and 4). An anti-FLAG western blot of total extracts indicated that conjugation was robust in all samples expressing the conjugation components, regardless of the point at which the cells were labeled with ^{35}S-cysteine (not shown). TCA precipitations of the extracts indicated that total protein labeling (dpm/μg of total protein) was similar among all samples (not shown). These results were consistent with the notion that proteins are only subject to ISG15 conjugation if they are synthesized in the window of time that the conjugation machinery is active.

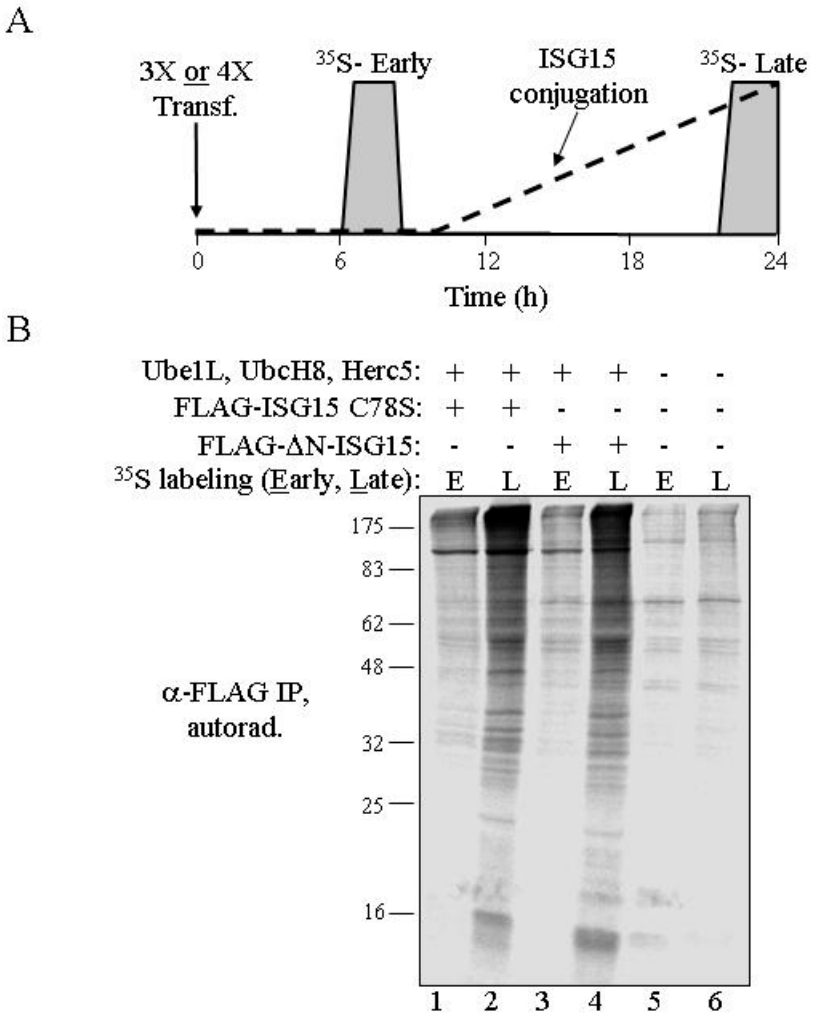

Figure 4.10: ^{35}S-Cysteine Metabolic Labeling Demonstrates that Pre-Existing Pools of Cellular Proteins Are Not Subject to ISG15 Conjugation.

A) Schematic of experimental design. HEK293T cells were transfected either with Ube1L, UbcH8, and Herc5 (3X) or Ube1L, UbcH8, Herc5, and either FLAG-ISG15 C78S or FLAG-ΔN-ISG15 (4X). Cells were labeled for two hours with ^{35}S -cysteine beginning either 6 or 22 hrs post-transfection (grey boxes), corresponding to periods before or during which ISG15 conjugation was occurring (approximate time course of ISG15 conjugation indicated by dashed line).
B) Immunoprecipitation of labeled cellular proteins conjugated to ISG15. ISG15 conjugates were immunoprecipitated with anti-FLAG beads, ^{35}S-labeled cellular proteins that were conjugated to ISG15 were analyzed by SDS-PAGE and autoradiography. Plasmids transfected are indicated in the figure. Early (E) refers to ^{35}S-labeling 6 hours post-transfection, while late (L) refers to ^{35}S-labeling 22 hours post-transfection.

A third assay utilized puromycin, which inhibits translation by covalent incorporation into the carboxy-terminal end of nascent polypeptide chains. Our hypothesis predicted that puromycin treatment of cells that were actively conjugating ISG15 would lead to the generation of polypeptides that contained both ISG15 and puromycin. Cells were therefore subjected to a four-plasmid transfection (FLAG-ISG15, Ube1L, UbcH8, Herc5) or a 3-plasmid transfections that omitted an individual enzyme component. Twenty-four hours later, cells were treated with puromycin for 2 minutes before preparation of cell extracts. ISG15 conjugates were immunoprecipitated with anti-FLAG antibody and then analyzed by immunoblotting with anti-puromycin antibody. As shown in Figure 4.11, cells expressing all four conjugation components contained a broad range of polypeptides that were modified with both ISG15 and puromycin. Such polypeptides were not detected in cells that were not treated with puromycin. Cells lacking Ube1L, UbcH8, or Herc5 had a very small amount of conjugates, corresponding to the low basal expression of these enzymes in non-IFN-treated cells (not shown). These results were therefore consistent with the model that newly synthesized proteins are targeted for ISGylation.

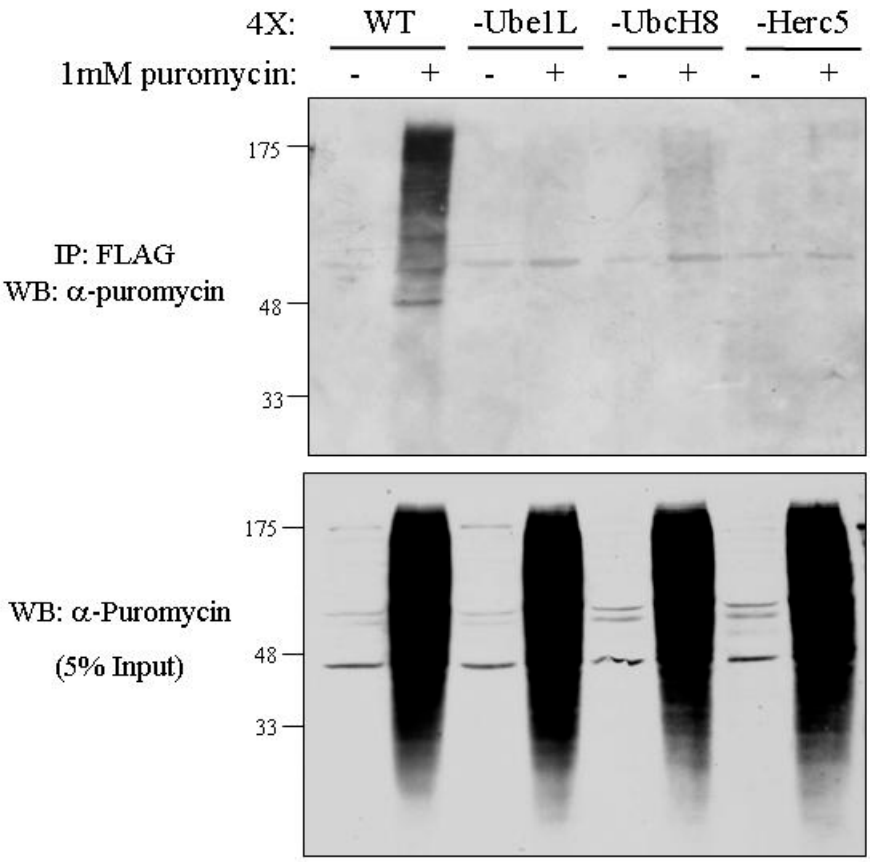

Figure 4.11: Cells treated with puromycin contain polypeptides that are modified with both puromycin and ISG15.

HEK293T cells were transfected with either four plasmids (FLAG-ISG15, Ube1L, UbcH8, and Herc5) or three plasmids (same, without either Ube1L, UbcH8, or Herc5). Twenty-four hours post-transfection, cells were harvested or treated with 1 mM puromycin for two minutes and cell extracts were prepared. Five percent of the extracts were immunoblotted with anti-puromycin (bottom). The remaining extracts were immunoprecipitated with anti-FLAG antibody and immunoblotted with anti-puromycin antibody (top).

4.2.3 Herc5 is associated with polyribosomes.

The ISGylation of newly synthesized proteins suggested that modification might occur co-translationally. We therefore determined whether endogenously expressed Herc5 co-fractionated with ribosomes and/or polysomes. HeLa cells were treated with IFN-β for 24 hours and cell extracts were fractionated by sucrose gradient sedimentation. Ribosome- and polysome-containing fractions, including the 40S and 60S ribosomal subunits, were identified by characteristic absorbance profiles at 254 nm and confirmed by immunoblotting with anti-ribosomal subunit antibodies. As shown in Figure 4.12A, the vast majority of Herc5 protein was within the polysome-containing fractions. Herc5 co-fractionated with 80S ribosomes when extracts were treated with RNase (Figure 4.12B), which destroys the polysomes and leads to a large increase in the amount of 80S ribosomes. This suggested that Herc5 was associated with polysomes via ribosomes, rather than mRNA. Consistent with this, Herc5 co-fractionated with 60S ribosomes when extracts were treated with EDTA (Figure 4.12C), which dissociates polysomes and 80S ribosomes into 40S and 60S subunits. EDTA also releases nascent polypeptides from the 60S subunit (Ullers et al., 2004; Valent et al., 1997), suggesting that Herc5 was unlikely to be tethered to ribosomes via nascent polypeptides. Herc4 is a HECT domain ligase that has 57% primary sequence similarity to Herc5 (Hochrainer et al., 2005), but it is not IFN-induced and does not function in ISG15 conjugation. Neither endogenously expressed Herc4 or another unrelated HECT E3, E6AP/Ube3A, co-fractionated with polysomes (Figure 4.12A).

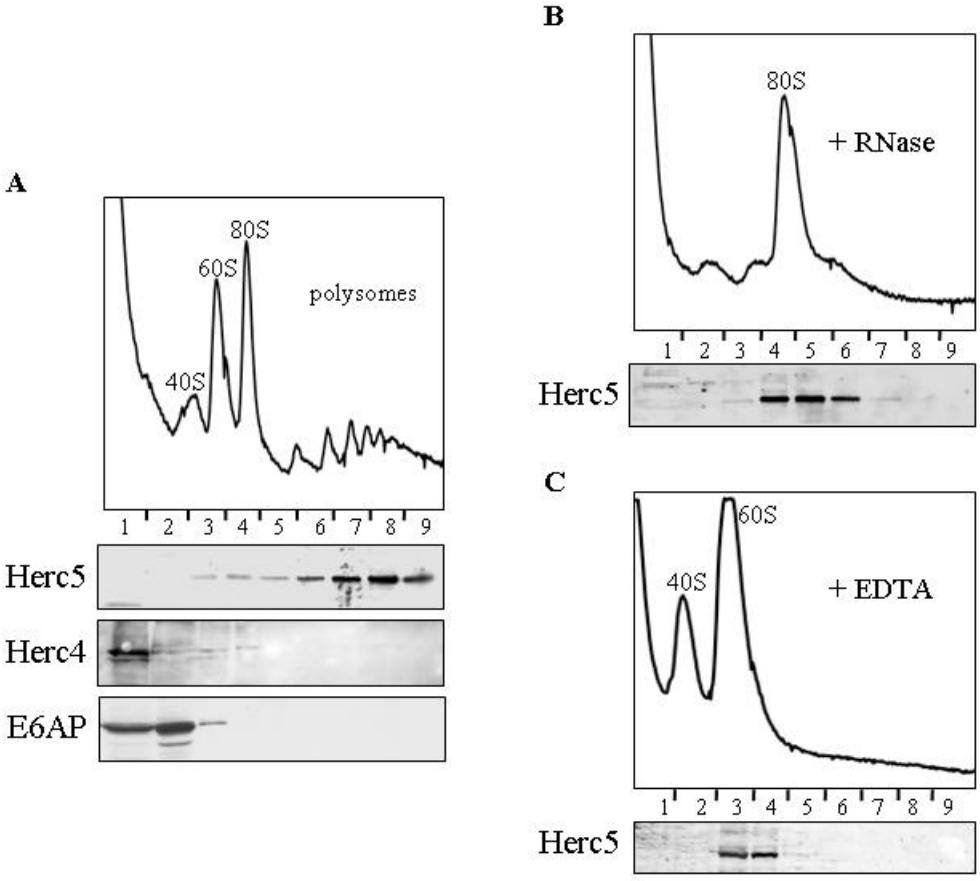

Figure 4.12: Herc5 fractionates with polysomes.

A) Herc5 fractionates with polysomes in HeLa cell extracts. HeLa cells were treated with IFN-β for 24 hours and subjected to polysome analysis (Methods). The A_{254} profile shows the positions of the 40S, 60S, 80S, and polysome fractions. Fractions were analyzed by immunoblotting with the indicated antibodies.
B) Herc5 fractionates with the 80S ribosomes after RNase treatment. HeLa cells were treated and analyzed as described in (A), however RNase was added to the cell lysate after harvest. Fractions were analyzed by immunoblotting with anti-Herc5 antibody.
C) Herc5 fractionates with the 60S ribosomal subunit after EDTA treatment. HeLa cells were treated and analyzed as described in (A), with addition of EDTA to the cell lysate after harvest. Fractions were analyzed by immunoblotting with anti-Herc5 antibody.

Herc5 contains four well-defined RCC repeats between residues 150 and 370 and three less well conserved repeats in the first 150 amino acids. Deletion of this entire region (ΔRCC) abrogates ISGylation of target proteins (not shown), as does deletion of amino acids 2-100 (Δ100), however both proteins retain catalytic activity based on auto-conjugation activity (Figure 4.13A). Full-length HA-tagged Herc5 expressed by transfection was present in the polysome fractions (Figure 4.13B), although it was present in earlier ribosome-containing fractions of the gradient, probably due to the approximate 5-fold overexpression of HA-Herc5 relative to the IFN-induced levels of Herc5 in HeLa cells. In contrast, both the HA-ΔRCC and HA-Δ100 Herc5 proteins were present almost exclusively in the earliest fractions of the gradient. Therefore, the RCC1 repeat region of Herc5 is essential for both ISGylation and polysome association.

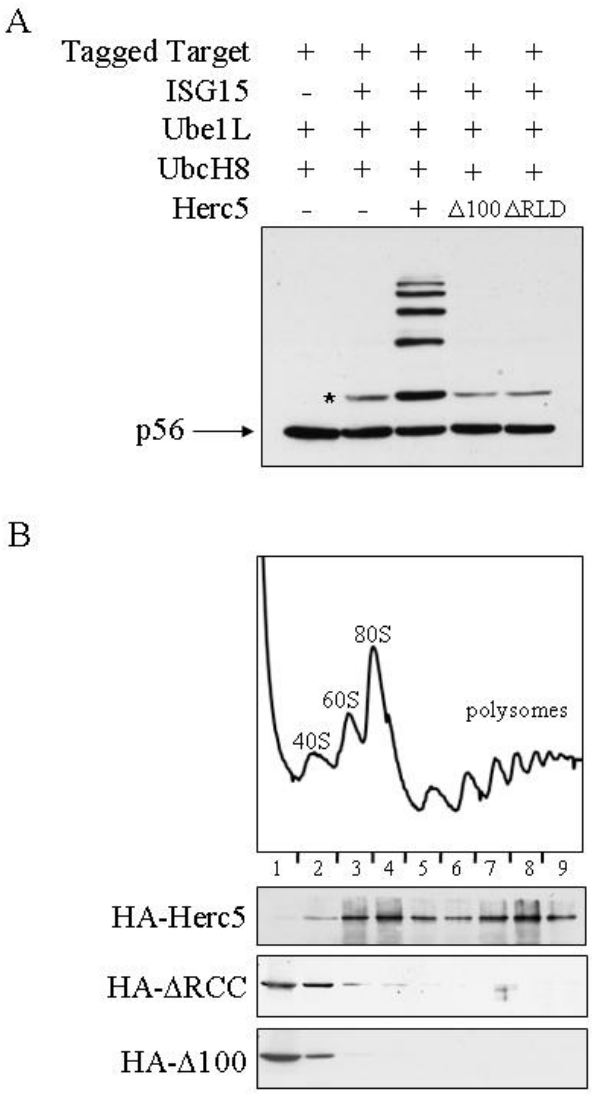

Figure 4.13: The RCC1 repeats are required for ISGylation of target proteins and co-sedimentation with polysomes.

A) Herc5-ΔRCC and Herc5-Δ100 cannot conjugate ISG15 to target proteins. Plasmids expressing FLAG-p56 were transfected into HEK293T cells along with plasmids expressing Ube1L, UbcH8, ISG15, and NTAP-Herc5 or the indicated Herc5 mutants. Cell extracts were prepared 48 hours post-transfection and ISGylation of p56 was determined by immunoblotting with anti-FLAG antibody. The asterisk marks ISG15 modification of p56 due to endogenous Herc5.

B) HEK293T cells were transfected with HA-Herc5, HA-ΔRCC, or HA-Δ100 expressing plasmids and harvested after 24 hours. Cell extracts were fractionated as above and analyzed by anti-HA immunoblotting.

4.3 DISCUSSION

We have shown here that the range of ISG15 target proteins is extremely broad, that newly synthesized proteins are the targets of ISGylation, and that Herc5 is associated with the translational machinery. These findings suggest that the ISG15 system is designed to target newly synthesized proteins, with limited target protein selectivity.

Herc5 protein in extracts of interferon-stimulated HeLa cells co-fractionated with polysomes, and further analyses suggested that it is associated with a core component of the 60S ribosomal subunit. As the exit tunnel for nascent polypeptides is on the 60S subunit (Kramer et al., 2009), an attractive model is that Herc5 modifies newly synthesized polypeptides co-translationally, as they emerge from the exit tunnel. Interestingly, other protein modification enzymes have been identified that are ribosome-associated and function near the exit tunnel, including methionine isopeptidase (Raue et al., 2007; Vetro and Chang, 2002), N-terminal acetyltransferases (Green et al., 1978; Pestana and Pitot, 1975), and chaperones that aid in co-translational folding of proteins (Kramer et al., 2009). Polysome association of Herc5 suggests that the inclusion of a translation system will be a requirement for reconstitution of *in vitro* ISGylation, which in turn is likely to be required for a direct test of the co-translational model. Also, it is important to note that while the range of ISG15 target proteins appears extremely broad, not all newly synthesized proteins were ISGylated in our assays. Factors that might influence susceptibility to modification include rates of translation, co-translational folding rates, and the sequence or secondary structure context of lysine acceptors.

The biochemical function of ISG15 conjugation remains unknown. The two most general possibilities are that ISG15 signals to another protein or protein complex (*e.g.*, in the way that ubiquitin signals to the proteasome), or it simply disrupts the function of

proteins to which it is conjugated. There is evidence to support the latter in studies that have examined individual target proteins (Jeon et al., 2009; Zou et al., 2005), and this may also be inferred by ISG15 protein sequence comparisons between mammalian species. Unlike ubiquitin and most other Ubls, ISG15 protein sequences are very divergent. Only 72 out of 157 residues (46%) are identical between the human, mouse, rat, dog, cow, and sheep ISG15 protein sequences. We suggest that these divergent mammalian ISG15 proteins are unlikely to have retained a common signaling function, and that the similarity retained reflects that which is required for maintaining the ubiquitin-like folds of ISG15 and for productive interaction with the conjugation enzymes. We therefore suggest that the function of ISG15 is to generally disrupt target protein function, and the functions of viral proteins, in particular.

But how could ISG15 conjugation be an effective defense against viruses when, even among the newly synthesized pool of a target protein, ISGylation is so inefficient? The answer may lay in the fact that structural proteins are generally among the most actively expressed of viral proteins, and capsid and nucleocapsid proteins must assemble into precise repeating geometric configurations to form infectious virus particles. Therefore, ISGylation of a small fraction of the total pool of a viral structural protein might have a strong dominant-negative effect on virus assembly or infectivity. Interestingly, a recent study identified a dominant-negative HIV1 gag protein that inhibited HIV1 infectivity (IC_{50}) at a ratio of 3-4% mutant to wild-type protein (Lee et al., 2009). Finally, the low efficiency of ISGylation may be tuned to minimize the collateral damage to newly synthesized cellular proteins. While this is a highly speculative model, the central experimental findings presented here – that ISG15 is broadly targeted to newly synthesized proteins - lead to testable hypotheses for the

identity of the biologically relevant targets of ISGylation in the innate immune response and the biochemical function of ISGylation.

Chapter 5: Implications for the anti-viral function of ISG15

5.1 INTRODUCTION

ISG15 is an interferon-induced and anti-viral ubiquitin-like protein (Ubl) (Farrell et al., 1979; Harty et al., 2009). The human ISG15 E1 enzyme is Ube1L (Yuan and Krug, 2001) and the E2 enzyme is UbcH8/Ube2L6 (Kim et al., 2004; Zhao et al., 2004). Herc5, the major E3 enzyme for ISG15, mediates the ISGylation of over 300 proteins in interferon-stimulated cells (Giannakopoulos et al., 2005; Wong et al., 2006; Zhao et al., 2005). In addressing this broad substrate selectivity of Herc5, we found that: 1) the range of substrates extends even further and includes many exogenously expressed foreign proteins, 2) ISG15 conjugation is restricted to newly synthesized pools of proteins, and 3) Herc5 is physically associated with polyribosomes (Durfee, In press). These results lead to a model for ISGylation in which Herc5 broadly modifies newly synthesized proteins in a co-translational manner.

Only modest progress has been made on determining the biochemical function of ISG15 conjugation. Currently, it is not possible to easily generate purified ISGylated target proteins because a complete *in vitro* ISGylation system has not yet been established. There are a few studies which have used cell-based approaches to examine ISG15 function: 1) ISGylated Ubc13 was shown to be defective for ubiquitin thioester formation (Takeuchi and Yokosawa, 2005; Zou et al., 2005), and 2) the ISGylation of filamin B was shown to lead to release of RAC1, MEKK1, and MKK4 from the scaffold, preventing JNK activation (Jeon et al., 2008). These studies suggest that ISG15 non-specifically disrupts the function of its target proteins by physical occlusion or obstruction. One major issue with these studies is only a very small fraction of the total

pool of any target protein is modified with ISG15 and therefore, it is unclear how modification of a small fraction of any individual target protein might have a significant effect on the overall activity of that protein.

Type 1 IFNs are secreted by virus-infected cells to establish an anti-viral state in uninfected surrounding cells (Samuel, 2001). As these cells are likely to be the next sites of virus infection, newly synthesized viral proteins may be the targets of the ISGylation system. In support of viral protein ISGylation, the influenza A viral protein, NS1, was recently shown to conjugated with ISG15 (Zhao et al., 2009). As with host cellular proteins, there is still the question of how modification of a small fraction of a viral protein could have a significant anti-viral effect. The answer may lay in the fact that structural proteins must often assemble into precise repeating geometric configurations to form infectious virus particles (*e.g.*, capsid proteins).

Human papillomavirus (HPV) is a non-enveloped icosahedral virus encapsidating an 8kb circular, double-stranded DNA. Papillomavirus virions are composed of 360 molecules of L1 (major capsid protein) and up to 72 molecules of L2 (minor capsid protein) (Buck et al., 2008). L1 and L2 assemble into virions and undergo a process by which inter-L1 disulfide bonds form and stabilize the virion (Buck et al., 2005b). During the maturation process the virions decrease in size to approximately 55 nm. HPV virion assembly has been well studied and there are established protocols for the production of pseudovirions (PsV) (Buck et al., 2005a). HPV PsV are similar to HPV virions, but instead of encapsidating the HPV genome, any double-stranded circular DNA ~8kb can be packaged. We therefore employed an HPV pseudovirus (PsV) system to determine if ISGylation had an effect on infectivity. The findings presented here provide a proof of

principle that low-level ISGylation of a virus structural protein can have dominant negative effects on virus infectivity.

5.2 RESULTS

5.2.1 ISG15 modification of HPV16 L1.

We first determined if HPV16 capsid proteins, L1 and L2, were modified by co-transfection of a plasmid expressing L1 and L2 (p16shell) with the ISGylation components. Figure 5.1 shows that HPV16 L1 is modified with ISG15. Currently, the status of L2 ISGylation is unknown. We have been testing multiple antibodies and have not achieved clear results yet. Next, we identified the ISG15 conjugation sites on the HPV16 L1 protein. 293TT cells were transfected as in Figure 5.1. The HPV16 L1-ISG15 conjugates were purified by immunoprecipitation with anti-HPV16 L1. Mass spectrometry analysis identified two lysines residues that were conjugated with ISG15: lysine 64 and lysine 309. These lysines are located in the BC-loop region and between the G1 and G2 β-strands, respectively (Chen et al., 2000).

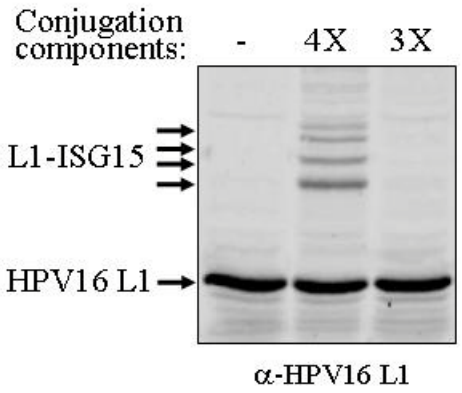

Figure 5.1: ISGylation of HPV16 L1.

293TT cells were co-transfected with p16shell, alone, or with plasmids expressing ISG15, Ube1L, UbcH8, and Herc5 (4X) or this set of plasmids without ISG15 (3X). Cells extracts were analyzed by SDS-PAGE and immunoblotting with anti-L1 antibody.

5.2.2 HPV16 Pseudovirus System

We therefore employed an HPV pseudovirus (PsV) system to measure the effect of ISGylation on infectivity (Buck et al., 2005a). When L1 and L2 are expressed in the presence of a ~8 kbp GFP expression plasmid, the plasmid is packaged as if it were viral genomic DNA; these PsV can then be isolated on velocity-density gradients and their infectivity measured by quantitating the delivery of the GFP reporter plasmid to naive cells (Figure 5.2). HPV16 pseudoviruses were generated in 293TT cells in which ISG15 conjugation was either occurring (co-transfection of ISG15 and E1, E2, E3 enzymes) or not occurring (co-transfection of ISG15 and inactive mutant forms of the E1, E2, and E3 enzymes).

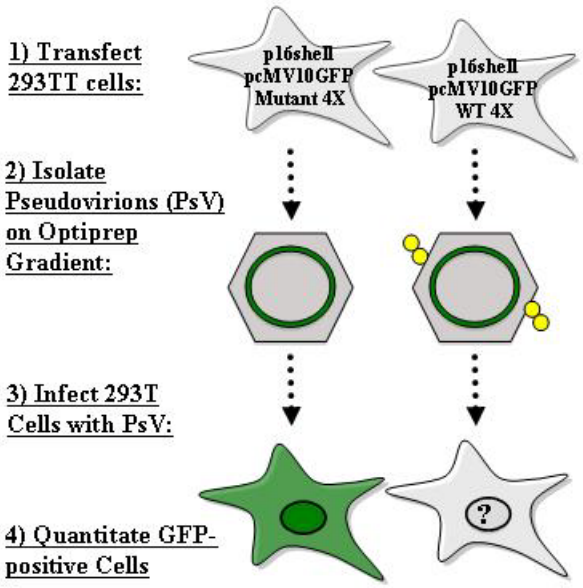

Figure 5.2: Schematic of HPV PsV Experimental Design.

Initially, HPV16 pseudoviruses were generated in 293TT cells in which ISG15 conjugation was not occurring. After ultracentrifugation through the Optiprep gradient, twelve fractions were obtained and analyzed for the presence of assembled PsV at the expected gradient fractions. Previous reports suggested that large amounts of properly assembled PsV would migrate to fractions five through eight; also known as the peak PsV fractions (Buck et al., 2004). This was confirmed by transmission electron microscopy of these fractions (Figure 5.3A) as well as by determination of the fraction infectivity by FACS analysis (Figure 5.3B).

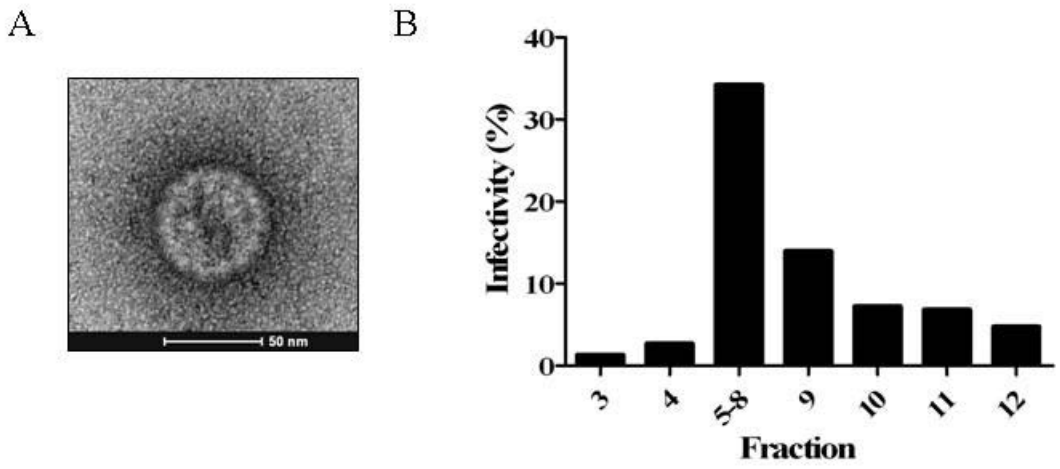

Figure 5.3: Confirmation of properly assembled HPV PsV.

A) Transmission electron microscopy (TEM) of HPV16 PsV. HPV16 PsV were isolated from an Optiprep gradient, absorbed to carbon-coated copper grids, and stained with 1% uranyl acetate before viewing.
B) Fractions 5-8 contain pronounced amounts of HPV16 PsV. Equal volumes of HPV16 PsV fractions obtained from Optiprep gradients were added to 293T cells. Sixty hours post-infection, GFP-positive cells were quantitated by FACS analysis.

5.2.3 The effect of HPV16 L1 ISGylation on PsV Infectivity.

HPV pseudovirions were generated in the presence of either a wild-type 4X or mutant 4X. Peak PsV fractions (fractions 5-8) from the Optiprep gradient were pooled for each and used to determine the ISGylation status of L1 as well as the infectivity. In the ISGylated PsV fractions, approximately 10% of the total L1 protein was ISGylated (Figure 5.4A). The total amount of L1 protein in ISGylated PsV fractions was approximately 30% less than in the control PsV fractions. Together, these observations indicated that ISGylated L1 was incorporated into PsV particles, but that the overall yield of PsV was decreased. To examine the infectivity of ISGylated and non-ISGylated PsV,

the peak gradient fractions were added to the culture media of 293T cells, followed by quantitation of GFP-positive cells by FACS analysis. Without normalization for total L1 concentration, the infectivity of ISGylated PsV was decreased approximately 80% relative to the non-ISGylated PsV in three independent experiments (Figure 5.4B). With normalization, the infectivity of ISGylated PsV was approximately 70% lower than non-ISGylated PsV (Figure 5.4B). These results establish that low-level ISGylation of a viral structural protein can have a dominant-negative effect on virus infectivity.

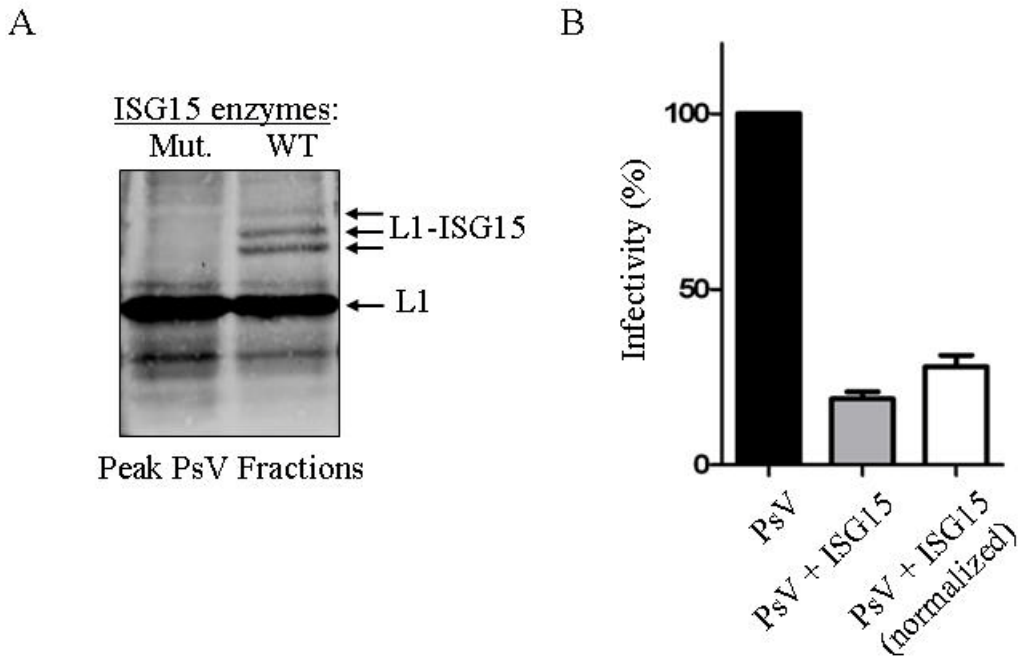

Figure 5.4: Low-level ISGylation of HPV16 L1 has a dominant-negative effect of virus infectivity.

A) ISGylated HPV16 L1 is detected in fractions containing HPV Pseudovirus. Equal volumes of PsV-containing fractions, prepared in cell expressing active ISGylation enzymes (WT) or inactive mutants (Mut.), were separated by SDS-PAGE and immunoblotted with anti-L1 antibody.
B) ISGylation of HPV16 L1 decreases the infectivity of HPV Pseudovirus. 293T cells were infected with equal volumes PsV from the fractions shown in Figure 7B, formed either in the absence (PsV) or presence (PsV + ISG15) of the ISG15 conjugation system. GFP-positive cells were counted 60 hours post-infection by FACS. The infectivity of wild type PsV was set to 100%. Results are presented both without (middle) and with (right) normalization for total L1 protein concentration. Error bars indicate standard error of the mean of three independent experiments performed in triplicate.

5.3 DISCUSSION

The findings presented here have implications for the identity of the biologically relevant targets of ISG15. Interferon-stimulated cells are primed to defend against an impending viral infection, which suggests that newly translated viral proteins might be

biologically relevant targets of the ISG15 system. The low degree of target protein selectivity of the ISG15 system is consistent with the requirement that the innate immune response protect cells against a wide range of pathogens. We previously proposed a model where Herc5 modifies newly synthesized polypeptides co-translationally (Durfee, In press). An implication of this model is that modification of cellular target proteins may be simply collateral damage in the attempt to target viral proteins. This, in turn, may be tied to the observation that ISGylation is relatively inefficient: an inefficient ISGylation system might protect against excessive damage to cellular proteins, while at the same time still be an effective anti-viral due to dominant-negative effects on abundantly expressed virus structural proteins (Figure 5.5).

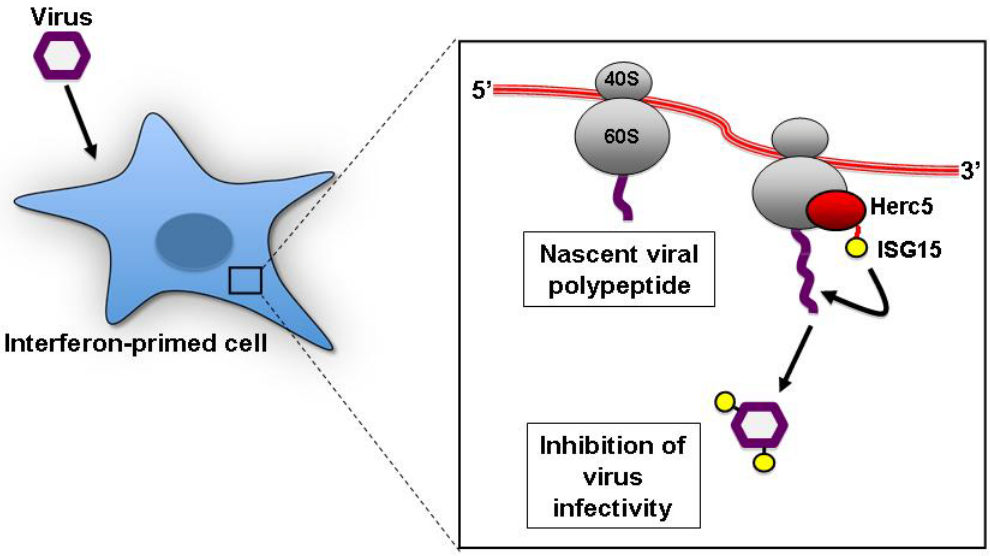

Figure 5.5: Model for the anti-viral function of ISG15 conjugation.

The HPV pseudovirus system provides a proof of principle that low-level ISGylation of a virus structural protein can have dominant negative effects on virus infectivity. The precise step in the infectivity of HPV pseudoviruses that is affected by

ISGylation of HPV capsids is not yet known, but could range from receptor recognition, to a defect in endocytosis or release from endocytic compartments, to the delivery of the packaged DNA to the nucleus. The lysines identified by the mass spectrometry do not correspond to lysine residues with previously published roles in HPV capsid formation or infection (Bishop et al., 2007; Knappe et al., 2007), but not all thirty-four lysines in HPV16 L1 have been characterized.

The effect of type 1 interferons on HPV replication is known to be complex (Beglin et al., 2009), however multiple studies have indicated that HPVs interfere with expression and/or function of components of the interferon response (Barnard and McMillan, 1999; Chang and Laimins, 2000; Nees et al., 2001; Ronco et al., 1998). In addition, topical IFN-α is an approved treatment for certain HPV lesions (Slade et al., 1998). The results presented here warrant an examination of the role of the ISG15 system in the response of HPV lesions to type 1 IFNs and, more broadly, of the effect on ISG15 on proteins of many other classes of viruses. For example, pseudovirion systems have been established for many other viruses. These systems can be used to examine if ISG15 disrupts virion formation of viruses besides HPV.

In addition to virion assembly, ISG15 may disrupt the function of other types of viral proteins that multimerize. HIV Rev is a good candidate as it oligomerizes to form a complex that transports viral mRNAs out of the nucleus (Dimattia et al., 2010). A recent example of non-structural viral protein ISGylation is the modification of the NS1A protein of H1N1 influenza A/WSN/33 (WSN) virus (Zhao et al., 2009). Zhao *et al.* demonstrated that approximately 5% of NS1A is ISGylated and mutation of one lysine residue, K41R, of NS1A led to a approximately 90% decrease in this ISGylation. In addition, this mutation in NS1A was shown to be important for inhibition of viral

replication. These results are another example of inhibition of viral replication by low-level ISGylation of a viral protein. The mechanism behind this inhibition is unknown.

Chapter 6: Future Directions

My thesis work has addressed two aspects of the human ISG15 conjugation system: 1) the specificity of the Ube1L-UbcH8 interaction and 2), the basis of substrate recognition by Herc5. I have shown that interactions between the UFD of Ube1L and the α1-helix and β1–β2 region within UbcH8 mediate the specific selection of UbcH8 by Ube1L. In addition, I have demonstrated that UbcH8 is unlikely to function as a Ub E2 in most cell lines. Based on the Herc5 work, I have proposed a model for ISGylation in which Herc5 broadly modifies newly synthesized proteins in a co-translational manner and suggested that, in the context of an interferon-stimulated cell, newly translated viral proteins may be primary targets of ISG15. Consistent with this, I have shown that ISGylation of the human papillomavirus (HPV) L1 capsid protein has a dominant-inhibitory effect on the infectivity of HPV16 pseudoviruses. These discoveries have greatly increased our understanding of the mechanism of ISG15 conjugation and raised many new questions regarding specificity within the ISG15 pathway, the mechanism for modification of newly synthesized proteins, and the dominant-negative inhibition of viral proteins.

6.1: SPECIFICITY WITHIN THE ISG15 PATHWAY

There are features of the ISG15 pathway that more closely resemble features of the Ub system than other Ubl systems. For example, human Ube1L is the most closely related E1 enzyme to human Ube1 ($E1^{Ub}$), and ISG15 is the only Ubl where the last six

residues of the protein (LRLRGG) are identical to that of Ub. In addition, UbcH8 was initially reported to be an E2 for the Ub pathway. Furthermore, Herc5 is the only HECT E3 enzyme known to function with a Ubl, rather than Ub. While my work has identified the basis for specific recruitment of UbcH8 by Ube1L, several questions remain.

Ube1L activates only ISG15 and Ube1 activates only Ub, but the basis for this specificity is unknown. The E1 enzymes for Nedd8 and SUMO do not charge Ub due to specific C-terminal residues in Ub that differ from those in their Ubls (Schulman and Harper, 2009). These residues are identical between ISG15 and Ub and therefore, it is unclear what restricts Ube1L from charging Ub. A recent structure of Uba1 (yeast $E1^{Ub}$) with Ub might shed some light on this question. Lee *et al.* identified residues within three interfaces responsible for the Ub-Uba1 interaction, including the C-terminal LRLRGG residues (Lee and Schindelin, 2008). Many of these residues are not conserved in Ube1L and the C-terminal half of ISG15. For example, hydrophobic residues in the adenylation domain of Uba1 interact with the canonical hydrophobic patch of Ub, but both ISG15 and Ube1L lack these types of residues in the corresponding regions.

While it has been established that no other E3 can substitute for Herc5 in the broad conjugation of ISG15 (Dastur et al., 2006; Dastur, 2007), it is possible that Herc5 participates in ubiquitination, or even further, catalyzes a ubiquitination event required for ISGylation. HECT E3 ligases are capable of autoconjugating Ub, but this has never been observed by western blot analysis of exogenously expressed Herc5 (Dastur, 2007). In contrast, Herc5 autoISGylation is easily detected when it is expressed with the ISG15 conjugation machinery. Therefore, there would appear to be mechanistic or structural features of Herc5 that distinguish it from Ub HECT E3s, or Herc5 might simply preferentially recruit UbcH8 over other E2s. *In vitro*, the Ub HECT E3s RSP5 and E6AP

can be forced to receive ISG15 from UbcH8 which suggests the Herc5-E2 interaction may be important for maintaining pathway specificity (Zhao et al., 2004).

In addition to Herc5, there are many questions surrounding the role of Herc6 in the ISG15 pathway. Previous results have shown that human Herc6 is, at best, a minor E3 ligase for ISG15 (Dastur et al., 2006; Dastur, 2007). It is possible that Herc6 has a limited number of target proteins or that Herc6 may participate in ubiquitination, although this has never been observed *in vivo*. Understanding the role of Herc6 is further complicated by the fact that rodents lack a direct equivalent to Herc5 and instead have only Herc6. Furthermore, recent results suggest mouse Herc6 can support broad ISGylation (Versteeg et al., 2010). Mouse Herc6 shares a similar domain organization and is interferon-induced like human Herc5 and Herc6, however it shares more identity with human Herc6 than Herc5. It is unclear why mouse Herc6 supports ISGylation, but not human Herc6. We are currently testing human and mouse Herc6 to see if they associate with polysome fractions in a manner similar to that of Herc5. Additionally, we need to examine these three enzymes more closely to identify determinants that prevent human Herc6 from functioning like mouse Herc6 and human Herc5.

6.2: MECHANISM FOR MODIFICATION OF NEWLY SYNTHESIZED PROTEINS

I have shown that Herc5 co-fractionates with polysomes and loss of the N-terminal RCC repeats of Herc5 shifts it out of the polysomes. Using RNase and EDTA treatments, I have demonstrated that Herc5 is not associated with polysomes via mRNA or nascent chains. Instead, these treatments suggest Herc5 is associated with a core component of the 60S ribosomal subunit. As the exit tunnel for nascent polypeptides is on the 60S subunit (Kramer et al., 2009), an attractive model is that Herc5 modifies newly synthesized polypeptides co-translationally, as they emerge from the exit tunnel.

Therefore, it is important to determine how Herc5 interacts with the ribosome. The eukaryotic exit tunnel consists primarily of rRNA in complex with the ribosomal proteins L4, L17, L25, and L39 (nearest to the exit) (Bhushan et al., 2010). One protein in particular, L25, is of interest because it has been shown to act as a docking protein for many proteins which act on nascent chains (Kramer et al., 2009). While Herc5 may associate directly with a protein such as L25, it is also possible that the interaction is mediated by another ribosomal associated protein or that Herc5 may bind rRNA. We initially attempted to use the yeast system to address the interaction because of the well characterized ribosomal mutant strains available. Unfortunately, Herc5 did not associate with polysomes in yeast. This was not entirely unexpected as yeast lack the ISG15 pathway. Currently, we are exploring the Herc5-ribosome interaction using immunoprecipitation (IP) techniques in conjunction with crosslinkers to stably link Herc5 to the ribosome before IP.

While I have shown that ISG15 modification occurs on newly synthesized proteins and that Herc5 associates with the ribosome, I have yet to determine if modification occurs co-translationally. One way to address this question is to isolate ribosomal bound nascent chains and examine them for ISG15 modification. Our current approach involves large-scale isolation of cycloheximide-treated ribosomes from mammalian cells transfected with the ISG15 components. The low level of nascent chains coupled with the inefficiency of ISGylation has precluded a definitive answer so far. A complete *in vitro* system would be helpful in testing this model because it would allow us to examine modification of a single, well-modified target protein under variable conditions.

Another interesting question involves the factors influencing ISG15 modification of newly synthesized proteins. It is important to note that although the list of ISG15 target proteins appears extremely broad, not all newly synthesized proteins were ISGylated. GFP, human Wbp2, and a fragment of paxillin were consistently not ISGylated in our assay system. In addition, examination of the modification sites of a limited number of ISGylated proteins suggests there are preferential modification sites within target proteins. Ubc13 is ISGylated only at K92, but contains eight other lysines, while mass spectrometry results for HPV16 L1 identified only two modification sites (K64 and K309) out of a potential thirty-four lysines. Identifying modification sites on additional target proteins would be helpful in determining if sequence or secondary structure context are factors in the selection of lysine acceptors. In addition, ISGylation might be influenced by translation rates or co-translation folding. In the future, we would like to see if altering the rate of translation alters the level of ISGylation. One option might be to stall translation by deleting the termination codon of a gene. Alternatively, larger proteins might be preferentially modified due to slow translating regions present to facilitate co-translational folding. Clearly, there are many potential factors to be explored.

Determining the mechanism for the modification of newly synthesized proteins is complicated by the fact that we are unable to reconstitute an *in vitro* ISGylation system. We can generate thioester formation between UbcH8 and ISG15 however, even with the addition of purified Herc5, we have been unable to transfer ISG15 from UbcH8 to Herc5 and therefore we have been unable to re-create ISGylation of target proteins. It has been unclear if purified Herc5 is inactive or if an additional factor(s) is required to support ISGylation. Polysome association of Herc5 suggests that the inclusion of a translation

system may be a requirement for reconstitution of *in vitro* ISGylation. We are in the process of examining rabbit reticulocyte lysate (RRL) as a possible *in vitro* translation system however, it is unknown if Herc5 can associate with rabbit ribosomal proteins. In addition, we are developing an *in vitro* translation system using polysomes isolated from mammalian cell lysate. An *in vitro* system would be useful not only for examining E3 ligase specificity as discussed above, but also for testing the ISG15 co-translational modification model and examining factors influencing modification.

6.4: DOMINANT-NEGATIVE INHIBITION OF VIRAL PROTEINS

I have shown that the human papillomavirus (HPV) L1 capsid protein can be ISGylated and although only a small fraction of L1 is modified, there is a significant decrease in the infectivity of ISGylated HPV pseudovirus (PsV). These results raise two major questions: 1) what is the precise step in the infectivity of HPV PsV that is affected by ISGylation of HPV capsids, and 2) is the ISG15 mediated decrease in infectivity observable *in vivo*? The decrease in infectivity could be stem from issues with DNA packaging or receptor recognition, to a defect in endocytosis or release from endocytic compartments, to the delivery of the packaged DNA to the nucleus. Preliminary experiments where ISG15 was removed from mature PsV showed these PsV had the same decrease in infectivity as mature PsV with ISG15. This suggests ISG15 somehow disrupted the PsV structure, but was not required once that alteration occurs. Observing the effect of ISG15 on HPV *in vivo* is much more complicated due to the requirement of differentiating epithelial cells for the life cycle of HPV. Raft tissue culture systems for HPV exist, however issues with transfection efficiency, the interferon response, and the long length of time required for differentiation would need to be addressed.

Alternatively, it will be important to test other viral structural and non-structural proteins to see if ISG15 mediates a dominant-negative effect similar to that seen in the HPV system. For example, a pseudovirion system has been established for murine leukemia virus (MLV). Similar to the HPV system, infectious MLV PsV can be generated by packaging a GFP reporter plasmid. Pseudovirion systems similar to MLV exist for HIV and can be examined as well. In addition to virion assembly, ISG15 may disrupt the function of other types of viral proteins that multimerize. HIV Rev is a good candidate as it oligomerizes to form a complex that transports viral mRNAs out of the nucleus. HIV Integrase would also be a good candidate because it is thought to function biologically as a tetramer and I have shown that it can be ISGylated.

Appendix I

A1.1 Experiment I.: Mutation of the ISG15 contact sites disrupts ISG15 conjugation.

The crystal structure of ISG15 identified several contact sites between the N-terminal and C-terminal domains of ISG15 (Narasimhan et al., 2005). These two domains contact each other via van der Waals interactions between N-terminal residues histidine 39 and phenylalanine 41 and the C-terminal residues proline 136 and glycine 138. We constructed an ISG15 C-terminal contact mutant (P136A/G138A) and an ISG15 N-terminal contact mutant (H39A/F41A), and examined ISGylation when expressed in HEK293 cells along with Ube1L, UbcH8, and Herc5. While the N terminal domain is not required for ISG15 conjugation (see Figure A2), disruption of the N contact sites reduces conjugation suggesting that, if the N terminal domain is improperly oriented, it can inhibit conjugation. The C contact mutations have a larger effect on conjugation, which could be due to a combination of a improper orientation and an effect on utilization of the C terminal domain by one or more enzymes of the pathway.

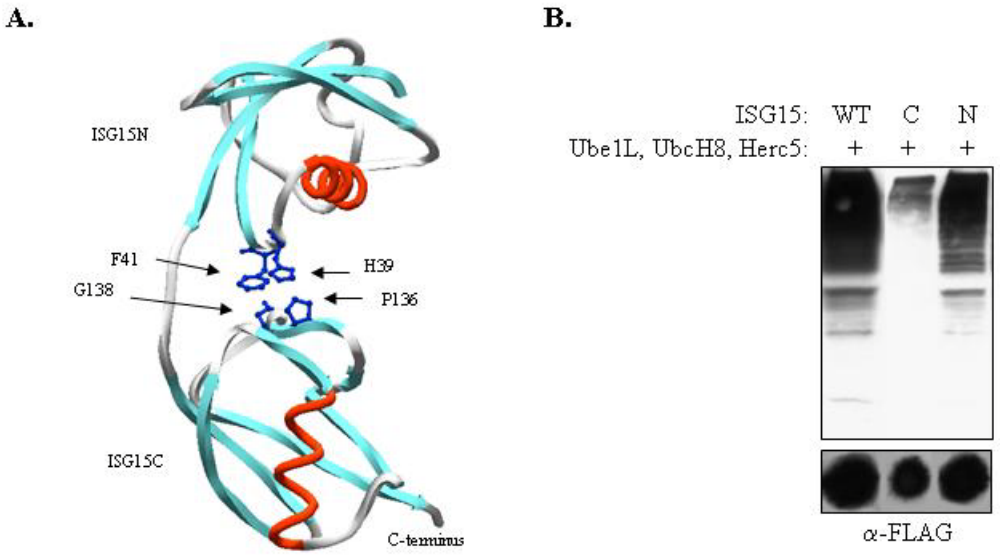

Figure A1. Mutation of the ISG15 contact sites.

A) Structure of ISG15 (PDB 1Z2M). The contact sites (dark blue) are indicated.
B) HEK293 cells were transfected with plasmids expressing Ube1L, UbcH8, Herc5, and either wild type (WT), C-terminal contact mutant (C), or N-terminal contact mutant (N) FLAG-ISG15. Cell extracts were prepared and analyzed by immunoblotting with anti-FLAG antibody to detect ISG15 conjugates (top). Expression of each FLAG-ISG15 construct was confirmed by applying the same amounts of cell extracts as in the top to nitrocellulose using the Bio-Dot Apparatus (Bio-Rad) and blotting with anti-FLAG antibody (bottom).

A1.2 EXPERIMENT II: ISG15-ΔN CAN SUPPORT ISG15 CONJUGATION

ISG15 consists of two Ub-like domains. To begin to characterize the determinants on ISG15 required for the recognition by Ube1L and UbcH8, we determined the effect of deleting the N-terminal Ub-like domain of ISG15 (ISG15-ΔN, deleted of residues 2-78). ISG15-ΔN was activated by wild-type Ube1L and transferred to UbcH8 *in vitro* (Figure A2A). Furthermore, ISG15-ΔN was conjugated to cellular proteins when expressed in HEK293 cells along with Ube1L, UbcH8, and Herc5 (Figure A2B). As with wild-type ISG15, conjugation was dependent on Ube1L, UbcH8, and Herc5. Conjugation of ISG15-ΔN was slightly less efficient than with wild-type ISG15, although this may have been due to a reproducibly lower expression of ISG15-ΔN compared to full-length ISG15 (not shown). These results suggest the primary determinants of ISG15 recognized by all of the central components of the conjugation system are located within the C-terminal Ub-like domain of ISG15. However, careful kinetic analyses of ISG15-ΔN is needed at each step of conjugation to determine to determine the role of the N-terminal lobe of ISG15.

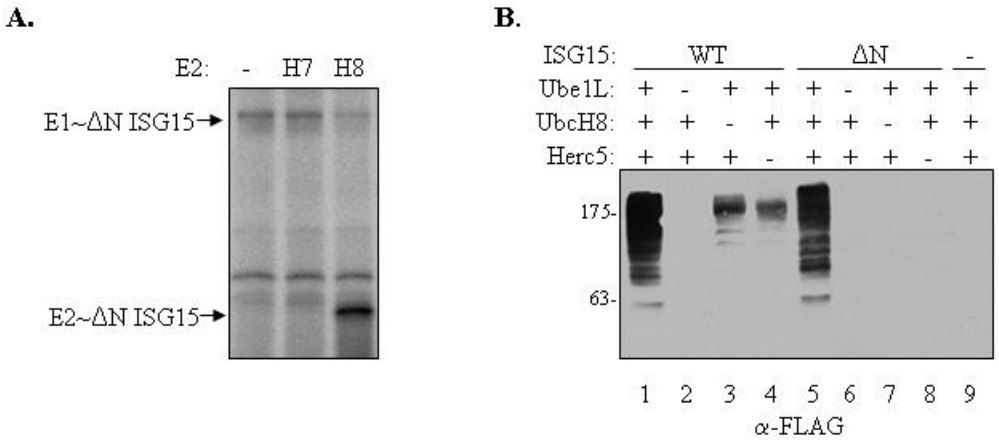

Figure A2: ISG15-ΔN can support ISG15 conjugation.

A) ^{32}P-ISG15ΔN was incubated with Ube1L and either no E2, UbcH7, or UbcH8. Reaction products were analyzed by SDS-PAGE without reducing agent. An E2-independent background band is indicated (*).
B) 293 cells were transfected with plasmids expressing FLAG-ISG15 (lanes 1-4) or FLAG-ISG15ΔN (lanes 5-8) and with or without plasmids expressing Ube1L, UbcH8, and Herc5, as indicated. Lane 9 contained no ISG15-expressing plasmid. Cell extracts were collected and immunoblotted with anti-FLAG antibody.

A1.3 METHODS FOR APPENDIX I.

Transfection Assays. Human HEK293 cells were grown in Dulbecco's modified Eagle's medium supplemented with 10% fetal bovine serum. Plasmid DNA transfections were performed with cells at 80% confluence using Lipofectamine transfection reagent (Invitrogen). For the experiment shown in Figure A1B, plasmids expressing Herc5 (0.5 μg), UbcH8 (0.25 μg), and Ube1L (0.25 μg) were transfected with either 1X-FLAG ISG15 wild type, C-terminal mutant, or N-terminal mutant (0.5 μg). For the experiment shown in Figure A2B, plasmids expressing Herc5 (0.5 μg), UbcH8 (0.25 μg), and Ube1L (0.25 μg) were transfected as indicated with either 1X-FLAG ISG15 wild type or 1X-FLAG ISG15-ΔN (0.5 μg). Cells were harvested and lysed 48 hours post-transfection in lysis buffer containing 1% Nonidet P-40, 100 mM Tris, pH 7.9, 100 mM NaCl, 1 mM DTT, 100 μM phenylmethylsulfonyl fluoride, 4 μM leupeptin, 0.3 μM aprotinin. 30 μg of total cell proteins were separated by SDS-PAGE, transferred to nitrocellulose membrane, and probed with anti-FLAG antibody (Sigma) to detect ISG15-conjugated proteins. Alternatively, 30 μg of total cell proteins were applied to nitrocellulose using the Bio-Dot Apparatus (Bio-Rad) in the bottom of Figure A1B.

Thioester Assay. The experiment in Figure A2A was performed similarly to that in Figure 3.2 as described in Chapter 2.1 under biochemical assays except that the incubation time was 30 minutes. ^{32}P-ISG15-ΔN was prepared as described for ^{32}P-ISG15 in Chapter 2.1 as well.

References

Ablasser, A., Bauernfeind, F., Hartmann, G., Latz, E., Fitzgerald, K.A. and Hornung, V. (2009) RIG-I-dependent sensing of poly(dA:dT) through the induction of an RNA polymerase III-transcribed RNA intermediate. *Nat Immunol*, **10**, 1065-1072.

Ank, N., Iversen, M.B., Bartholdy, C., Staeheli, P., Hartmann, R., Jensen, U.B., Dagnaes-Hansen, F., Thomsen, A.R., Chen, Z., Haugen, H., Klucher, K. and Paludan, S.R. (2008) An important role for type III interferon (IFN-lambda/IL-28) in TLR-induced antiviral activity. *J Immunol*, **180**, 2474-2485.

Ank, N. and Paludan, S.R. (2009) Type III IFNs: new layers of complexity in innate antiviral immunity. *Biofactors*, **35**, 82-87.

Barnard, P. and McMillan, N.A. (1999) The human papillomavirus E7 oncoprotein abrogates signaling mediated by interferon-alpha. *Virology*, **259**, 305-313.

Bayer, P., Arndt, A., Metzger, S., Mahajan, R., Melchior, F., Jaenicke, R. and Becker, J. (1998) Structure determination of the small ubiquitin-related modifier SUMO-1. *J Mol Biol*, **280**, 275-286.

Beaudenon, S. and Huibregtse, J.M. (2005) High level expression and purification of recombinant E1 enzyme. *Meth. Enzym.*, **in press**.

Beglin, M., Melar-New, M. and Laimins, L. (2009) Human papillomaviruses and the interferon response. *J Interferon Cytokine Res*, **29**, 629-635.

Bencsath, K.P., Podgorski, M.S., Pagala, V.R., Slaughter, C.A. and Schulman, B.A. (2002) Identification of a multifunctional binding site on Ubc9p required for Smt3p conjugation. *J Biol Chem*, **277**, 47938-47945.

Bennett, E.J. and Harper, J.W. (2008) DNA damage: ubiquitin marks the spot. *Nat Struct Mol Biol*, **15**, 20-22.

Bernier-Villamor, V., Sampson, D.A., Matunis, M.J. and Lima, C.D. (2002) Structural basis for E2-mediated SUMO conjugation revealed by a complex between ubiquitin-conjugating enzyme Ubc9 and RanGAP1. *Cell*, **108**, 345-356.

Bhushan, S., Gartmann, M., Halic, M., Armache, J.P., Jarasch, A., Mielke, T., Berninghausen, O., Wilson, D.N. and Beckmann, R. (2010) alpha-Helical nascent polypeptide chains visualized within distinct regions of the ribosomal exit tunnel. *Nat Struct Mol Biol*, **17**, 313-317.

Birmachu, W., Gleason, R.M., Bulbulian, B.J., Riter, C.L., Vasilakos, J.P., Lipson, K.E. and Nikolsky, Y. (2007) Transcriptional networks in plasmacytoid dendritic cells stimulated with synthetic TLR 7 agonists. *BMC Immunol*, **8**, 26.

Bishop, B., Dasgupta, J. and Chen, X.S. (2007) Structure-based engineering of papillomavirus major capsid l1: controlling particle assembly. *Virol J*, **4**, 3.

Blomstrom, D.C., Fahey, D., Kutny, R., Korant, B.D. and Knight, E., Jr. (1986) Molecular characterization of the interferon-induced 15-kDa protein. Molecular cloning and nucleotide and amino acid sequence. *J Biol Chem*, **261**, 8811-8816.

Buck, C.B., Cheng, N., Thompson, C.D., Lowy, D.R., Steven, A.C., Schiller, J.T. and Trus, B.L. (2008) Arrangement of L2 within the papillomavirus capsid. *J Virol*, **82**, 5190-5197.

Buck, C.B., Pastrana, D.V., Lowy, D.R. and Schiller, J.T. (2004) Efficient intracellular assembly of papillomaviral vectors. *J Virol*, **78**, 751-757.

Buck, C.B., Pastrana, D.V., Lowy, D.R. and Schiller, J.T. (2005a) Generation of HPV pseudovirions using transfection and their use in neutralization assays. *Methods Mol Med*, **119**, 445-462.

Buck, C.B., Thompson, C.D., Pang, Y.Y., Lowy, D.R. and Schiller, J.T. (2005b) Maturation of papillomavirus capsids. *J Virol*, **79**, 2839-2846.

Catic, A., Fiebiger, E., Korbel, G.A., Blom, D., Galardy, P.J. and Ploegh, H.L. (2007) Screen for ISG15-crossreactive deubiquitinases. *PLoS ONE*, **2**, e679.

Chang, Y.E. and Laimins, L.A. (2000) Microarray analysis identifies interferon-inducible genes and Stat-1 as major transcriptional targets of human papillomavirus type 31. *J Virol*, **74**, 4174-4182.

Chang, Y.G., Yan, X.Z., Xie, Y.Y., Gao, X.C., Song, A.X., Zhang, D.E. and Hu, H.Y. (2008) Different roles for two ubiquitin-like domains of ISG15 in protein modification. *J Biol Chem*, **283**, 13370-13377.

Chen, X.S., Garcea, R.L., Goldberg, I., Casini, G. and Harrison, S.C. (2000) Structure of small virus-like particles assembled from the L1 protein of human papillomavirus 16. *Mol Cell*, **5**, 557-567.

Chin, L.S., Vavalle, J.P. and Li, L. (2002) Staring, a novel E3 ubiquitin-protein ligase that targets syntaxin 1 for degradation. *J Biol Chem*, **277**, 35071-35079.

Chiu, Y.H., Macmillan, J.B. and Chen, Z.J. (2009) RNA polymerase III detects cytosolic DNA and induces type I interferons through the RIG-I pathway. *Cell*, **138**, 576-591.

Chiu, Y.H., Sun, Q. and Chen, Z.J. (2007) E1-L2 activates both ubiquitin and FAT10. *Mol Cell*, **27**, 1014-1023.

Ciechanover, A. (2009) Tracing the history of the ubiquitin proteolytic system: the pioneering article. *Biochem Biophys Res Commun*, **387**, 1-10.

Ciehanover, A., Hod, Y. and Hershko, A. (1978) A heat-stable polypeptide component of an ATP-dependent proteolytic system from reticulocytes. *Biochem Biophys Res Commun*, **81**, 1100-1105.

Clementz, M.A., Chen, Z., Banach, B.S., Wang, Y., Sun, L., Ratia, K., Baez-Santos, Y.M., Wang, J., Takayama, J., Ghosh, A.K., Li, K., Mesecar, A.D. and Baker, S.C. (2010) Deubiquitinating and interferon antagonism activities of coronavirus papain-like proteases. *J Virol*, **84**, 4619-4629.

Dar, A.C., Dever, T.E. and Sicheri, F. (2005) Higher-order substrate recognition of eIF2alpha by the RNA-dependent protein kinase PKR. *Cell*, **122**, 887-900.

Dastur, A., Beaudenon, S., Kelley, M., Krug, R.M. and Huibregtse, J.M. (2006) Herc5, an interferon-induced HECT E3 enzyme, is required for conjugation of ISG15 in human cells. *J Biol Chem*, **281**, 4334-4338.

Dastur, A.R. (2007) Characterization of Herc5: the major ligase for ISG15, an antiviral ubiquitin-like protein. University of Texas at Austin, Austin, Vol. PhD.

Der, S.D., Zhou, A., Williams, B.R. and Silverman, R.H. (1998) Identification of genes differentially regulated by interferon alpha, beta, or gamma using oligonucleotide arrays. *Proc Natl Acad Sci U S A*, **95**, 15623-15628.

Deshaies, R.J. and Joazeiro, C.A. (2009) RING domain E3 ubiquitin ligases. *Annu Rev Biochem*, **78**, 399-434.

Dimattia, M.A., Watts, N.R., Stahl, S.J., Rader, C., Wingfield, P.T., Stuart, D.I., Steven, A.C. and Grimes, J.M. (2010) Implications of the HIV-1 Rev dimer structure at 3.2 A resolution for multimeric binding to the Rev response element. *Proc Natl Acad Sci U S A*, **107**, 5810-5814.

Duda, D.M., Borg, L.A., Scott, D.C., Hunt, H.W., Hammel, M. and Schulman, B.A. (2008) Structural insights into NEDD8 activation of cullin-RING ligases: conformational control of conjugation. *Cell*, **134**, 995-1006.

Durfee, L.A., Kelley, M.L. and Huibregtse, J.M. (2008) The basis for selective E1-E2 interactions in the ISG15 conjugation system. *J Biol Chem*, **283**, 23895-23902.

Durfee, L.A., Lyon, N., Seo, K., and Huibregtse, J.M. (In press) The ISG15 conjugation system broadly targets newly synthesized proteins: implications for
the anti-viral function of ISG15. *Molecular Cell*.

Eletr, Z.M., Huang, D.T., Duda, D.M., Schulman, B.A. and Kuhlman, B. (2005) E2 conjugating enzymes must disengage from their E1 enzymes before E3-dependent ubiquitin and ubiquitin-like transfer. *Nat Struct Mol Biol*, **12**, 933-934.

Eletr, Z.M. and Kuhlman, B. (2007) Sequence Determinants of E2-E6AP Binding Affinity and Specificity. *J Mol Biol*, **369**, 419-428.

Farrell, P.J., Broeze, R.J. and Lengyel, P. (1979) Accumulation of an mRNA and protein in interferon-treated Ehrlich ascites tumour cells. *Nature*, **279**, 523-525.

Fortier, J.M. and Kornbluth, J. (2006) NK lytic-associated molecule, involved in NK cytotoxic function, is an E3 ligase. *J Immunol*, **176**, 6454-6463.

French, M.E., Kretzmann, B.R. and Hicke, L. (2009) Regulation of the RSP5 ubiquitin ligase by an intrinsic ubiquitin-binding site. *J Biol Chem*, **284**, 12071-12079.

Frias-Staheli, N., Giannakopoulos, N.V., Kikkert, M., Taylor, S.L., Bridgen, A., Paragas, J., Richt, J.A., Rowland, R.R., Schmaljohn, C.S., Lenschow, D.J., Snijder, E.J., Garcia-Sastre, A. and Virgin, H.W.t. (2007) Ovarian tumor domain-containing viral proteases evade ubiquitin- and ISG15-dependent innate immune responses. *Cell Host Microbe*, **2**, 404-416.

Geiss-Friedlander, R. and Melchior, F. (2007) Concepts in sumoylation: a decade on. *Nat Rev Mol Cell Biol*, **8**, 947-956.

Giannakopoulos, N.V., Arutyunova, E., Lai, C., Lenschow, D.J., Haas, A.L. and Virgin, H.W. (2009) ISG15 Arg151 and the ISG15-conjugating enzyme UbE1L are important for innate immune control of Sindbis virus. *J Virol*, **83**, 1602-1610.

Giannakopoulos, N.V., Luo, J.K., Papov, V., Zou, W., Lenschow, D.J., Jacobs, B.S., Borden, E.C., Li, J., Virgin, H.W. and Zhang, D.E. (2005) Proteomic identification of proteins conjugated to ISG15 in mouse and human cells. *Biochem Biophys Res Commun*, **336**, 496-506.

Green, R.M., Elce, J.S. and Kisilevsky, R. (1978) Acetylation of peptidyl-tRNA on rat liver polyribosomes. *Can J Biochem*, **56**, 1075-1081.

Guerra, S., Caceres, A., Knobeloch, K.P., Horak, I. and Esteban, M. (2008) Vaccinia virus E3 protein prevents the antiviral action of ISG15. *PLoS Pathog*, **4**, e1000096.

Haas, A.L. (2006) *Protein Degradation*. Wiley-VCH, Weinheim.

Hadjebi, O., Casas-Terradellas, E., Garcia-Gonzalo, F.R. and Rosa, J.L. (2008) The RCC1 superfamily: from genes, to function, to disease. *Biochim Biophys Acta*, **1783**, 1467-1479.

Haglund, K. and Dikic, I. (2005) Ubiquitylation and cell signaling. *Embo J*, **24**, 3353-3359.

Haller, O., Kochs, G. and Weber, F. (2006) The interferon response circuit: induction and suppression by pathogenic viruses. *Virology*, **344**, 119-130.

Haller, O., Staeheli, P. and Kochs, G. (2007) Interferon-induced Mx proteins in antiviral host defense. *Biochimie*, **89**, 812-818.

Harty, R.N., Pitha, P.M. and Okumura, A. (2009) Antiviral activity of innate immune protein ISG15. *J Innate Immun*, **1**, 397-404.

Hay, R.T. (2005) SUMO: a history of modification. *Mol Cell*, **18**, 1-12.

Hayden, M.S. and Ghosh, S. (2008) Shared principles in NF-kappaB signaling. *Cell*, **132**, 344-362.

Hershko, A., Heller, H., Elias, S. and Ciechanover, A. (1983) Components of ubiquitin-protein ligase system. Resolution, affinity purification, and role in protein breakdown. *J Biol Chem*, **258**, 8206-8214.

Hicke, L. (2001) Protein regulation by monoubiquitin. *Nat Rev Mol Cell Biol*, **2**, 195-201.

Ho, Y.D., Joyal, J.L., Li, Z. and Sacks, D.B. (1999) IQGAP1 integrates Ca2+/calmodulin and Cdc42 signaling. *J Biol Chem*, **274**, 464-470.

Hochrainer, K., Mayer, H., Baranyi, U., Binder, B., Lipp, J. and Kroismayr, R. (2005) The human HERC family of ubiquitin ligases: novel members, genomic organization, expression profiling, and evolutionary aspects. *Genomics*, **85**, 153-164.

Honda, K. and Taniguchi, T. (2006) IRFs: master regulators of signalling by Toll-like receptors and cytosolic pattern-recognition receptors. *Nat Rev Immunol*, **6**, 644-658.

Honda, K., Yanai, H., Negishi, H., Asagiri, M., Sato, M., Mizutani, T., Shimada, N., Ohba, Y., Takaoka, A., Yoshida, N. and Taniguchi, T. (2005) IRF-7 is the master regulator of type-I interferon-dependent immune responses. *Nature*, **434**, 772-777.

Hovanessian, A.G. and Justesen, J. (2007) The human 2'-5'oligoadenylate synthetase family: unique interferon-inducible enzymes catalyzing 2'-5' instead of 3'-5' phosphodiester bond formation. *Biochimie*, **89**, 779-788.

Hsiang, T.Y., Zhao, C. and Krug, R.M. (2009) Interferon-induced ISG15 conjugation inhibits influenza A virus gene expression and replication in human cells. *J Virol*, **83**, 5971-5977.

Huang, D.T., Ayrault, O., Hunt, H.W., Taherbhoy, A.M., Duda, D.M., Scott, D.C., Borg, L.A., Neale, G., Murray, P.J., Roussel, M.F. and Schulman, B.A. (2009) E2-RING expansion of the NEDD8 cascade confers specificity to cullin modification. *Mol Cell*, **33**, 483-495.

Huang, D.T., Hunt, H.W., Zhuang, M., Ohi, M.D., Holton, J.M. and Schulman, B.A. (2007) Basis for a ubiquitin-like protein thioester switch toggling E1-E2 affinity. *Nature*, **445**, 394-398.

Huang, D.T., Miller, D.W., Mathew, R., Cassell, R., Holton, J.M., Roussel, M.F. and Schulman, B.A. (2004) A unique E1-E2 interaction required for optimal conjugation of the ubiquitin-like protein NEDD8. *Nat Struct Mol Biol*.

Huang, D.T., Paydar, A., Zhuang, M., Waddell, M.B., Holton, J.M. and Schulman, B.A. (2005) Structural basis for recruitment of Ubc12 by an E2 binding domain in NEDD8's E1. *Mol Cell*, **17**, 341-350.

Huang, D.T., Zhuang, M., Ayrault, O. and Schulman, B.A. (2008) Identification of conjugation specificity determinants unmasks vestigial preference for ubiquitin within the NEDD8 E2. *Nat Struct Mol Biol*, **15**, 280-287.

Huang, L., Kinnucan, E., Wang, G., Beaudenon, S., Howley, P.M., Huibregtse, J.M. and Pavletich, N.P. (1999) Structure of an E6AP-UbcH7 complex: insights into ubiquitination by the E2-E3 enzyme cascade. *Science*, **286**, 1321-1326.

Huibregtse, J.M., Scheffner, M., Beaudenon, S. and Howley, P.M. (1995) A family of proteins structurally and functionally related to the E6-AP ubiquitin-protein ligase. *Proc. Natl. Acad. Sci. U. S. A.*, **92**, 2563-2567.

Huibregtse, J.M., Scheffner, M. and Howley, P.M. (1991) A cellular protein mediates association of p53 with the E6 oncoprotein of human papillomavirus types 16 or 18. *EMBO J.*, **10**, 4129-4135.

Ichimura, Y., Kirisako, T., Takao, T., Satomi, Y., Shimonishi, Y., Ishihara, N., Mizushima, N., Tanida, I., Kominami, E., Ohsumi, M., Noda, T. and Ohsumi, Y. (2000) A ubiquitin-like system mediates protein lipidation. *Nature*, **408**, 488-492.

Imai, Y., Soda, M. and Takahashi, R. (2000) Parkin suppresses unfolded protein stress-induced cell death through its E3 ubiquitin-protein ligase activity. *J Biol Chem*, **275**, 35661-35664.

Jeon, Y.J., Choi, J.S., Lee, J.Y., Yu, K.R., Ka, S.H., Cho, Y., Choi, E.J., Baek, S.H., Seol, J.H., Park, D., Bang, O.S. and Chung, C.H. (2008) Filamin B serves as a molecular scaffold for type I interferon-induced c-Jun NH2-terminal kinase signaling pathway. *Mol Biol Cell*, **19**, 5116-5130.

Jeon, Y.J., Choi, J.S., Lee, J.Y., Yu, K.R., Kim, S.M., Ka, S.H., Oh, K.H., Kim, K.I., Zhang, D.E., Bang, O.S. and Chung, C.H. (2009) ISG15 modification of filamin B negatively regulates the type I interferon-induced JNK signalling pathway. *EMBO Rep*, **10**, 374-380.

Jin, J., Li, X., Gygi, S.P. and Harper, J.W. (2007) Dual E1 activation systems for ubiquitin differentially regulate E2 enzyme charging. *Nature*, **447**, 1135-1138.

Joazeiro, C.A., Wing, S.S., Huang, H., Leverson, J.D., Hunter, T. and Liu, Y.C. (1999) The Tyrosine Kinase Negative Regulator c-Cbl as a RING-Type, E2- Dependent Ubiquitin-Protein Ligase. *Science*, **286**, 309-312.

Jones, J., Wu, K., Yang, Y., Guerrero, C., Nillegoda, N., Pan, Z.Q. and Huang, L. (2008) A targeted proteomic analysis of the ubiquitin-like modifier nedd8 and associated proteins. *J Proteome Res*, **7**, 1274-1287.

Kamadurai, H.B., Souphron, J., Scott, D.C., Duda, D.M., Miller, D.J., Stringer, D., Piper, R.C. and Schulman, B.A. (2009) Insights into ubiquitin transfer cascades from a structure of a UbcH5B approximately ubiquitin-HECT(NEDD4L) complex. *Mol Cell*, **36**, 1095-1102.

Kato, H., Takeuchi, O., Mikamo-Satoh, E., Hirai, R., Kawai, T., Matsushita, K., Hiiragi, A., Dermody, T.S., Fujita, T. and Akira, S. (2008) Length-dependent recognition of double-stranded ribonucleic acids by retinoic acid-inducible gene-I and melanoma differentiation-associated gene 5. *J Exp Med*, **205**, 1601-1610.

Kato, H., Takeuchi, O., Sato, S., Yoneyama, M., Yamamoto, M., Matsui, K., Uematsu, S., Jung, A., Kawai, T., Ishii, K.J., Yamaguchi, O., Otsu, K., Tsujimura, T., Koh, C.S., Reis e Sousa, C., Matsuura, Y., Fujita, T. and Akira, S. (2006) Differential roles of MDA5 and RIG-I helicases in the recognition of RNA viruses. *Nature*, **441**, 101-105.

Kawakami, T., Chiba, T., Suzuki, T., Iwai, K., Yamanaka, K., Minato, N., Suzuki, H., Shimbara, N., Hidaka, Y., Osaka, F., Omata, M. and Tanaka, K. (2001) NEDD8 recruits E2-ubiquitin to SCF E3 ligase. *Embo J*, **20**, 4003-4012.

Kerscher, O., Felberbaum, R. and Hochstrasser, M. (2006) Modification of proteins by ubiquitin and ubiquitin-like proteins. *Annu Rev Cell Dev Biol*, **22**, 159-180.

Kim, H.C. and Huibregtse, J.M. (2009) Polyubiquitination by HECT E3s and the determinants of chain type specificity. *Mol Cell Biol*, **29**, 3307-3318.

Kim, H.T., Kim, K.P., Lledias, F., Kisselev, A.F., Scaglione, K.M., Skowyra, D., Gygi, S.P. and Goldberg, A.L. (2007) Certain pairs of ubiquitin-conjugating enzymes (E2s) and ubiquitin-protein ligases (E3s) synthesize nondegradable forked ubiquitin chains containing all possible isopeptide linkages. *J Biol Chem*, **282**, 17375-17386.

Kim, K.I., Giannakopoulos, N.V., Virgin, H.W. and Zhang, D.E. (2004) Interferon-Inducible Ubiquitin E2, Ubc8, Is a Conjugating Enzyme for Protein ISGylation. *Mol Cell Biol*, **24**, 9592-9600.

Knappe, M., Bodevin, S., Selinka, H.C., Spillmann, D., Streeck, R.E., Chen, X.S., Lindahl, U. and Sapp, M. (2007) Surface-exposed amino acid residues of HPV16 L1 protein mediating interaction with cell surface heparan sulfate. *J Biol Chem*, **282**, 27913-27922.

Knobeloch, K.P., Utermohlen, O., Kisser, A., Prinz, M. and Horak, I. (2005) Reexamination of the role of ubiquitin-like modifier ISG15 in the phenotype of UBP43-deficient mice. *Mol Cell Biol*, **25**, 11030-11034.

Kramer, G., Boehringer, D., Ban, N. and Bukau, B. (2009) The ribosome as a platform for co-translational processing, folding and targeting of newly synthesized proteins. *Nat Struct Mol Biol*, **16**, 589-597.

Kumar, S., Kao, W.H. and Howley, P.M. (1997) Physical interaction between specific E2 and Hect E3 enzymes determines functional cooperativity. *J Biol Chem*, **272**, 13548-13554.

Kurz, T., Chou, Y.C., Willems, A.R., Meyer-Schaller, N., Hecht, M.L., Tyers, M., Peter, M. and Sicheri, F. (2008) Dcn1 functions as a scaffold-type E3 ligase for cullin neddylation. *Mol Cell*, **29**, 23-35.

Lai, C., Struckhoff, J.J., Schneider, J., Martinez-Sobrido, L., Wolff, T., Garcia-Sastre, A., Zhang, D.E. and Lenschow, D.J. (2009) Mice lacking the ISG15 E1 enzyme UbE1L demonstrate increased susceptibility to both mouse-adapted and non-mouse-adapted influenza B virus infection. *J Virol*, **83**, 1147-1151.

Lee, I. and Schindelin, H. (2008) Structural insights into E1-catalyzed ubiquitin activation and transfer to conjugating enzymes. *Cell*, **134**, 268-278.

Lee, S.K., Harris, J. and Swanstrom, R. (2009) A strongly transdominant mutation in the human immunodeficiency virus type 1 gag gene defines an Achilles heel in the virus life cycle. *J Virol*, **83**, 8536-8543.

Lee, S.S., Weiss, R.S. and Javier, R.T. (1997) Binding of human virus oncoproteins to hDlg/SAP97, a mammalian homolog of the Drosophila discs large tumor suppressor protein. *Proc Natl Acad Sci U S A*, **94**, 6670-6675.

Lenschow, D.J., Giannakopoulos, N.V., Gunn, L.J., Johnston, C., O'Guin, A.K., Schmidt, R.E., Levine, B. and Virgin, H.W.t. (2005) Identification of interferon-stimulated gene 15 as an antiviral molecule during Sindbis virus infection in vivo. *J Virol*, **79**, 13974-13983.

Lenschow, D.J., Lai, C., Frias-Staheli, N., Giannakopoulos, N.V., Lutz, A., Wolff, T., Osiak, A., Levine, B., Schmidt, R.E., Garcia-Sastre, A., Leib, D.A., Pekosz, A., Knobeloch, K.P., Horak, I. and Virgin, H.W.t. (2007) IFN-stimulated gene 15 functions as a critical antiviral molecule against influenza, herpes, and Sindbis viruses. *Proc Natl Acad Sci U S A*, **104**, 1371-1376.

Lindner, H.A., Lytvyn, V., Qi, H., Lachance, P., Ziomek, E. and Menard, R. (2007) Selectivity in ISG15 and ubiquitin recognition by the SARS coronavirus papain-like protease. *Arch Biochem Biophys*, **466**, 8-14.

Loeb, K.R. and Haas, A.L. (1992) The interferon-inducible 15-kDa ubiquitin homolog conjugates to intracellular proteins. *J Biol Chem*, **267**, 7806-7813.

Lois, L.M. and Lima, C.D. (2005) Structures of the SUMO E1 provide mechanistic insights into SUMO activation and E2 recruitment to E1. *Embo J*, **24**, 439-451.

Love, K.R., Catic, A., Schlieker, C. and Ploegh, H.L. (2007) Mechanisms, biology and inhibitors of deubiquitinating enzymes. *Nat Chem Biol*, **3**, 697-705.

Malakhov, M.P., Malakhova, O.A., Kim, K.I., Ritchie, K.J. and Zhang, D.E. (2002) UBP43 (USP18) specifically removes ISG15 from conjugated proteins. *J Biol Chem*, **277**, 9976-9981.

Malakhova, O.A., Kim, K.I., Luo, J.K., Zou, W., Kumar, K.G., Fuchs, S.Y., Shuai, K. and Zhang, D.E. (2006) UBP43 is a novel regulator of interferon signaling independent of its ISG15 isopeptidase activity. *Embo J*, **25**, 2358-2367.

Malakhova, O.A. and Zhang, D.E. (2008) ISG15 inhibits Nedd4 ubiquitin E3 activity and enhances the innate antiviral response. *J Biol Chem*, **283**, 8783-8787.

Malathi, K., Dong, B., Gale, M., Jr. and Silverman, R.H. (2007) Small self-RNA generated by RNase L amplifies antiviral innate immunity. *Nature*, **448**, 816-819.

Martinez-Noel, G., Niedenthal, R., Tamura, T. and Harbers, K. (1999) A family of structurally related RING finger proteins interacts specifically with the ubiquitin-conjugating enzyme UbcM4. *FEBS Lett*, **454**, 257-261.

Melchior, F. (2000) SUMO--nonclassical ubiquitin. *Annu Rev Cell Dev Biol*, **16**, 591-626.

Michelle, C., Vourc'h, P., Mignon, L. and Andres, C.R. (2009) What was the set of ubiquitin and ubiquitin-like conjugating enzymes in the eukaryote common ancestor? *J Mol Evol*, **68**, 616-628.

Mizushima, N., Sugita, H., Yoshimori, T. and Ohsumi, Y. (1998) A new protein conjugation system in human. The counterpart of the yeast Apg12p conjugation system essential for autophagy. *J Biol Chem*, **273**, 33889-33892.

Mogensen, T.H. (2009) Pathogen recognition and inflammatory signaling in innate immune defenses. *Clin Microbiol Rev*, **22**, 240-273, Table of Contents.

Moynihan, T.P., Ardley, H.C., Nuber, U., Rose, S.A., Jones, P.F., Markham, A.F., Scheffner, M. and Robinson, P.A. (1999) The ubiquitin-conjugating enzymes UbcH7 and UbcH8 interact with RING finger/IBR motif-containing domains of HHARI and H7-AP1. *J Biol Chem*, **274**, 30963-30968.

Mukhopadhyay, D. and Riezman, H. (2007) Proteasome-independent functions of ubiquitin in endocytosis and signaling. *Science*, **315**, 201-205.

Muller, U., Steinhoff, U., Reis, L.F., Hemmi, S., Pavlovic, J., Zinkernagel, R.M. and Aguet, M. (1994) Functional role of type I and type II interferons in antiviral defense. *Science*, **264**, 1918-1921.

Nakasato, N., Ikeda, K., Urano, T., Horie-Inoue, K., Takeda, S. and Inoue, S. (2006) A ubiquitin E3 ligase Efp is up-regulated by interferons and conjugated with ISG15. *Biochem Biophys Res Commun*, **351**, 540-546.

Narasimhan, J., Wang, M., Fu, Z., Klein, J.M., Haas, A.A. and Kim, J.J. (2005) Crystal structure of the interferon-induced ubiquitin-like protein ISG15. *J Biol Chem*.

Nees, M., Geoghegan, J.M., Hyman, T., Frank, S., Miller, L. and Woodworth, C.D. (2001) Papillomavirus type 16 oncogenes downregulate expression of interferon-responsive genes and upregulate proliferation-associated and NF-kappaB-responsive genes in cervical keratinocytes. *J Virol*, **75**, 4283-4296.

Niwa, J., Ishigaki, S., Doyu, M., Suzuki, T., Tanaka, K. and Sobue, G. (2001) A novel centrosomal ring-finger protein, dorfin, mediates ubiquitin ligase activity. *Biochem Biophys Res Commun*, **281**, 706-713.

Nyman, T.A., Matikainen, S., Sareneva, T., Julkunen, I. and Kalkkinen, N. (2000) Proteome analysis reveals ubiquitin-conjugating enzymes to be a new family of interferon-alpha-regulated genes. *Eur J Biochem*, **267**, 4011-4019.

Ogunjimi, A.A., Briant, D.J., Pece-Barbara, N., Le Roy, C., Di Guglielmo, G.M., Kavsak, P., Rasmussen, R.K., Seet, B.T., Sicheri, F. and Wrana, J.L. (2005) Regulation of Smurf2 ubiquitin ligase activity by anchoring the E2 to the HECT domain. *Mol Cell*, **19**, 297-308.

Ogunjimi, A.A., Wiesner, S., Briant, D.J., Varelas, X., Sicheri, F., Forman-Kay, J. and Wrana, J.L. The ubiquitin binding region of the Smurf HECT domain facilitates polyubiquitylation and binding of ubiquitylated substrates. *J Biol Chem*, **285**, 6308-6315.

Okumura, A., Lu, G., Pitha-Rowe, I. and Pitha, P.M. (2006) Innate antiviral response targets HIV-1 release by the induction of ubiquitin-like protein ISG15. *Proc Natl Acad Sci U S A*, **103**, 1440-1445.

Okumura, A., Pitha, P.M. and Harty, R.N. (2008) ISG15 inhibits Ebola VP40 VLP budding in an L-domain-dependent manner by blocking Nedd4 ligase activity. *Proc Natl Acad Sci U S A*, **105**, 3974-3979.

Olsen, S.K., Capili, A.D., Lu, X., Tan, D.S. and Lima, C.D. (2010) Active site remodelling accompanies thioester bond formation in the SUMO E1. *Nature*, **463**, 906-912.

Osiak, A., Utermohlen, O., Niendorf, S., Horak, I. and Knobeloch, K.-P. (2005) ISG15, an interferon-stimulated ubiquitin-like protein, is not essential for STAT1-signaling and responses against Vesicular Stomatitis and Lymphocytic Choriomeningitis Virus. *Mol. Cell. Biol.*, **in press**.

Pandya, R.K., Partridge, J.R., Love, K.R., Schwartz, T.U. and Ploegh, H.L. (2010) A structural element within the HUWE1 HECT domain modulates self-ubiquitination and substrate ubiquitination activities. *J Biol Chem*, **285**, 5664-5673.

Papouli, E., Chen, S., Davies, A.A., Huttner, D., Krejci, L., Sung, P. and Ulrich, H.D. (2005) Crosstalk between SUMO and ubiquitin on PCNA is mediated by recruitment of the helicase Srs2p. *Mol Cell*, **19**, 123-133.

Passmore, L.A. and Barford, D. (2004) Getting into position: the catalytic mechanisms of protein ubiquitylation. *Biochem J*, **379**, 513-525.

Peng, J., Schwartz, D., Elias, J.E., Thoreen, C.C., Cheng, D., Marsischky, G., Roelofs, J., Finley, D. and Gygi, S.P. (2003) A proteomics approach to understanding protein ubiquitination. *Nat Biotechnol*, **21**, 921-926.

Perry, J.J., Tainer, J.A. and Boddy, M.N. (2008) A SIM-ultaneous role for SUMO and ubiquitin. *Trends Biochem Sci*, **33**, 201-208.

Pestana, A. and Pitot, H.C. (1975) Acetylation of nascent polypeptide chains on rat liver polyribosomes in vivo and in vitro. *Biochemistry*, **14**, 1404-1412.

Petroski, M.D. and Deshaies, R.J. (2005) Function and regulation of cullin-RING ubiquitin ligases. *Nat Rev Mol Cell Biol*, **6**, 9-20.

Pfander, B., Moldovan, G.L., Sacher, M., Hoege, C. and Jentsch, S. (2005) SUMO-modified PCNA recruits Srs2 to prevent recombination during S phase. *Nature*, **436**, 428-433.

Pickart, C.M. (2001) Mechanisms underlying ubiquitination. *Annu. Rev. Biochem.*, **70**, 503-533.

Pickart, C.M. and Rose, I.A. (1985) Functional heterogeneity of ubiquitin carrier proteins. *J Biol Chem*, **260**, 1573-1581.

Pincetic, A., Kuang, Z., Seo, E.J. and Leis, J. (2010) The interferon-induced gene ISG15 blocks retrovirus release from cells late in the budding process. *J Virol*, **84**, 4725-4736.

Pitluk, Z.W., McDonough, M., Sangan, P. and Gonda, D.K. (1995) Novel CDC34 (UBC3) ubiquitin-conjugating enzyme mutants obtained by charge-to-alanine scanning mutagenesis. *Mol Cell Biol*, **15**, 1210-1219.

Potu, H., Sgorbissa, A. and Brancolini, C. (2010) Identification of USP18 as an important regulator of the susceptibility to IFN-alpha and drug-induced apoptosis. *Cancer Res*, **70**, 655-665.

Rabut, G. and Peter, M. (2008) Function and regulation of protein neddylation. 'Protein modifications: beyond the usual suspects' review series. *EMBO Rep*, **9**, 969-976.

Rape, M. (2009) Ubiquitin, infinitely seductive: symposium on the many faces of ubiquitin. *EMBO Rep*, **10**, 558-562.

Raue, U., Oellerer, S. and Rospert, S. (2007) Association of protein biogenesis factors at the yeast ribosomal tunnel exit is affected by the translational status and nascent polypeptide sequence. *J Biol Chem*, **282**, 7809-7816.

Reverter, D. and Lima, C.D. (2005) Insights into E3 ligase activity revealed by a SUMO-RanGAP1-Ubc9-Nup358 complex. *Nature*, **435**, 687-692.

Ritchie, K.J., Malakhov, M.P., Hetherington, C.J., Zhou, L., Little, M.T., Malakhova, O.A., Sipe, J.C., Orkin, S.H. and Zhang, D.E. (2002) Dysregulation of protein modification by ISG15 results in brain cell injury. *Genes Dev*, **16**, 2207-2212.

Ronco, L.V., Karpova, A.Y., Vidal, M. and Howley, P.M. (1998) Human papillomavirus 16 E6 oncoprotein binds to interferon regulatory factor-3 and inhibits its transcriptional activity. *Genes Dev*, **12**, 2061-2072.

Rotin, D. and Kumar, S. (2009) Physiological functions of the HECT family of ubiquitin ligases. *Nat Rev Mol Cell Biol*, **10**, 398-409.

Ryman, K.D., Klimstra, W.B., Nguyen, K.B., Biron, C.A. and Johnston, R.E. (2000) Alpha/beta interferon protects adult mice from fatal Sindbis virus infection and is an important determinant of cell and tissue tropism. *J Virol*, **74**, 3366-3378.

Samuel, C.E. (2001) Antiviral actions of interferons. *Clin Microbiol Rev*, **14**, 778-809, table of contents.

Satoh, T., Kato, H., Kumagai, Y., Yoneyama, M., Sato, S., Matsushita, K., Tsujimura, T., Fujita, T., Akira, S. and Takeuchi, O. LGP2 is a positive regulator of RIG-I- and MDA5-mediated antiviral responses. *Proc Natl Acad Sci U S A*, **107**, 1512-1517.

Scheffner, M., Huibregtse, J.M., Vierstra, R.D. and Howley, P.M. (1993) The HPV-16 E6 and E6-AP Complex Functions as a Ubiquitin-Protein Ligase in the Ubiquitination of p53. *Cell*, **75**, 495-505.

Scheffner, M., Nuber, U. and Huibregtse, J.M. (1995) Protein ubiquitination involving an E1-E2-E3 enzyme ubiquitin thioester cascade. *Nature*, **373**, 81-83.

Schroder, K., Muruve, D.A. and Tschopp, J. (2009) Innate immunity: cytoplasmic DNA sensing by the AIM2 inflammasome. *Curr Biol*, **19**, R262-265.

Schulman, B.A. and Harper, J.W. (2009) Ubiquitin-like protein activation by E1 enzymes: the apex for downstream signalling pathways. *Nat Rev Mol Cell Biol*, **10**, 319-331.

Shimura, H., Hattori, N., Kubo, S., Mizuno, Y., Asakawa, S., Minoshima, S., Shimizu, N., Iwai, K., Chiba, T., Tanaka, K. and Suzuki, T. (2000) Familial Parkinson disease gene product, parkin, is a ubiquitin-protein ligase. *Nat Genet*, **25**, 302-305.

Siepmann, T.J., Bohnsack, R.N., Tokgoz, Z., Baboshina, O.V. and Haas, A.L. (2003) Protein interactions within the N-end rule ubiquitin ligation pathway. *J Biol Chem*, **278**, 9448-9457.

Slade, H.B., Owens, M.L., Tomai, M.A. and Miller, R.L. (1998) Imiquimod 5% cream (Aldara). *Expert Opin Investig Drugs*, **7**, 437-449.

Sommereyns, C., Paul, S., Staeheli, P. and Michiels, T. (2008) IFN-lambda (IFN-lambda) is expressed in a tissue-dependent fashion and primarily acts on epithelial cells in vivo. *PLoS Pathog*, **4**, e1000017.

Soucy, T.A., Smith, P.G., Milhollen, M.A., Berger, A.J., Gavin, J.M., Adhikari, S., Brownell, J.E., Burke, K.E., Cardin, D.P., Critchley, S., Cullis, C.A., Doucette, A., Garnsey, J.J., Gaulin, J.L., Gershman, R.E., Lublinsky, A.R., McDonald, A., Mizutani, H., Narayanan, U., Olhava, E.J., Peluso, S., Rezaei, M., Sintchak, M.D., Talreja, T., Thomas, M.P., Traore, T., Vyskocil, S., Weatherhead, G.S., Yu, J., Zhang, J., Dick, L.R., Claiborne, C.F., Rolfe, M., Bolen, J.B. and Langston, S.P. (2009) An inhibitor of NEDD8-activating enzyme as a new approach to treat cancer. *Nature*, **458**, 732-736.

Souphron, J., Waddell, M.B., Paydar, A., Tokgoz-Gromley, Z., Roussel, M.F. and Schulman, B.A. (2008) Structural dissection of a gating mechanism preventing misactivation of ubiquitin by NEDD8's E1. *Biochemistry*, **47**, 8961-8969.

Sridharan, H., Zhao, C. and Krug, R.M. (2010) Species specificity of the NS1 protein of influenza B virus: NS1 binds only human and non-human primate ubiquitin-like ISG15 proteins. *J Biol Chem*, **285**, 7852-7856.

Su, A.I., Cooke, M.P., Ching, K.A., Hakak, Y., Walker, J.R., Wiltshire, T., Orth, A.P., Vega, R.G., Sapinoso, L.M., Moqrich, A., Patapoutian, A., Hampton, G.M., Schultz, P.G. and Hogenesch, J.B. (2002) Large-scale analysis of the human and mouse transcriptomes. *Proc Natl Acad Sci U S A*, **99**, 4465-4470.

Sullivan, M.L. and Vierstra, R.D. (1991) Cloning of a 16-kDa ubiquitin carrier protein from wheat and Arabidopsis thaliana. *J. Biol. Chem.*, **266**, 23878-23885.

Takaoka, A., Wang, Z., Choi, M.K., Yanai, H., Negishi, H., Ban, T., Lu, Y., Miyagishi, M., Kodama, T., Honda, K., Ohba, Y. and Taniguchi, T. (2007) DAI (DLM-1/ZBP1) is a cytosolic DNA sensor and an activator of innate immune response. *Nature*, **448**, 501-505.

Takeuchi, T., Kobayashi, T., Tamura, S. and Yokosawa, H. (2006) Negative regulation of protein phosphatase 2Cbeta by ISG15 conjugation. *FEBS Lett*, **580**, 4521-4526.

Takeuchi, T. and Yokosawa, H. (2005) ISG15 modification of Ubc13 suppresses its ubiquitin-conjugating activity. *Biochem Biophys Res Commun*, **336**, 9-13.

Talis, A.L., Huibregtse, J.M. and Howley, P.M. (1998) The role of E6AP in the regulation of p53 protein levels in human papillomavirus (HPV)-positive and HPV-negative cells. *J Biol Chem*, **273**, 6439-6445.

Tateishi, K., Omata, M., Tanaka, K. and Chiba, T. (2001) The NEDD8 system is essential for cell cycle progression and morphogenetic pathway in mice. *J Cell Biol*, **155**, 571-579.

Terenzi, F., Hui, D.J., Merrick, W.C. and Sen, G.C. (2006) Distinct induction patterns and functions of two closely related interferon-inducible human genes, ISG54 and ISG56. *J Biol Chem*, **281**, 34064-34071.

Trinchieri, G. and Sher, A. (2007) Cooperation of Toll-like receptor signals in innate immune defence. *Nat Rev Immunol*, **7**, 179-190.

Ullers, R.S., Luirink, J., Harms, N., Schwager, F., Georgopoulos, C. and Genevaux, P. (2004) SecB is a bona fide generalized chaperone in Escherichia coli. *Proc Natl Acad Sci U S A*, **101**, 7583-7588.

Urano, T., Saito, T., Tsukui, T., Fujita, M., Hosoi, T., Muramatsu, M., Ouchi, Y. and Inoue, S. (2002) Efp targets 14-3-3 sigma for proteolysis and promotes breast tumour growth. *Nature*, **417**, 871-875.

Valent, Q.A., de Gier, J.W., von Heijne, G., Kendall, D.A., ten Hagen-Jongman, C.M., Oudega, B. and Luirink, J. (1997) Nascent membrane and presecretory proteins synthesized in Escherichia coli associate with signal recognition particle and trigger factor. *Mol Microbiol*, **25**, 53-64.

Verdecia, M.A., Joazeiro, C.A., Wells, N.J., Ferrer, J.L., Bowman, M.E., Hunter, T. and Noel, J.P. (2003) Conformational flexibility underlies ubiquitin ligation mediated by the WWP1 HECT domain E3 ligase. *Mol. Cell*, **11**, 249-259.

Versteeg, G.A., Hale, B.G., van Boheemen, S., Wolff, T., Lenschow, D.J. and Garcia-Sastre, A. (2010) Species-specific antagonism of host ISGylation by the influenza B virus NS1 protein. *J Virol*.

Vertegaal, A.C. (2010) SUMO chains: polymeric signals. *Biochem Soc Trans*, **38**, 46-49.

Vetro, J.A. and Chang, Y.H. (2002) Yeast methionine aminopeptidase type 1 is ribosome-associated and requires its N-terminal zinc finger domain for normal function in vivo. *J Cell Biochem*, **85**, 678-688.

Wheeler, T.C., Chin, L.S., Li, Y., Roudabush, F.L. and Li, L. (2002) Regulation of synaptophysin degradation by mammalian homologues of seven in absentia. *J Biol Chem*, **277**, 10273-10282.

Winn, P.J., Religa, T.L., Battey, J.N., Banerjee, A. and Wade, R.C. (2004) Determinants of functionality in the ubiquitin conjugating enzyme family. *Structure*, **12**, 1563-1574.

Wong, J.J., Pung, Y.F., Sze, N.S. and Chin, K.C. (2006) HERC5 is an IFN-induced HECT-type E3 protein ligase that mediates type I IFN-induced ISGylation of protein targets. *Proc Natl Acad Sci U S A*, **103**, 10735-10740.

Xu, P., Duong, D.M., Seyfried, N.T., Cheng, D., Xie, Y., Robert, J., Rush, J., Hochstrasser, M., Finley, D. and Peng, J. (2009) Quantitative proteomics reveals the function of unconventional ubiquitin chains in proteasomal degradation. *Cell*, **137**, 133-145.

Ye, Y. and Rape, M. (2009) Building ubiquitin chains: E2 enzymes at work. *Nat Rev Mol Cell Biol*, **10**, 755-764.

Yuan, W. and Krug, R.M. (2001) Influenza B virus NS1 protein inhibits conjugation of the interferon (IFN)-induced ubiquitin-like ISG15 protein. *EMBO J*, **20**, 362-371.

Yunus, A.A. and Lima, C.D. (2009) Structure of the Siz/PIAS SUMO E3 ligase Siz1 and determinants required for SUMO modification of PCNA. *Mol Cell*, **35**, 669-682.

Zeng, W., Sun, L., Jiang, X., Chen, X., Hou, F., Adhikari, A., Xu, M. and Chen, Z.J. (2010) Reconstitution of the RIG-I pathway reveals a signaling role of unanchored polyubiquitin chains in innate immunity. *Cell*, **141**, 315-330.

Zhang, Y., Gao, J., Chung, K.K., Huang, H., Dawson, V.L. and Dawson, T.M. (2000) Parkin functions as an E2-dependent ubiquitin- protein ligase and promotes the degradation of the synaptic vesicle-associated protein, CDCrel-1. *Proc Natl Acad Sci U S A*, **97**, 13354-13359.

Zhao, C., Beaudenon, S.L., Kelley, M.L., Waddell, M.B., Yuan, W., Schulman, B.A., Huibregtse, J.M. and Krug, R.M. (2004) The UbcH8 ubiquitin E2 enzyme is also the E2 enzyme for ISG15, an IFN-alpha/beta-induced ubiquitin-like protein. *Proc Natl Acad Sci U S A*, **101**, 7578-7582.

Zhao, C., Denison, C., Huibregtse, J.M., Gygi, S. and Krug, R.M. (2005) Human ISG15 conjugation targets both IFN-induced and constitutively expressed proteins functioning in diverse cellular pathways. *Proc Natl Acad Sci U S A*, **102**, 10200-10205.

Zhao, C., Hsiang, T.Y., Kuo, R.L. and Krug, R.M. (2009) ISG15 conjugation system targets the viral NS1 protein in influenza A virus-infected cells. *Proc Natl Acad Sci U S A*, **107**, 2253-2258.

Zheng, N., Wang, P., Jeffrey, P.D. and Pavletich, N.P. (2000) Structure of a c-Cbl-UbcH7 complex: RING domain function in ubiquitin- protein ligases. *Cell*, **102**, 533-539.

Zou, W., Papov, V., Malakhova, O., Kim, K.I., Dao, C., Li, J. and Zhang, D.E. (2005) ISG15 modification of ubiquitin E2 Ubc13 disrupts its ability to form thioester bond with ubiquitin. *Biochem Biophys Res Commun*, **336**, 61-68.

Zou, W. and Zhang, D.E. (2006) The interferon-inducible ubiquitin-protein isopeptide ligase (E3) EFP also functions as an ISG15 E3 ligase. *J Biol Chem*, **281**, 3989-3994.

Vita

Larissa Anne Durfee was born in Lubbock, Texas in 1978. She is the daughter of Howard and Rebecca Durfee. In May 2003, she graduated from the University of Texas at Austin with a Bachelor of Science degree in Biology. She worked as a laboratory technician for Dr. Karen Artzt until 2004, when she began her graduate education in the Cellular and Molecular Biology program at the University of Texas at Austin. In 2005, she joined the lab of Dr. Jon Huibregtse for her doctoral studies.

Permanent address: 565 Leeward Way, Sacramento, CA 95831

This dissertation was typed by Larissa Anne Durfee.